DEVELOPMENT OF A NOVEL MICROFLUIDIC PLATFORM TO STUDY T CELL SIGNALING

By

Shannon Leigh Faley

Dissertation

Submitted to the Faculty of the

Graduate School of Vanderbilt University

In partial fulfillment of the requirements

for the degree of

DOCTOR OF PHILOSOPHY

in

Biomedical Engineering

August, 2007

Nashville Tennessee

Approved:

Professor John P. Wikswo

Professor E. Duco Jansen

Professor Derya Unutmaz

Professor Franz Baudenbacher

Professor David Wright

ACKNOWLEDGEMENTS

First and foremost, I would like to thank my incredible family for all their undying support over the past several years. My parents are truly inspiring people who have been anything I needed them to be and for that I will be eternally grateful. To say I wouldn't be here without them is a drastic understatement. "Thank you" seems so trivial for such devotion, but I will forever offer it nonetheless. I can only hope to be as good a parent to my son they have been to me.

I also have to give huge thanks to my firecracker of a son, Andrew. He has been by far my biggest motivator and best teacher. I've learned more about humanity and family from this little boy in the past 7 years than in the 22 years I spent without him. Andrew continues to inspire me daily with his intense curiousity and courage to run against the grain. I am so proud.

In addition, I have to thank my "grad-school family" which consists of all the wonderful people at Vanderbilt whom I've come to know and love. Huge thanks go out to my fellow cell-mates in the graduate student bullpens for being comic relief, offering great scientific advice, as well as lending their ear to my occasional rants. Marcella Woods has been a tremendous support to me, both professionally and personally, and I will continue to be inspired by her work ethic and intense attention to detail. I will miss our conversations.

I have enjoyed tremendously working closely with Kevin Seale during the course of my research. Kevin spared my sanity many times with his ingenious trouble shooting skills and inventive solutions. Together we made a great team that produced results of which I am very proud.

Finally, I have to extend my utmost gratitude to my advisor, John Wikswo. He has been a fantastic mentor whose enthusiasm and love for science continues to inspire and motivate me. I have enjoyed tremendously working with him and I will be forever grateful for his encouragement and support.

TABLE OF CONTENTS

LIST OF FIGURES

LIST OF ABBREVIATIONS

aAPC..... Artificial Antigen Presenting Cells

Ab .....Antibody

APC..... Antigen Presenting Cell

Ca^{2+}.....Calcium

CBW..... Chemical and Biological Warfare

CCD .....Charge-Coupled Device

CCL19.....Chemokine Ligand 19

CCR7 ..... Chemokine Receptor 7

CD8+..... Cytotoxic T cell

Cipro .....Ciprofloxacin

CO_2 ..... Carbon Dioxide

DAG .....Diacylglycerol

DC..... Dendritic Cell

DIC..... Differential Interference Contrast

ELISA..... Enzyme-Linked ImmunoSorbent Assay

ER.....Endoplasmic Recticulum

FACS ..... Fluorescence Activated Cell Sorting

FBS..... Fetal Bovine Serum

FC .....Flow Cytometry

FITC..... Fluorescein Isothiocyanate

FOV..... Field of View

GM-CSF..... Granulocyte Maturing Colony Stimulating Factor

iDC..... Immature Dendritic Cell

IL2..... Interleukin 2

IL2Rα, CD25 ..... Interleukin 2 Receptor Alpha

IL4 ..... Interleukin 4

Iono ..... Ionomycin

IP_3 ..... Inositol 1,4,5-triphosphate

LPS ..... Lipopolysaccharide

MAPK ..... Mitogen-Activated Protein Kinase

mDC ..... Mature Dendritic Cell

MHC ..... Major Histocompatibility Complex

NFAT ..... Nuclear Factor of Activation in T cells

NFκB ..... Nuclear Facotr kappa B

nTC ..... Naïve T Cell

PBMC ..... Peripheral Blood Mononuclear Cell

PDMS ..... Polydimethylsiloxane

PEEK ..... Polyetheretherketone

PhD ..... six years of hard work

PIP_2 ..... Phophatidylinositol 4,5-bisphosphate

PLC ..... Phospholipase C

PMA ..... Phorbol Myristoyl Acetate

QD ..... Quantum Dot

RPM ..... Revolutions per minute

SEB ..... Staphylococcal Enterotoxin B

TC ..... T Cell

TCR, CD3 ..... T Cell Receptor

Th, CD4+ ..... T helper cell

Th1 ..... T helper, subtype 1

Th2 ..... T helper, subtype 2

TRITC ..... Tetramethylrhodamine Isothiocyanate

VIIBRE ..... Vanderbilt Institute for Integrative Biosystems Research and Education

CHAPTER I

INTRODUCTION

Motivation & Significance

The adaptive immune response is a highly complex, critical life system which allows the human body to combat never before seen pathogens. This intricate dance which is called immunity involves well-timed sequences of signaling mechanisms and cellular interactions which is constantly working to maintain that delicate balance between outright war upon invaders and preservation of that which is self. A misjudged step in either direction results in either defeat or self-destruction. Lack of an intact immune system as observed in individuals diagnosed with severe combined immunodeficiency (SCID) or acquired immune deficiency syndrome (AIDS) demonstrates its incompatibility with life as both syndromes are fatal without drastic medical intervention. In addition to the primary duties of warding off potentially life threatening invaders, the immune system also plays major roles in wound healing[1-4], autoimmune diseases, tumor growth and survival[2;5], as well as producing chemical signaling agents that communicate and influence various bodily tissues[6] including both the heart[7] and the brain[8;9]. Thus, understanding the goings on of the immune system is an area of intense scrutiny and certain to have widespread impact in human biology and medicine.

T cells play a central role in cellular mediated adaptive immune responses as they are responsible for recognizing and responding to foreign/dangerous antigens. Deciphering the modus operandi of T cells in action is of utmost importance understanding the adaptive immune response as a whole. While the intracellular signaling pathways the govern T cell response are some of the most intensely studied, the intricacies of many signaling mechanisms remain unclear. Conventional cell culture methodologies involve analyzing bulk responses from million

of T cells which may average out key, rare signaling events important in the progression of a successful immune response. Thus it is desirable to follow both individual and populations of cells over time to obtain a clearer understanding of T cell signaling states. However, studying single T cells over time is difficult as their non-adherent nature generates the need for a method of tethering cells to a cell culture surface using antibodies or fibronectin which induce intracellular signaling cascades on their own. Hence, the main motivating factor driving this project was the desire to create a platform which overcomes limitations in conventional immunological and cell culture techniques to allow key information concerning T cell signaling pathways associated with cellular activation to be ascertained in an efficient as well as economic manner. The primary objective being the development, validation, and successful implementation of a novel microfluidic platform that allows controlled activation, manipulation, and monitoring of signaling pathways in multiple single T cells simultaneously.

Overview

The primary objective of this research was to develop a microfluidic platform for the study of T cell signaling pathways. To accomplish this, the following goals were set forth: (1) Design and produce a microfluidic device capable of passively trapping hundreds of single T cells in parallel. (2) Validate the ability of this device to trap primary T cells without compromising viability as well as maintain primary T cells for at least 24 hours within the device with a similar mortality rate as that found in cell culture. Long-term observation of T cells is essential to fully understanding the outcome of signaling cascades stimulated upon activation and as such this platform must be able to stably sustain primary T cells for extended lengths of time. (3) Demonstrate the ability to activate primary T cells within the microfluidic device using chemical, antibody and cellular based stimulation methods. While cellular based activation methods are most relevant physiologically, all three methods are utilized in conventional

immunological procedures and thus must be included to add credence to the assertion that this platform be a suitable substitute to current methodologies. (4) Utilize the microfluidic platform to study intracellular calcium signaling in primary T cells during activation. Calcium release from intracellular stores is a very early event in T cell activation and one that had been extensively characterized. However, utilizing this platform which allows the analysis of hundreds of individual cells over time may reveal nuances not clearly apparent in previous studies. At the very least, these experiments will further validate our platform as a useful tool in the study of T cell signaling.

Background

Immunology & T cell Biology

Thymocytes (T cells) are the major signal transducer with respect to the adaptive immune response in mammalian systems. These cells accept generic information from antigen presenting cells (APCs), rapidly distinguish between dangerous and benign peptides, then initiate signaling pathways to spark immune reaction specific to antigens perceived as threatening. Capabilities such as these make T cells an ideal target for developing cell based biosensor technologies. However, in order to utilize T cells to discriminate between or identify various stimuli, the internal signaling cascades must be well understood. Many of the experiments described within this proposal are

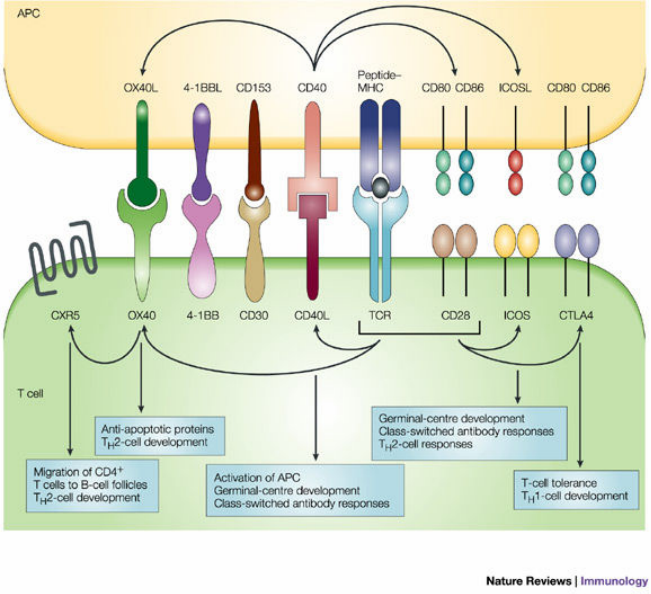

Figure 1. Illustration of Immune synapse

designed to facilitate the ability to gain more insight into the intricacies of T cell signaling pathways by developing a platform for studying multiple independent signaling pathways in single cells. Preliminary, proof-of-principle experiments will be based upon well known signaling events occurring during T cells activation.

Antigen Processing & Immune Synapse

Antigen presenting cells, primarily dendritic cells, can be considered the sentinels of the adaptive immune system as their primary functions is to indiscriminately break down all peptides, including those of self and non-self origins, and express the peptide fragments bound to the MHC receptor. It is the MHC complex to which the T cell receptor (TCR) binds to and discriminates between dangerous and non-threatening antigens. There are two classes of MHC receptor, class I MHC and class II MHC that respond to cytosolic peptides or endosomal peptides, respectively. While not an absolute division, the MHC class I receptors present mainly viral peptides while the MHC class II bind primarily bacterial antigens. Cytotoxic T cells (CD8+) interact with class I MHC while helper T cells (CD4+) bind the class II MHC receptor.

The immune synapse is formed by the strong interaction between T cells and antigen presenting cells (APCs) during which information on a particular antigen is transmitted to the T cell. If the MHC receptor contains a self, non-dangerous peptide fragment, the binding affinity between the TCR and the MHC receptor will be too week to transmit a signal resulting in the dissociation of the T cell and APC. When a pathogen is presented instead, the TCR and MHC bind tightly and recruit additional signaling and adhesion molecules to the synapse as shown in figure 1. This results in the amplification and propagation of activation signals through intracellular pathways causing stimulatory cytokine production and clonal expansion of the reacting T cell line (details described below).

T Cell Activation Pathways

Given the centrality of T cells and their activation to this proposal, it is useful to understand the sequence of events that occur with T cell activation. Figure 2 illustrates the major signaling pathways leading to IL-2 and IL-2Rα production. Successful engagement of the T-cell receptor (TCR) and coreceptors by antigen presenting cells (APCs) results in a cascade of intracellular events that ultimately result in the transcription of gene products necessary for T-cell proliferation and effector functions. This cascade of events can initiate several important signaling pathways, including the DAG (diacylglycerol), IP_3 (inositol 1,4,5-triphosphate), and MAPK (mitogen-activated protein kinase) pathways. Activation of phospholipase C (PLCγ1) by adaptor proteins and ZAP-70 results in the cleavage of phosphatidylinositol 4,5bisphosphate (PIP_2) to produce IP_3 and DAG. IP_3 binds to the endoplasmic reticulum and releases calcium stores. This increase in intracellular calcium concentration activates transcription factor NFAT (nuclear factor of activation in T cells), which then moves to the nucleus. DAG recruits and activates protein kinase C (PKC) in the lipid membrane [10]. There are several calcium-dependant and -independent isoforms of PKC whose substrates are not clearly defined. However, studies have shown that PKC is integral in the activation of NFκB (nuclear factor kappa beta)[11] and AP-1[12]. In particular, the PKC θ isoform is essential for the production of TCR-induced IL-2[13]. Once in

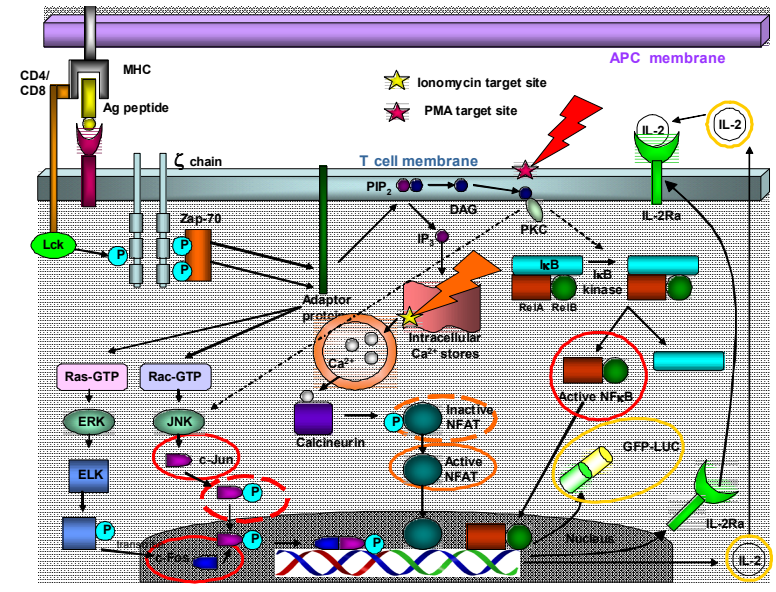

Figure 2. Major intracellular T cell activation pathways leading to the production of IL-2 and IL-2Rα.

the nucleus, the transcription factors NFAT, NFκB, and AP-1 act in concert to coordinate the activation of many genes involved in host defense and inflammatory responses, such as cytokine IL-2 to promote T cell activation and proliferation. It is estimated that together these transcription factors generate more than 250 gene products upon activation.

In vivo, T cell activation occurs by direct cell-cell contact with an APC. In vitro, T cell stimulation can be artificially induced by using 2 chemicals, phorbol myrastoyl acetate (phorbol ester or PMA) and ionomycin[14]. Both PKC and Ras-GRP (precursor to MAPK cascade) possess phorbol ester binding sites and are thus stimulated by PMA resulting in the activation of NFkb and AP-1[15]. Ionomycin stimulates calcium release from intracellular stores which results in the activation of NFAT. Thus, administration of these two chemicals simultaneously upregulates all three transcription factors.

NFκB: Five members of the mammalian NFκB/Rel family have been identified. The preponderant form of NFκβ in most cells consists of a heterodimer containing p50 and RelA (p65), which contains a transactivation domain[16-18]. In quiescent cells, NFκB complexes are sequestered in the cytoplasm by inhibitory proteins (IκB-α, IκB -β, IκB -ε)[19]. Stimulation of the NFκB pathway is mediated by diverse signal transduction cascades, resulting in phosphorylation of IκBs. Phosphorylated IκB-α (or IκB -β) is ubiquitinated and degraded by the 26S proteasome, allowing nuclear translocation of the NFκB complexes [20;21]. Activation of NFκB is necessary for maximal transcription of many adhesion molecules, enzymes, cytokines, and chemokines important in the initiation of inflammation and has been shown to be an essential component in signaling pathways of macrophages, dendritic cells, T and B-lymphocytes[22;23]. Still, the independent effects of cell and tissue specific activation of this transcription factor complex are largely undefined.

NFAT: There are four members of the NFAT family (NFAT 1-4), all of which share a high degree of DNA binding region sequence homology with the NFkB/Rel family of

transcription factors. NFAT 1 and 4 are constitutively expressed in T cells, while NFAT-2 transcription is induced by T cell activation. Previous studies have shown that NFAT 1,2 ,and 4 exert overlapping control in the initiation of IL-2 production in that cells may be deficient in one isoform without suffering significant decrease in IL-2 levels. However, cells deficienct in 2 or more isoforms result in marked impairment of IL-2 production [24]. Under resting conditions, a phosphorylated NFAT resides in the cytosol. Increase in intracellular calcium during activation results in calcineurin activation and subsequent binding to NFAT. The NFAT/calcineurin complex rapidly (5-10 minutes following activation translocates to the nucleus where NFAT associates with AP-1 to initiate transcription of various gene products including IL-2, IL-4, Il-5, TNF-α, and GM-CSF [24-27]). High intracellular calcium levels are required to sustain NFAT activity in the nucleus as calcineurin dissociation results in the movement of NFAT from the nucleus back to the cytosol [24].

AP-1: Activator protein -1 (AP-1) is a potent transcription factor consisting of 2 basic region-leucine zipper proteins (bZIP), c-Jun and c-Fos [28]. Ligation of the TCR activates MAPK cascades, ERK (extracellular receptor-activated kinase) and JNK (c-Jun N-terminal Kinase), that lead to the de novo synthesis of c-Jun and c-Fos in parallel pathways, respectively. A third MAPK, FRK, facilitates the dimerization of c-Jun and c-Fos by phosphorylating the C-terminal of c-Fos. Both c-Jun and c-Fos can act as transcription factors, but are more stable as a heterodimer and thus increase their DNA-binding ability[29]. In T cells AP-1 is known to associate with NFAT and NFκB in the production of IL-2, among other gene products.

IL-2: Interleukin-2 (IL-2), also known as T cell growth factor, is the major activating cytokine in T cells. Antigen stimulated naïve T cells (both CD4+ and CD8+) generate high levels of IL-2 which acts in autocrine fashion to promote clonal expansion, expression of IL-2 receptor-alpha (IL-2Rα), and increased cytokine production[10]. Because IL-2 is not produced

in naïve T cells, it is a good indicator of T cell activation. IL-2 synthesis requires transcriptional activation by NFκB, NFAT, and AP-1 and typically peaks 8 to 12 hours following antigen stimulation in primary T cells [30].

Jurkat T cells/ T cell hybridoma: Generating a stable cell line from T cells freshly isolated from peripheral blood samples is difficult due to their inherent volatility and relatively short lifetime. In addition, the peripheral blood will contain a very diverse population of T cells in terms of maturity and receptor type. T cell hybridomas overcome these limitations by fusing a particular normal T cell line with a lymphoma cell line. Fused cells are immortal and thus are stable over time, but also retain many of the characteristics of the normal T cell. In this experiment we propose to use Jurkat cells (ATCC, clone E6-1), a well studied T cell hybridoma generated from leukemia lymphoma by Schneider et al [31]. However, the Jurkat cell line is only a model of normal CD4 T cells. Because of their ease of use Jurkat cells will be used to optimize many of the experimental protocols, but the ultimate goal is to conduct experiments with primary CD4+ T cells isolated from peripheral blood of human donors in order to generate more scientifically relevant results.

Conventional Cell Cuture Techniques

Because the primary objective of this research is to develop a platform to replace current immunological experimental techniques, it is useful to summarize the strengths and weaknesses of some of the most widely used tools. The reason for developing the microfluidic platform is to have an easy method of analyzing multiple single T cells over extended periods of time. The following techniques are undoubtedly important in immunological experimentation, but none alone are able to fulfill these criteria.

Flourescence Activated Cell Sorting (FACS): FACS is a highly useful flow cytometry technique for quickly identifying subset populations in bulk aliquots of cells and is one of the

most frequently used techniques in the field of immunology. The reason being that the state (activated vs anergic, mature vs. immature) of an immune cell can often be narrowed by the protein expressed on the cell surface. These cell surface protein are easily tagged with fluorescently labeled antibodies and FACS provides a methods for quickly assessing the size of labeled and unlabeled cells within a large population.

FACS works by employing a laser beam (most commercial FACS machines have multiple lasers which are utilized based upon the fluorescent markers labeling the cells) focused upon a fluid stream that is hydrodynamically focused such that the width is on the order of a single cell, thus allowing single cell analysis. Several detectors are arranged such that forward scatter, side scatter, and fluorescence signals are simultaneously collected from the passing cells. This collection of scatter data combined with one or more fluorescent marker signals, is used in a statistical manner to draw conclusions on the state of the cells as well as to sort them into predefined populations for further study. FACS is extremely fast requiring only minutes to analyze millions of individual cells and is one of the few experimental techniques that allows for the analysis single cells. However, the data collected from FACS is a single snapshot of the cell in time. Obtaining time resolved information required multiple FACS runs most often on different cells from the same culture. It is nearly impossible to track any given individual cell over time.

Cell Culture Based Methods: The term cell culture based methods is meant to refer to experiments completed in the context of cell culture dish. Most experiments designed to gather information on entire populations of cells typically begin in cell culture as the environmental conditions of the cells in question are modified to address a given hypothesis, but in the end the analysis is very often performed using FACS. However, cell culture has the potential to allow the assessment of a given cell or population of cells over time. There are several issues with traditional cell culture experimentation that are particularly significant in studying immune cells.

One such issue is the typically large volume of media compared to cell volume in traditional cell culture setup. For example, it is customary to culture primary CD4+ T cells at a ratio of $5x10^5$ cells/ml such that there is approximately 10 μl of cell culture media available per cell. Primary naïve CD4+ T cells have a diameter of approximately 7 μm which gives a cellular volume of close to one picoliter. Thus, the media to cell volume ratio is 10μl:1pl which is equivalent to a ratio of $1x10^6$ to 1. While this setup provides a surplus of nutrients for cells, this superfluous volume also hinders normal T cell function. It is well known that both autocrine and paracrine signaling agents such as cytokines or chemokines are absolutely critical in the functioning of a normal T cell. The tremendous media to cell volume ratio results in the dilution of the cell based signals. In addition, cell-cell interactions are also very important in the progression of immune response, especially during activation. Dendritic cells (DCs) are larger than T cells with an approximate cellular volume closer to 5 picoliters such that the media to cell volume ratio is reduced to roughly $5x10^6$:1, but this is still sufficiently large that there is significant media volume between cells. Activation experiments requiring DCs and T cells to closely interact with one another must allow sufficient time for cells to "find" each other. This process can be hampered by the dilution of intercellular chemical agents. In addition, it is difficult to analyze the initial interactions between DCs and T cells as the exact position and time of interface is nearly impossible to predict. The solution to this problem leads us to the second major drawback of traditional cell culture techniques used to study T cell activation: tethering cells to the cell culture surface.

Because immune cells are non-adherent and there typically exists a large media to cell volume ratio in culture, studying the interactions between cells can be extremely difficult. One solution to this problem is attempting to tether one cell population to the cell culture surface so that there is a fixed point at which you expect the cellular interactions to occur. This is usually done using antibodies to cell surface proteins or an adhesive protein such as fibronection. The

problem with this approach is that any type of cell surface binding event will result in the triggering of internal signaling cascades that will affect the state of the cell. There are more passive methods of isolating cells such as optical trapping, but this allows the study of only a few cells at a time and requires an expensive setup. Thus, it is extremely desirable to have a method for passively isolating cells to minimize the variables during a given experiment without the need for a highly specialized and expensive experimental assembly.

Microfluidics

Overview

Microfluidics falls under the umbrella of "Lab-on-a-chip" technology, which in essence means translating traditional lab bench scale experiments to a micro-, or even nano-, scale. There are several reason that this is desirable, the first being the ability to integrate several laboratory functions in a single chip, thus decreasing time of experimentation and maximizing output. In addition, then miniaturization itself has several key advantages including reduction in reagents required for a given experiment (including cells for cell-based applications), increase in reaction times due to small volumes yielding shorter diffusion times[32;33], as well as tighter control of the system as a whole due to small size and low fluid volume[34-36]. Finally, once a platform has been designed it is typically very easy and inexpensive to mass produce disposable chips[37].

The materials used in making these devices depends upon the intended application, but for many biological including those presented within this body of work, microfluidic devices are constructed of polydimethylsiloxane (PDMS). PDMS is an elastomeric compound that is optically transparent making it well suited for microscopy applications and bio-inert such that biological organism or fluids do not react with the device surface upon contact[38]. However,

both PDMS and glass surfaces are easily functionalized using methods such as self-assembled monolayers (SAMs) associated with cell surface antibodies[37], or coating with bioreactive compounds (e.g. fibronectin)[39]. Furthermore, PDMS is gas permeable to nonpolar gases such as oxygen and carbon dioxide, a characteristic which is extremely important when dealing with mammalian cell culture that requires a steady exchange of oxygen and carbon dioxide to maintain metabolic equilibrium[37].

Fabrication

Microfluidic devices are fabricated using soft lithography, a process that has roots in the photolithographic methods developed to manufacture microelectronics. The process was adapted for microfluidic applications by lab-on-a-chip pioneers, George Whitesides and Steve Quake[33;37;40]. A simplified overview of the current fabrication process is illustrated in Figure 3. The design of the microfluidic device is first composed using Auto-CAD (Autodesk, Inc.), then transferred to a chrome mask via a commercial partner. A master is generated from the mask by first spin coating a layer of a photo-curable polymer, also known as photoresist, onto a silicon wafer. The photoresist is then exposed through the chrome mask with UV light. Areas that have been etched on the chrome will allow UV rays to penetrate the mask and cured the exposed photoresist. The uncured photoresist is then washed away leaving positive relief structures on

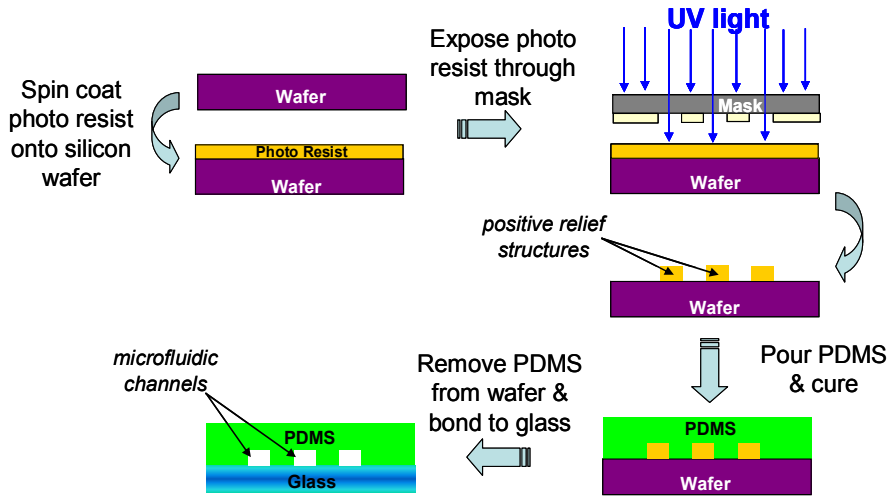

Figure 3. Overview of microfluidic device fabrication.

the surface of the silicon wafer. This becomes the master; a mold which can be used repeatedly to generated microfluidic devices out of PDMS. To generate a device from the master, a thick layer of PDMS is poured over the master and allowed to cure for 1 hour at 70^{o}C. The PDMS is then carefully peeled from the master. Narrow access ports are punched using standard 25 gauge hypodermic needle just prior to plasma bonding the device to a glass coverslip. The positive relief structure from the master result in open channels that are bound on the top and sides by PDMS, and glass on the bottom. The device is now ready for cellular applications.

Microfluidic devices to study single cells

The utilization of microfluidic devices for cellular applications has exploded over the past 10 years with the promise of lower production and reagent cost, tighter control of experimental paramenters, and quicker reaction times along with reduced diffusion times compared to traditional cell culture techniques[34;36;41]. The latter point opens the possibility of interrogating cellular activities that occur in time scales to quick to observe with conventional techniques[42]. Flexible and relatively easy fabrication allows incorporation of more complicated microfluidic designs including valves, pumps, and switches which enhance the manipulative ability of the cellular micro-environment[33;37;40]. Furthermore, culturing cells in a constant flow-thru environment is arguably more physiologically relevant than maintaining cells in a relatively large, stagnant pool of media as done in conventional cell culture.

The ability to maintain mammalian cells for extended periods of time has been demonstrated in adherent cell lines[43-45]. Cells readily adhere to the glass surface (sometimes functionalized to promote adhesion) and are able to be studied individually or en mass. When working with suspension cells, however, the same sequestration problem that plagues traditional cell culture methods is true for microfluidics as well. Methods to adhere cells

to a surface (antibodies or adhesion proteins) will induce undesired intracellular signaling pathways that alter the state of the cell.

One solution to this problem is to use suction to hold a cell in a “trap”, which has been demonstrated to be very effective with cardiac myocytes[46-48]. However, T cells, one of the main focuses of this research, are extremely small compared to cardiac myocytes with diameters of naïve T cells ranging between 5-7 μm. The diameter of the suction channels would ideally be much smaller than the diameter of the cell, but this aspect ratio is nearing the resolution limit for out current fabrication facilities. Furthermore, T cells are highly deformable and sensitive to pressure. Suction easily lyses these cells and those that remain intact are destined for apoptosis. Thus, for analysis of T cells, it is essential to have a passive trapping process.

McClain et al avoided the trapping problem in their novel platform to study Jurkat T cells[49]. Their high-throughput device allowed the interrogation and subsequent lysis of individual cells as they passed through the device. We are interested, however, in long term analysis of T cells and thus this technique isn’t applicable.

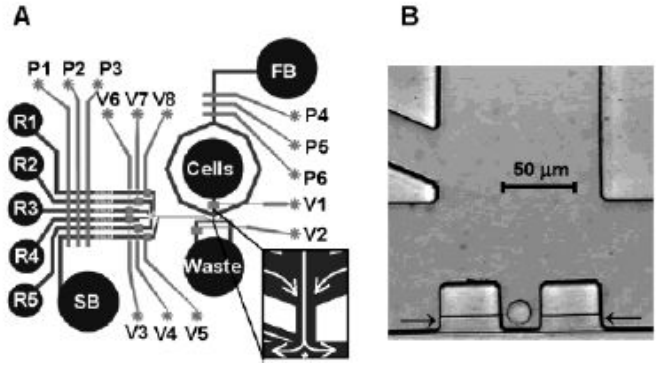

Figure 4. Single-cell analysis device. (A) Schematic of device: fluidic channels are dark; control channels are light. R1-R5 are reactant inlets, SB and FB are shield and focusing buffer inlets, respectively. Valves are actuated by applying pressure to control inlets V1-V8. Pumps are activated by actuating P1-P3 or P4-P6 in series. The serpentine regions of reagent and shield buffer channels diminish flow pulsing resulting from pump activation. Inset: closeup of cell trapping region. Cells are pushed by hydrostatic pressure from cell inlet to waste; they are focused to the center of the stream by the focusing buffer. Note the point of stagnation formed at *. (B) CCDimage of an individual Jurkat T-cell trapped in cell dock.
Reproduced from Wheeler et al. Anal Chem. 2003, 75, 3249-3254

A truly passive trapping mechanism was developed by Wheeler et al[35]. A clever device design incorporating on-chip valves allowed high precision control of fluid flow such that individual T cells could be directed into a bucket-shaped chamber (see **Figure 4**). Once trapped,

the intricate hydrodynamic controls allowed the cell to be directly addressable by dyes, stimulants, or lysing agents. However, the design was arranged such that only a single cell was trapped and interrogated during a single experiment. This is highly inefficient for collecting information concerning a population of T cells. To maximize the quantity and quality of data extracted from a given experiment, it is desirable to have many (hundreds to thousands) individually trapped and fluidically addressable T cells within a single microfluidic platform. To our knowledge, such a platform for analysis of T cells does not yet exist. Thus the impetus to develop and validate a microfluidic platform designed specifically to analyze T cells. Such a platform will facilitate the long-term study of hundreds of passively trapped individual T cells simultaneously, as well as other suspension cells of the immune system, without using antibodies or proteins to adhere cells to the culture surface and still allowing microscopic evaluation. In addition, this cell-based platform will be easily compatible with a multitude of detection modalities to maximize information extracted from any given experiment.

Bibliography

[1] A. D. Agaiby and M. Dyson, "Immuno-inflammatory cell dynamics during cutaneous wound healing," *J Anat.*, vol. 195 (Pt 4), pp. 531-542, Nov.1999.

[2] P. Grandics, "The cancer stem cell: evidence for its origin as an injured autoreactive T cell," *Mol. Cancer*, vol. 5, p. 6, 2006.

[3] S. Hendrix and R. Nitsch, "The role of T helper cells in neuroprotection and regeneration," *J Neuroimmunol.*, vol. 184, no. 1-2, pp. 100-112, Mar.2007.

[4] A. K. Tsirogianni, N. M. Moutsopoulos, and H. M. Moutsopoulos, "Wound healing: immunological aspects," *Injury*, vol. 37 Suppl 1, pp. S5-12, Apr.2006.

[5] J. C. Becker, T. Brabletz, C. Czerny, C. Termeer, and E. B. Brocker, "Tumor escape mechanisms from immunosurveillance: induction of unresponsiveness in a specific MHC-restricted CD4+ human T cell clone by the autologous MHC class II+ melanoma," *Int. Immunol*, vol. 5, no. 12, pp. 1501-1508, Dec.1993.

[6] A. Marques-Deak, G. Cizza, F. Eskandari, S. Torvik, I. C. Christie, E. M. Sternberg, and T. M. Phillips, "Measurement of cytokines in sweat patches and plasma in healthy women: validation in a controlled study," *J Immunol Methods*, vol. 315, no. 1-2, pp. 99-109, Aug.2006.

[7] J. E. Blalock, "The immune system as the sixth sense," *J Intern. Med.*, vol. 257, no. 2, pp. 126-138, Feb.2005.

[8] E. M. Sternberg, "Neuroendocrine regulation of autoimmune/inflammatory disease," *J Endocrinol.*, vol. 169, no. 3, pp. 429-435, June2001.

[9] E. M. Sternberg, "Neural regulation of innate immunity: a coordinated nonspecific host response to pathogens," *Nat Rev. Immunol*, vol. 6, no. 4, pp. 318-328, Apr.2006.

[10] A. Abbas, *Cellular and Molecular Immunology* Saunders, 2003.

[11] N. Coudronniere, M. Villalba, N. Englund, and A. Altman, "NF-kappa B activation induced by T cell receptor/CD28 costimulation is mediated by protein kinase C-theta," *Proc Natl Acad Sci U S A*, vol. 97, no. 7, pp. 3394-9, 2000.

[12] A. Kvanta, E. Kontny, M. Jondal, S. Okret, and B. B. Fredholm, "Mitogen stimulation of T-cells increases c-Fos and c-Jun protein levels, AP-1 binding and AP-1 transcriptional activity," *Cell Signal*, vol. 4, no. 3, pp. 275-86, 1992.

[13] G. Baier, "The PKC gene module: molecular biosystematics to resolve its T cell functions," *Immunol Rev*, vol. 192, pp. 64-79, 2003.

[14] A. Truneh, F. Albert, P. Golstein, and A. M. Schmitt-Verhulst, "Early steps of lymphocyte activation bypassed by synergy between calcium ionophores and phorbol ester," *Nature*, vol. 313, no. 6000, pp. 318-20, 1985.

[15] J. Hawiger, "Innate immunity and inflammation: a transcriptional paradigm," *Immunol Res*, vol. 23, no. 2-3, pp. 99-109, 2001.

[16] T. S. Blackwell and J. W. Christman, "The role of nuclear factor-kappa B in cytokine gene regulation," *Am J Respir Cell Mol Biol*, vol. 17, no. 1, pp. 3-9, 1997.

[17] D. Ron and M. G. Kazanietz, "New insights into the regulation of protein kinase C and novel phorbol ester receptors," *Faseb J*, vol. 13, no. 13, pp. 1658-76, 1999.

[18] T. R. Torgerson, A. D. Colosia, J. P. Donahue, Y. Z. Lin, and J. Hawiger, "Regulation of NF-kappa B, AP-1, NFAT, and STAT1 nuclear import in T lymphocytes by noninvasive delivery of peptide carrying the nuclear localization sequence of NF-kappa B p50," *J Immunol*, vol. 161, no. 11, pp. 6084-92, 1998.

[19] J. W. Christman, R. T. Sadikot, and T. S. Blackwell, "The role of nuclear factor-kappa B in pulmonary diseases," *Chest*, vol. 117, no. 5, pp. 1482-7, 2000.

[20] M. L. Schmitz and P. A. Baeuerle, "The p65 subunit is responsible for the strong transcription activating potential of NF-kappa B," *EMBO J*, vol. 10, no. 12, pp. 3805-17, 1991.

[21] I. M. Verma, J. K. Stevenson, E. M. Schwarz, D. Van Antwerp, and S. Miyamoto, "Rel/NF-kappa B/I kappa B family: intimate tales of association and dissociation," *Genes Dev*, vol. 9, no. 22, pp. 2723-35, 1995.

[22] A. S. Baldwin, Jr., "The NF-kappa B and I kappa B proteins: new discoveries and insights," *Annu Rev Immunol*, vol. 14, pp. 649-83, 1996.

[23] A. A. Beg and A. S. Baldwin, Jr., "The I kappa B proteins: multifunctional regulators of Rel/NF-kappa B transcription factors," *Genes Dev*, vol. 7, no. 11, pp. 2064-70, 1993.

[24] P. A. Baeuerle and T. Henkel, "Function and activation of NF-kappa B in the immune system," *Annu Rev Immunol*, vol. 12, pp. 141-79, 1994.

[25] P. J. Barnes, "Nuclear factor-kappa B," *Int J Biochem Cell Biol*, vol. 29, no. 6, pp. 867-70, 1997.

[26] J. Liu, N. Koyano-Nakagawa, Y. Amasaki, F. Saito-Ohara, T. Ikeuchi, S. Imai, T. Takano, N. Arai, T. Yokota, and K. Arai, "Calcineurin-dependent nuclear translocation of a murine transcription factor NFATx: molecular cloning and functional characterization," *Mol Biol Cell*, vol. 8, no. 1, pp. 157-70, 1997.

[27] E. Serfling, F. Berberich-Siebelt, S. Chuvpilo, E. Jankevics, S. Klein-Hessling, T. Twardzik, and A. Avots, "The role of NF-AT transcription factors in T cell activation and differentiation," *Biochim Biophys Acta*, vol. 1498, no. 1, pp. 1-18, 2000.

[28] J. H. Oum, J. Han, H. Myung, M. Hleb, S. Sharma, and J. Park, "Molecular mechanism of NFAT family proteins for differential regulation of the IL-2 and TNF-alpha promoters," *Mol Cells*, vol. 13, no. 1, pp. 77-84, 2002.

[29] G. W. Cockerill, A. G. Bert, G. R. Ryan, J. R. Gamble, M. A. Vadas, and P. N. Cockerill, "Regulation of granulocyte-macrophage colony-stimulating factor and E-selectin expression in endothelial cells by cyclosporin A and the T-cell transcription factor NFAT," *Blood*, vol. 86, no. 7, pp. 2689-98, 1995.

[30] E. Shaulian and M. Karin, "AP-1 as a regulator of cell life and death," *Nat Cell Biol*, vol. 4, no. 5, pp. 131-6, 2002.

[31] M. Karin, "The regulation of AP-1 activity by mitogen-activated protein kinases," *J Biol Chem*, vol. 270, no. 28, pp. 16483-6, 1995.

[32] S. Takayama, E. Ostuni, P. LeDuc, K. Naruse, D. E. Ingber, and G. M. Whitesides, "Selective chemical treatment of cellular microdomains using multiple laminar streams," *Chem. Biol*, vol. 10, no. 2, pp. 123-130, Feb.2003.

[33] G. M. Whitesides, "The origins and the future of microfluidics," *Nature*, vol. 442, no. 7101, pp. 368-373, July2006.

[34] P. Mitchell, "Microfluidics--downsizing large-scale biology," *Nat Biotechnol.*, vol. 19, no. 8, pp. 717-721, Aug.2001.

[35] A. R. Wheeler, W. R. Throndset, R. J. Whelan, A. M. Leach, R. N. Zare, Y. H. Liao, K. Farrell, I. D. Manger, and A. Daridon, "Microfluidic device for single-cell analysis," *Anal. Chem.*, vol. 75, no. 14, pp. 3581-3586, July2003.

[36] J. P. Wikswo, A. Prokop, F. Baudenbacher, D. Cliffel, B. Csukas, and M. Velkovsky, "Engineering challenges of BioNEMS: the integration of microfluidics, micro- and nanodevices, models and external control for systems biology," *IEE. Proc. Nanobiotechnol.*, vol. 153, no. 4, pp. 81-101, Aug.2006.

[37] G. M. Whitesides, E. Ostuni, S. Takayama, X. Jiang, and D. E. Ingber, "Soft lithography in biology and biochemistry," *Annu. Rev. Biomed. Eng*, vol. 3, pp. 335-373, 2001.

[38] S. K. Sia and G. M. Whitesides, "Microfluidic devices fabricated in poly(dimethylsiloxane) for biological studies," *Electrophoresis*, vol. 24, no. 21, pp. 3563-76, 2003.

[39] J. El-Ali, P. K. Sorger, and K. F. Jensen, "Cells on chips," *Nature*, vol. 442, no. 7101, pp. 403-411, July2006.

[40] M. A. Unger, H. P. Chou, T. Thorsen, A. Scherer, and S. R. Quake, "Monolithic microfabricated valves and pumps by multilayer soft lithography," *Science*, vol. 288, no. 5463, pp. 113-116, Apr.2000.

[41] S. K. Sia and G. M. Whitesides, "Microfluidic devices fabricated in poly(dimethylsiloxane) for biological studies," *Electrophoresis*, vol. 24, no. 21, pp. 3563-3576, Nov.2003.

[42] J. Voldman, "Engineered systems for the physical manipulation of single cells," *Curr. Opin. Biotechnol.*, vol. 17, no. 5, pp. 532-537, Oct.2006.

[43] C. D. Di, L. Y. Wu, and L. P. Lee, "Dynamic single cell culture array," *Lab Chip.*, vol. 6, no. 11, pp. 1445-1449, Nov.2006.

[44] L. Kim, Y. C. Toh, J. Voldman, and H. Yu, "A practical guide to microfluidic perfusion culture of adherent mammalian cells," *Lab Chip.*, vol. 7, no. 6, pp. 681-694, June2007.

[45] A. Prokop, Z. Prokop, D. Schaffer, E. Kozlov, J. Wikswo, D. Cliffel, and F. Baudenbacher, "NanoLiterBioReactor: long-term mammalian cell culture at nanofabricated scale," *Biomed. Microdevices.*, vol. 6, no. 4, pp. 325-339, Dec.2004.

[46] N. Klauke, G. Smith, and J. M. Cooper, "Microfluidic systems to examine intercellular coupling of pairs of cardiac myocytes," *Lab Chip.*, vol. 7, no. 6, pp. 731-739, June2007.

[47] N. Klauke, G. L. Smith, and J. M. Cooper, "Microfluidic partitioning of the extracellular space around single cardiac myocytes," *Anal. Chem.*, vol. 79, no. 3, pp. 1205-1212, Feb.2007.

[48] A. A. Werdich, E. A. Lima, B. Ivanov, I. Ges, M. E. Anderson, J. P. Wikswo, and F. J. Baudenbacher, "A microfluidic device to confine a single cardiac myocyte in a sub-nanoliter volume on planar microelectrodes for extracellular potential recordings," *Lab Chip.*, vol. 4, no. 4, pp. 357-362, Aug.2004.

[49] M. A. McClain, C. T. Culbertson, S. C. Jacobson, N. L. Allbritton, C. E. Sims, and J. M. Ramsey, "Microfluidic devices for the high-throughput chemical analysis of cells," *Anal. Chem.*, vol. 75, no. 21, pp. 5646-5655, Nov.2003.

CHAPTER II

QUANTUM DOT PROBES FOR MONITORING DYNAMIC CELLULAR RESPONSE: REPORTERS OF T CELL ACTIVATION

Abstract

Antibody-conjugated quantum dots (QDs) have been used to map the expression dynamics of the cytokine receptor interleukin-2 receptor (IL-2R) following Jurkat T cell activation. Maximal receptor expression was observed 48 h after activation, followed by a sharp decrease consistent with IL-2R internalization subsequent to IL-2 engagement. Verification of T cell activation and specificity of QD labeling were demonstrated using fluorescence microscopy, ELISA, and FACS analyses. These antibody conjugates provide a versatile means to rapidly determine cell state and interrogate membrane associated proteins involved in cell signaling pathways. Ultimately, incorporation with a microfluidic platform capable of simultaneously monitoring several cell signaling pathways will aid in toxin detection and discrimination.

Introduction

Quantum Dots (QDs) have shown a great deal of promise in fluorescent imaging applications since their first reported use as biological probes in 1998 [1], [2]. Their unique photophysical properties overcome several limitations of conventional fluorophores. Specifically, QDs continuous absorption spectra and narrow, size-dependant fluorescent emission make them ideally suited for multiplexed fluorescence detection, while their improved brightness and photostability permit long-term, dynamic imaging applications. Biological specificity has been

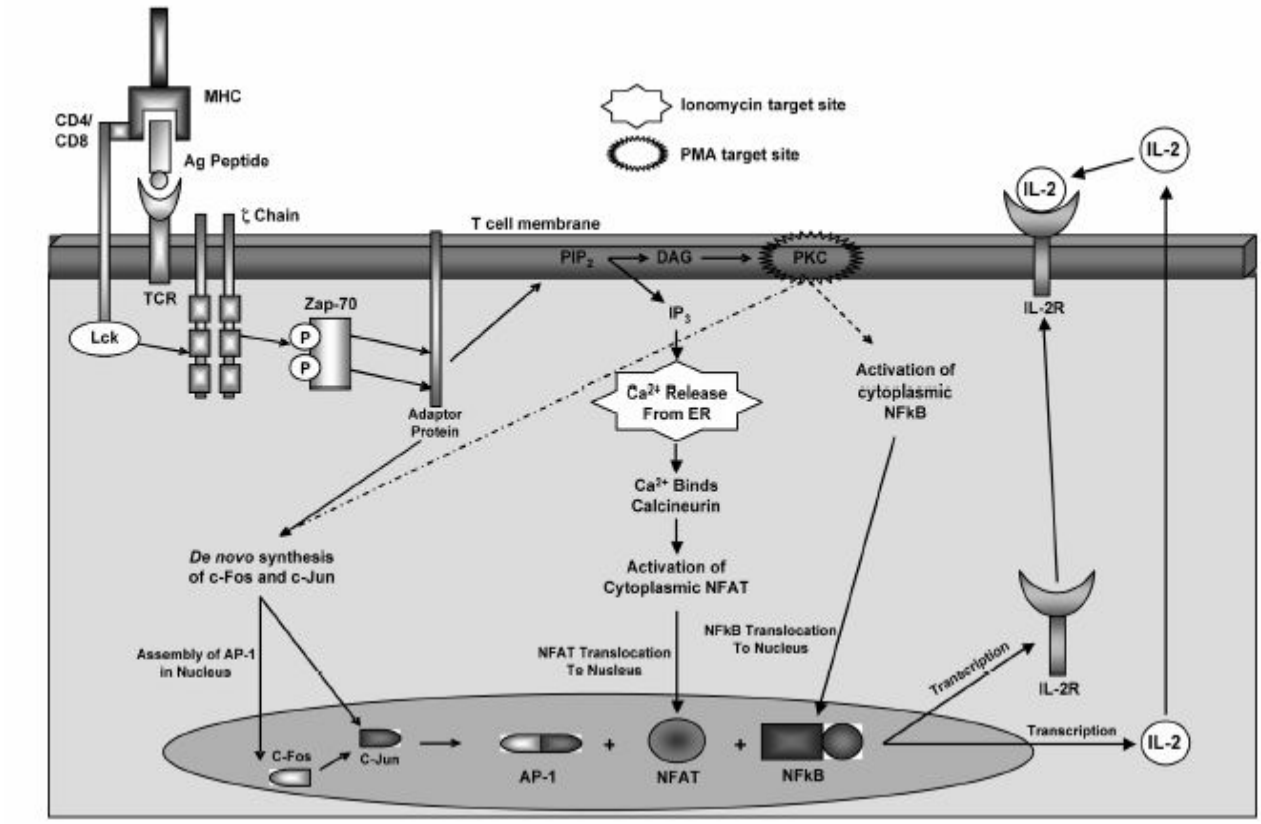

Figure 5. Signaling pathway associated with T cell activation. Engagement of the TCR and coreceptors by an APC results in a signaling cascade producing transcription factors NFAT, NFkB, and AP-1 required for successful activation of the T cell and expression of IL-2 and IL-2R□. As indicated, chemical stimulation can occur by treatment with PMA and ionomycin. PMA activates PKC, initiating the signaling cascades responsible for the transcription of AP-1 and NFkB, while ionomycin causes a release of intracellular calcium stores resulting in transcription of NFAT. Thus, treatment with both PMA and ionomycin upregulates all three transcription factors required for successful activation and expression of IL-2Rα and IL-2.

introduced through a number of different surface modifications. Some noteworthy imaging applications have utilized small molecule [3], peptide [4], [5], and antibody [6]–[8] QD

conjugates. In addition, PEGylation strategies have been shown to both minimize nonspecific interactions in cellular imaging applications [9] as well as extend clearance rates for in vivo imaging applications [10].

In this paper we examine the feasibility of using QDs as nanoprobes of T cell signaling events with the intention of demonstrating the benefits of incorporating QDs as a major read-out component of a proposed T cell based cell-signaling platform. To date, there have been a limited number of imaging applications which interrogate a dynamic cellular response utilizing QDs, despite their improved photostability. An initial dynamic imaging application employed nontargeted, endocytic loading of QDs into both mammalian and *D.discoideum* cell lines and confirmed no deleterious effects on cellular physiology [7]. Single-quantum dot tracking methods have since been used to elucidate diffusion dynamics of glycine receptors in the neuronal membrane over time frames ranging from seconds to minutes [11]. More recently, QDs were used to demonstrate retrograde transport of epidermal growth factor receptors and track their subsequent endosomal trafficking [12]. Peptide-conjugated QDs have also been used intracellularly, following transfection, for imaging nuclear targets allowing visualization of the transport of the QDs from the cytoplasm to the nucleus [5]. It is apparent, given their unique optical properties, that QDs can ultimately allow for unprecedented temporal resolution for imaging dynamic cellular processes. Thymocytes (T cells) are the major signal transducers of the adaptive immune response in mammalian systems. In the presence of a perceived threat, T cells undergo a process of activation and proliferation to coordinate an antigen specific immune response. Cell surface expression of the cytokine receptor interleukin-2 receptor- (IL-2R), as well as secretion of the cytokine interleukin-2 (IL-2), in T cells is widely used as an indicator of T cell activation. **Figure 1** illustrates the major signaling pathways leading to IL-2 and IL-2R production. Successful engagement of the T-cell receptor (TCR) by antigen presenting cells (APCs) results in a cascade of intracellular events including the DAG (diacylglycerol), IP (inositol 1,4,5-triphosphate), and MAPK (mitogen-activated protein kinase) pathways. Activation

of phospholipase C PLC by adaptor proteins and ZAP-70 results in the cleavage of phosphatidylinositol 4,5-bisphosphate PIP to produce IP and DAG. IP binds to the endoplasmic reticulum and releases calcium stores, activating transcription factor NFAT (nuclear factor of activation in T cells), which then moves to the nucleus. The recruitment and activation of protein kinase C (PKC) by DAG [13] have been shown to be integral to the activation of NFkB (nuclear factor kappa beta) [14] and AP-1 [15], [16].

Alternatively, T cell activation can be chemically induced *in vitro* by treatment with phorbol myrastoyl acetate (phorbol ester or PMA) and ionomycin, which act together to upregulate NFAT, NFkB, and AP-1 [17]. Once in the nucleus, the transcription factors NFAT, NF B, and AP-1 act in concert to coordinate the activation of several genes involved in host defense and inflammatory responses, including production of IL-2 and expression of IL-2Rα. This high level of complexity and discriminatory ability within the signaling pathways of T cells not only allows these cells to be highly effective for mediating immune responses against novel pathogens, but may also permit the cells to be utilized as biosensors to gain insight into methods of detection, prevention, and treatment for biological warfare agents.

We believe that construction of a detection system with the ability to sense novel pathogens of both known and unknown pathogenesis can be accomplished by utilizing T cells as biosensors and taking advantage of the discriminatory power of their diverse intracellular signaling pathways. Previous studies support the feasibility of this premise as both anthrax toxin [18] and immunomodulatory agents [19] have been shown to suppress T cell activation with a significantly varied response on cytokine production levels. We are currently developing platforms to study signaling dynamics of single T cells and other cells by utilizing technology that allows the simultaneous detection of multiple signals in live cells [20]. It is desirable to detect signaling on an individual cell basis to avoid averaging out either rare but important signaling events or spatial and relational correlations of signaling events with regard to the overall signaling cascade. Incorporation of QDs in this platform will ultimately allow for the interrogation of multiple pathways given their narrow fluorescent emission spectra, while the inherent brightness of QD probes provides an improved chance of detecting the limited amounts of cytokine production at the level of a single cell. Finally, their intrinsic photostability permits

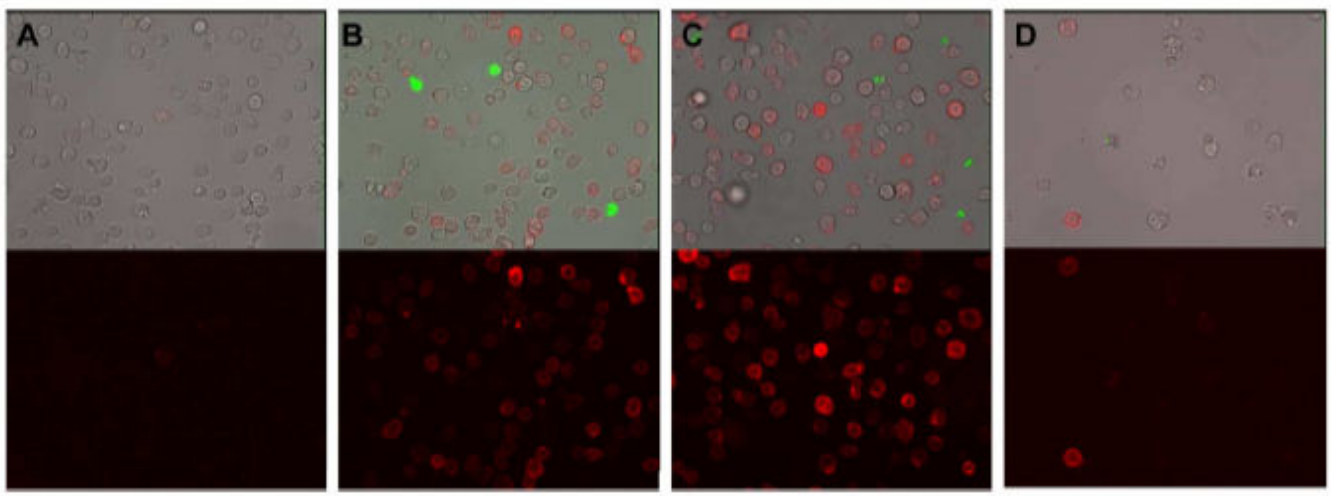

Figure 6. Time course of IL-2Rα expression. Bright field overlay (top) and QD fluorescence (bottom) images of Jurkat cells labeled with anti-IL2Rα-conjugated 655 QDs at different time points subsequent to activation with 10 M PMA and 4 M ionomycin. Green fluorescence in the overlaid images indicates nonviable cells using YOPRO-1 (Molecular Probes) cell viability stain. An increase in QD fluorescent intensity is observed from: (A) unactivated cells to cells activated for (B) 24 h and (C) 48 h indicating an increase in IL-2Rα expression. By 72 h (D) most cells have internalized IL-2Rα for lysosomal degradation and fluorescent intensity has correspondingly dropped off.

further investigation into the temporal dynamics of receptor expression and subsequent localization following expression.

Results & Discussion

Representative fluorescent images obtained from the 0, 24, 48, and 72 h time points are illustrated in **Figure 2**. Unactivated cells [**Figure 2(a)**], which do not express IL-2Rαand serve as a negative control, show minimal nonspecific fluorescent interactions. Receptor expression and, correspondingly, fluorescent intensity increase from 24 to 48 h and then drop off following 48 h. This decrease in fluorescent intensity is consistent with the expected wax and wane of IL-2R expression as the receptor is internalized upon engagement of secreted IL-2 for lysosomal degradation [13]. Additionally, internalization of the IL-2 • IL-2R

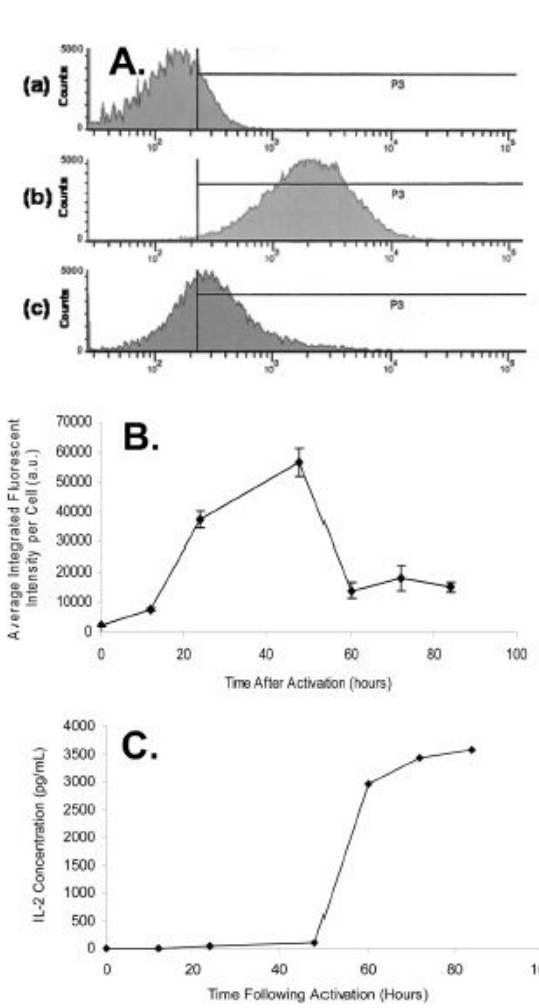

Figure 7. Quantification of IL-2 and IL-2Rα response. (A) FACS analysis of anti-IL2R□-conjugated QD fluorescence at selected points subsequent to activation. Minimal background fluorescent intensity is observed for: (a) unactivated cells compared to (b) those cells activated for 48 h which exhibit a large increase in fluorescent intensity per cell. This increase correspondingly drops off by 72 h (c) with only a small population still exhibiting increased fluorescence. (B) Average fluorescent intensity per cell obtained from fluorescent images using Metamorph image analysis software provides a graphical representation of the time course of receptor expression. Background subtracted fluorescent intensities were averaged over all viable cells imaged throughout the time course of one activation experiment. Error bars represent one standard deviation of the mean. (C) Quantification of IL-2 production by an ELISA provides verification of activation. IL-2R acts to clear IL-2 from the supernatant initially, but decreased expression of IL-2R allows for an accumulation of IL-2 concentration at later time points.

complex acts in an autoregulatory manner to down-regulate further transcription of IL-2R, further decreasing receptor expression and attenuating the T cell's IL-2 responsiveness [21]. FACS analysis provided confirmation of receptor expression and subsequent internalization [**Figure 3(a)**]. Minimal fluorescence is observed for unactivated cells (a) and by 48 h (b) most cells have shifted to higher fluorescent intensity, which correspondingly drops off by 72 h (c) for all but a small number of cells that remain activated. A graphical representation of the relative fluorescent intensity per cell throughout the entire time course of activation was obtained by fluorescent image analysis using Metamorph software package [**Figure 3(b)**]. Since activation is also accompanied by secretion of IL-2, analysis of the supernatants from each time point by means of an IL-2 ELISA provided verification of successful activation [**Figure 3(c)**].

Initial examination of the IL-2 ELISA data seemed to indicate a delayed response, as IL-2 secretion is expected to coincide with IL-2Rαexpression. However, since IL-2R acts to clear secreted IL-2 from the supernatant, accumulation of IL-2 in the supernatant is only observed after a significant portion of the expressed IL-2R has been internalized, resulting in a sharp spike following the 48 h time point. Thus, the IL-2 ELISA results confirm activation of the T cell populations by PMA and ionomycin.

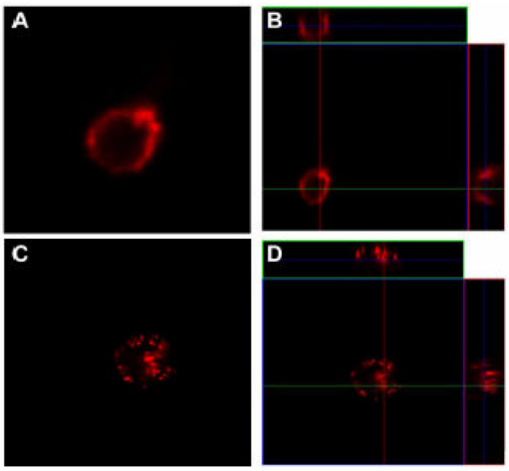

Figure 8. Receptor localization subsequent to QD labeling. Jurkat cells activated with PMA and ionomycin for 72 h were labeled with anti-IL2R conjugated 655 QDs. Cells were fixed: (A), (B) immediately following QD labeling and (C), (D) 24 h after labeling. Confocal images (A) and (C): center slice views; (B) and (D): orthogonal views of the z-stack) indicate only membrane associated QDs for the cells fixed immediately following labeling. Cells fixed 24 h later, however, have clearly internalized at least a portion of the QD conjugates.

Confocal microscopy provided direct evidence of receptor internalization subsequent to expression and anti-IL2Rα–QD labeling (Figure 4). Cells that had been activated for 72 h were labeled as before with 10 nM anti-IL2Rα-conjugated QDs for 30 min. Following centrifugation, the

labeled cells were resuspended in fresh media from which a small population of cells were immediately fixed with 4% paraformaldehyde on poly-L-lysine coated glass slides and mounted with Aqua PolyMount (Polysciences Inc.) for confocal microscopy. The remaining cells were allowed to remain in culture for an additional 24 h before fixation and mounting. Confocal images of cells fixed immediately after labeling [**Figure 4(a)–(b)**] show membrane associated extracellular labeling, while cells that have been allowed to remain in culture subsequent to labeling [**Figure 4(b)–(c)**] demonstrate internalization of the QDs (Panels A and C are the center-slices from the z-stack of confocal images, while panels B and D provide orthogonal views of the XZ and YZ planes). This indicates that the QD-receptor interaction is sufficiently strong as to undergo internalization, and that the relatively bulky QD probe does not prevent this internalization.

Conclusions

We have demonstrated controlled activation of populations of Jurkat T cells and shown that the dynamics of receptor expression can be monitored using antibody conjugated fluorescent QD probes. Incorporation with a microfluidic platform capable of isolating and maintaining nonadherent cells, currently being developed in our group, will allow these time course studies to be performed in real time on thousands of individual cells in a massively parallel format. Additionally, other signaling pathways can be simultaneously monitored in a similar manner by varying the emission wavelength of the QD probes and targeting these probes to other relevant membrane associated receptors. Future experiments will address simultaneous detection of multiple cell surface targets in order to more accurately portray the signaling state of the cell. In addition, it may prove to be beneficial to compare the brightness of these QD conjugates to fluorophores traditionally used for low expression applications, although the improved sensitivity of QD probes has been demonstrated extensively. Furthermore, we are

currently working on methods to use QDs intracellularly and obtain functional information of earlier events occurring within the signaling pathways that may be used in discrimination or prediction of cellular response to toxins. Ultimately, QDs will be used as nanoprobes to aid in the detection and discrimination of toxin exposure in T cells. The effect of toxin exposure on expression dynamics will provide insights not only into the toxin exposure itself, but also provide information on the method of pathogenesis as well as treatment.

References

[1] M. P. Bruchez, M. Moronne, P. Gin, S. Weiss, and A. P. Alivisatos,"Semiconductor nanocrystals as fluorescent biological labels," Science,vol. 281, no. 5385, pp. 2013-2016, Sep. 1998.

[2] W. C. W. Chan and S. Nie, "Quantum dot bioconjugates for ultrasensi-tive nonisotopic detection," Science, vol. 281, no. 5385, pp. 2016-2018,Sep. 1998.

[3] S. J. Rosenthal, I. D. Tomlinson, E. M. Adkins, S. Schroeter, S. Adams, L. Swafford, J. McBride, Y. Wang, L. J. DeFelice, and R. D. Blakely, "Targeting cell surface receptors with ligand-conjugated nanocrystals,"J. Amer. Chem. Soc., vol. 124, no. 17, pp. 4586-4594, Apr. 2002.

[4] M. E. Akerman, W. C. W. Chan, P. Laakkonen, S. N. Bahtia, and E. Ruoslahti, "Nanocrystal targeting in vivo," Proc. Nat. Acad. Sci. USA, vol. 99, no. 20, pp. 12 617-12 621, Sep. 2002.

[5] F. Chen and D. Gerion, "Fluorescent CdSe/ZnS nanocrystal-peptide conjugates for long-term, nontoxic imaging and nuclear targeting in living cells," Nano Lett., vol. 4, no. 10, pp. 1827-1832, Oct. 2004.

[6] X. Wu, H. Liu, J. Liu, K. N. Haley, J. A. Treadway, J. P. Larson, N. Ge, F. Peale, and M. P. Bruchez, "Immunofluorescent labeling of cancer marker Her2 and other cellular targets with semiconductor quantum dots," Nature Biotechnol., vol. 21, pp. 41-46, Jan. 2003.

[7] J. K. Jaiswal, H. Mattoussi, J. M. Mauro, and S. M. Simon, "Long-term multiple color imaging of live cells using quantum dot bioconjugates,"Nature Biotechnol., vol. 21, pp. 47-51, Jan. 2003.

[8] E. L. Bentzen, F. House, T. J. Utley, J. E. Crowe, and D. W. Wright, "Progression of respiratory syncytial virus infection monitored by fluorescent quantum dot probes," Nano Lett., vol. 5, no. 4, pp. 591-595,Mar. 2005.

[9] E. L. Bentzen, I. D. Tomlinson, J. Mason, P. Gresch, M. R. Warnement, D. Wright, E. Sanders-Bush, R. D. Blakely, and S. J. Rosenthal, "Surface modification to reduce nonspecific binding of quantum dots in live cell assays," Bioconjugate. Chem., vol. 16, no. 6, pp. 1488-1494, Nov.2005.

[10] B. Ballou, B. C. Lagerholm, L. A. Ernst, M. P. Bruchez, and A. S. Waggoner, "Noninvasive imaging of quantum dots in mice," Bioconjugate.Chem., vol. 15, no. 1, pp. 79-86, Jan. 2004.

[11] M. Dahan, S. Levi, C. Luccardini, P. Rostaing, B. Riveau, and A. Triller, "Diffusion dynamics of glycine receptors revealed by single-quantum dot tracking," Science, vol. 302, pp. 442-445, Oct.2003.

[12] D. S. Lidke, P. Nagy, R. Heintzmann, D. J. Arndt-Jovin, J. N. Post, H. E. Grecco, E. A. Jares-Erijman, and T. M. Jovin, "Quantum dot ligands provide new insights into

erbB/HER receptor mediated signal transduction," Nature Biotechnol., vol. 22, pp. 198-203, Feb. 2004. [13] A. K. Abbas and A. H. Lichtman, Cellular and Molecular Immunology, 5 ed. Philadelphia, PA: Saunders, 2003, ch. 8.

[14] N. Coudronniere, M. Villalba, N. Englund, and A. Altman, "NF-Kb activation induced by T cell receptor/Cd28 costimulation is mediated by protein kinase C-q," Proc. Nat. Acad. Sci. USA, vol. 97, no. 7, pp. 3394-3399, Mar. 2000.

[15] A. Kvanta, E. Kontny, M. Jondal, S. Okret, and B. B. Fredholm, "Mitogen stimulation of T-cells increases c-Fos and c-Jun protein levels, AP-1 binding and AP-1 transcriptional activity," Cell. Signal., vol. 4, no. 3, pp. 275-286, May 1992.

[16] G. Baier, "The PKC gene module: molecular biosystematics to resolveits T cell functions," Immunol. Rev., vol. 192, no. 1, pp. 64-79. [17] A. Truneh, F. Albert, P. Golstein, and A. M. Schmitt-Verhulst, "Early steps of lymphocyte activation bypassed by synergy between calcium ionophores and phorbol ester," Nature, vol. 313, no. 6000, pp. 318-320, Jan. 1985.

[18] S. R. Paccani, F. Tonello, R. Ghittoni, M. Natale, L. Muraro, M. M. D'Elios, W. J. Tang, C. Montecucco, and C. T. Baldari, "Anthrax toxins suppress T lymphocyte activation by disrupting antigen receptor signaling," J. Exp. Med., vol. 201, no. 3, pp. 325-331, Feb. 2005.

[19] T. Ringerike, E. Ulleras, R. Volker, B. Verlaan, A. Eikeset, D. Trzaska, V. Adamczewska, J. Arkusz, H. van Loveren, G. Nilsson, M. Lovik, J. Dastych, and R. J. Vandebriel, "Detection of immunotoxicity using T-cell based cytokine reporter cell lines ('cell chip')," Toxicology, vol. 206, no. 2, pp. 257-272, Jan. 2005.

[20] J. P. Wikswo, A. Prokop, F. Baudenbacher, D. Cliffel, B. Csukas, and M. Velkovsky, "Engineering challenges of bioNEMS: The integration of microfluidics, micro- and nanodevices, models, and external control for systems biology," IEE Proc.— Nanobiotechnol., vol. 153, no. 4, pp. 81-101, 2006.

[21] D. Z. Chang, Z. Wu, and T. Ciardelli, "A point mutation in interleukin-2 that alters ligand internalization," J. Biol. Chem., vol. 271, no. 23, pp. 13349-13 355, Jun. 1996.

CHAPTER III

MACRO TO NANO: A SIMPLE METHOD FOR TRANSPORTING CULTURED CELLS FROM MILLILITER SCALE TO NANOLITER SCALE

Abstract

We describe simple procedures that address the long-standing problem of introducing efficient introduction of cells and cell culture media into microfluidic devices using polyetheretherketone (PEEK) tubing and Hamilton gastight syringes. Suspension or adherent cells grown in cell culture flasks are extracted directly from the centrifuge pellet into the end of the PEEK tubing by aspiration. The tube end is then coupled to pre-punched channels in the polydimethylsiloxane (PDMS) microfluidic device by friction fitting. Depression of the syringe plunger expels the cells into the microfluidic device seconds following aspiration. The gastight syringes and PEEK tubing with PEEK fittings provide a noncompliant source of pressure and suction with a rapid response time that is well suited for short term intra-microfluidic cellular studies. The benefits of this method are its simplicity, modest expense, and the short preparation time required for loading appropriate numbers of cells.

Introduction

An often cited obstacle to widespread use or commercialization of microfluidic BioMicroElectroMechanical (BioMEMS) devices is the “world-to-chip”[1] or “macro-to-micro”[2] problem of how to introduce samples from milliliter sized volumes into the micro and nanoliter volumes of microfluidic devices. This problem is characterized by low Reynold’s number perfusion within a noncompliant, very small-volume, high surface-tension device that is resistant to flow. The world-to-chip problem is compounded in the case of cellular studies by an increased cellular

volume fraction inside the device and a more rapid auto-toxification of the cellular microenvironment by metabolic activity of the cell. We have approached this challenge by noting the similarity to the requirement for input impedance matching for maximum power transfer in the design of electronic equipment[3]. A driving circuit having lower or higher impedance than a load circuit will result in less than optimal power transfer. Input impedance matching of test circuitry is required for accurate control and measurement of electronic circuits. For microfluidic circuits, the surface tensions, capacitances and resistance to flow must be considered for high fidelity control of the fluid flow within the device. Several good solutions to this problem have been put forth[4-15], but most either require specialized microfabrication or are limited to specific assays and are inappropriate for cellular studies. Here we describe an inexpensive and simple method for accessing, loading and controlling micro and nanofluidic devices for short to long term cellular studies.

Cell Density

The study of cultured cells requires long term containment and nourishment of primary and/or immortalized cell lines[16]. The cells under study are usually kept in environmentally controlled incubators at bulk concentrations of approximately $1x10^6$ cells/ml or 1 cell per nanoliter or less in container sizes of 5 to 50 ml. For short duration experiments lasting minutes to hours, smaller volumes may be extracted from the bulk containers with pipettors into vials of approximately 1 ml. At these concentrations, a cell occupies one out of every 1000 possible positions in a suspension of cells with the balance being pure media, assuming a spherical cell with 5 □m radius and approximately 1 pL volume. Since adherent cells are often separated from their substrate and released into solution by an enzymatic digestion (i.e. trypsin) for transport or splitting, they may be assumed to exhibit roughly the same volume distribution.

Microfluidic devices for cellular studies are essentially two-dimensional flow chambers, often with vessel heights on the order of one cell diameter. The sparse cellular volume fraction of macro cell culture preparations leads to long loading times of microfluidic devices since every cell is not closely packed with neighboring cells. The cell-cell separation within the device is determined by the volume fraction of cells in the loaded media and a typical 650 × 870 micron field of view from a wide field microscope provided by a 20X objective will contain only 14 cells when loaded with media containging suspended cells from a macro culture vial. Integrated microfluidic filters may be used to help retain the cells that arrive early until later cells appear, but this is accomplished at the expense of time and is not always effective since cells are deformable, subject to mechanical damage, and tend to squeeze through small gaps in the filters.

Flow Control and Switching

The instantaneous fluid velocity within a microfluidic device with a chamber height of approximately one cell diameter is sensitive to seemingly mild sources of perturbation such as temperature, evaporation and mechanical jostling of supply tubing. The resistance of the device is often very high and compliance is low. Proper coupling of the fluidic resistance and capacitance of the input apparatus is necessary for good flow control. Tubing, fittings and syringes that are relatively noncompliant in the macro world must be re-examined for their ability to interface with fluidic channels of sub-nanoliter volumes. To realize the full advantage that microfluidic systems offer in terms of cellular microenvironment control, the driving system should be capable of rapid flow adjustments and switching between different flow sources as well as excellent absolute flow control. We have found that ordinary silicone based tubing and plastic syringes commonly used in the lab are far too compliant to supply microfluidic devices except in cases of steady-flow and slow flow switching. It is also advantageous to have the capability of switching between many

sources of flow in a single experiment without being limited by mechanical or stearic hindrances of large diameter tubing and syringes.

Transit Time

Finally, transit time of reagents from the macro to the micro world becomes an important consideration when conducting cellular experiments inside the microfluidic device. In many cell biology studies it is desirable to introduce agents sequentially such as a primary antibody, secondary antibody and fluorescent marker in an immunofluorescence experiment, or putative agents in a drug discovery screening. When switching from normal media to media containing a bioactive agent, it becomes increasingly important for a rapid effect in the cell chamber as more agents are included in a single experiment. Small volume microfluidic drivers such as the glass syringe/PEEK tube system described here enable the conservation of expensive reagents and reduce the transit time into the chamber containing the cells, which increases data throughput by minimizing the duration of experiments. Indeed, one of the great promises of microfluidic “lab on a chip” technology is high throughput, data-dense studies.

For these reasons we have examined the use of small-volume glass body Hamilton Gastight syringes (Hamilton Company 80920) and polyetheretherketone (PEEK) tubing and fittings (Upchurch Scientific) as flow drivers for microfluidic structures. We developed the techniques described in this technical note for loading cells into microfluidic cell-trapping devices of approximately 100 nanoliter overall volume from the condensed cell pellet. Our goal is to decrease reagent waste, decrease the need to seperate cells from media on-chip, and increase experimental throughput by minimizing delays due to sparseness of cells.

Methods

Primary human T cells were obtained from healthy donors using separation methods described elsewhere[17]. The T cells were stored in liquid nitrogen in aliquots of approximately $1x10^6$ cells per tube. For experiments, the cells were thawed rapidly, washed and re-suspended in RPMI complete media in a 100 ml flat bottom culture flask and maintained at 37°C and 5% CO_2 in an incubator for 4-5 days. During this time, precise volumes of media and cells were removed by sterile pipetting from the culture flask and dispensed into 1.6 ml microcentrifuge tubes. Centrifugation of the microcentrifuge tube at 1000×G for 1 minute caused the formation of a cell pellet near the bottom of the tube. Positioning the PEEK tube end near or within the pellet (see Figure 9) during retraction of the syringe plunger allowed us to harvest cells by gentle aspiration into the PEEK tubing. We routinely use this aspiration method in our laboratory with cell pellets of 10,000 or more suspension or adherent cells of various types and sizes. After aspiration, the end of the PEEK tubing is immediately placed into a pre-punched hole in the PDMS device (see Figure 10). To avoid bubble formation at the junction of the PEEK tubing and the fluid within the microfluidic device, we first make sure the inlet channel to the device in completely filled with media. We then push media through the PEEK tubing using the syring pumps until we observe droplet formation on the end of the tubing. The droplet on the end of the tubing is then joined with the media on the surface the device entrance port to form an air-tight seal around the tubing. The tubing is then

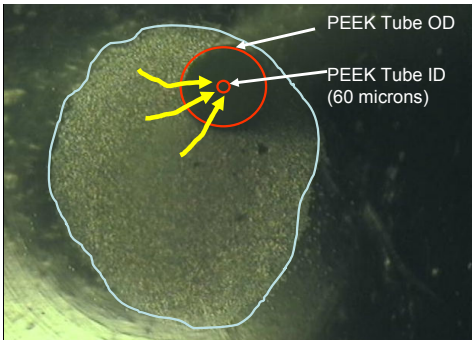

Figure 9. An inverted microscope image of a 500,000 cell pellet in the bottom of a 1.6 ml microcentrifuge tube during aspiration. Red overlay: PEEK tube end, Yellow overlay: Direction of cell motion into tube.

inserted into the channel without having trapped any air in the process which could cause catastrophic issues later in the experiment.

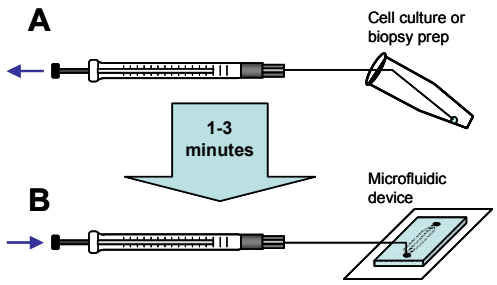

Figure 10. (A) Aspiration of cells from the pellet in a microcentrifuge tube (B) Loading of cells into PDMS microfluidic device using a simple friction-fit coupling between PDMS and PEEK tubing. Normally actuation of the syringe plunger is controlled with a syringe pump.

The entrance port itself is punched with sharpened 0.25 gauge needle stock (McMaster-Carr #75165A686). Typically our PDMS structures are 2-5 mm thick leading to 2-5 mm of contact between the outer surface of the PEEK tube and the inner PDMS surface of the punched hole. We have found this friction fit is more than adequate to support flow rates of 0-3000 nl/min. Due to the low dead volume and low compliance of the system, cells begin appearing in the channels of the device immediately upon coupling of the tube to the device, or at time delays selectable by aspiration of a leading plug of pure media.

To guage the effects of aspiration and residence time in the PEEK tubing on cell viability, controlled studies were performed comparing residence times from 0 minutes (no residence in the PEEK tubing) to 90 minutes. During experiments, great effort is taken to keep cell residence time within the tubing to a minimum and typically does not exceed 15 minutes. As shown in Figure 4, no appreciable decrease in cell viability was noted in samples that were resident in the tubing up to 30 minutes. Furthermore, long-term experiments performed using cells transferred to devices using this method reveal that both Jurkat and primary CD4+ T cells remain viable for more than 24 hours indicating that PEEK tubing aspiration does not induce apoptosis (data not shown). Taken together this suggests that this aspiration method is well suited for cellular applications.

Discussion

We have loaded microfluidic devices with both adherent and suspension cells using our technique for aspirating cells from the centrifuge pellet. The small-bore, low compliance tubing enables the suction of high cell-fraction media from the pellet and immediate loading into a perfused microfluidic device. We have used this aspiration method with a variety of cells including the Jurkat T cell line, primary T and B cells, dendritic cells and adherent cell lines.

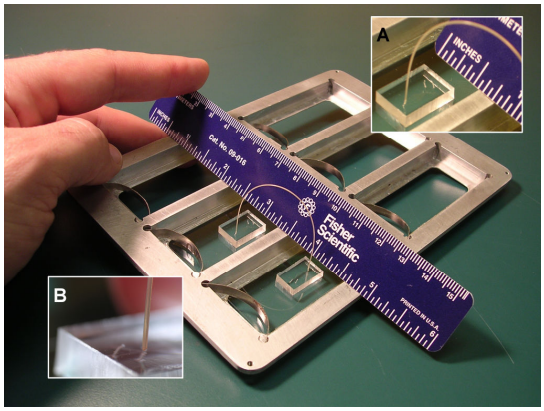

Figure 11. Image of a multi-device stage insert containing two devices interconnected with PEEK tubing. Interconnection volume is approximately 100 nanoliters. Inset A: close-up of device. Inset B: close-up of 300 □m tubing to be inserted into punched hole.

The low compliance PEEK tubing and glass body syringes with syringe pumps allow us to control absolute flow and switch between many flow sources very rapidly with short delays. The small bore of the PEEK tubing and the ease with which it can be cut and bent allow the access to the high density cell centrifugation pellet. Aspiration of cells from the pellet with this setup leads to very rapid transition from cell culture volumes and concentrations to microfluidic volumes and concentrations, with the whole technique being (including centrifugation) accomplished in 3-5 minutes. The small outside diameter and 60 μm inside diameter and the easy deformability of the PEEK tubing allows interconnection of microfluidic devices with the output from one device providing input to a downstream device, etc. (See Figure 11)

Using these methods, we have supplied devices with 3-5 different perfusion sources routinely and can switch rapidly between supplies or any combination or mixture of supplies. We could potentially achieve a dozen or more supply lines in a single device using these small, deformable tubes. Finally, we have extracted cells from microfluidic devices back into the PEEK tubing where they may be re-dispensed into macro cell culture vials for possible long-term traditional culture in incubators.

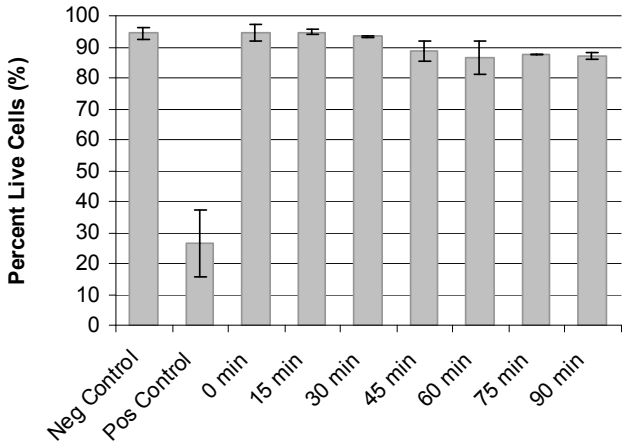

Figure 12. Graph illustrating the percentages of live Jurkat T cells remaining following various lengths of time housed inside PEEK tubing after aspiration from pellet. Negative control samples consist of cells taken straight from cell pellet following centrifugation. Cells were incubated in 70% water/media solution for 5 minutes to obtain positive control viability data. The remaining time points were obtained after allowing aspirated cells to reside within PEEK tubing, then released onto a Petri dish with media containing yopro-1 for imaging. No noticeable decrease in viability occurs prior to 30 minutes while more that 85% of cells remain viable following 90 minute incubation. Error bars indicate +/- one standard deviation.

Conclusions

The methods described here offer four advantages over other methods for conducting cellular studies within microfluidic devices: 1) Small volume flow drivers conserve samples and experiment time; 2) non-compliant drivers lead to fast flow response and rapid switching; 3) small tubing bore and outside diameter facilitates the aspiration of cells from centrifuge pellets; 4) the low expense, small size and deformability of the PEEK tubing facilitates the interfacing of microfluidic devices with many different perfusion sources.

Rigid, low-compliance, low dead volume perfusion systems reduce the time required to set up cell studies in microfluidic devices. Aspiration from the centrifuge pellet as demonstrated here enables

rapid access to sparse cells in macro cell culture dishes. Many independent perfusion mixtures may access the same microfluidic chip and any combination of switching or mixing may be rapidly accomplished during an experiment. Interconnection of separate microfluidic devices is easily achieved with PEEK tubing with very low transit time between devices. Cells that have been studied or treated within he device can also be easily off-loaded from the device and return to conventional cell culture flasks using this system if sterility is maintained throughout the experiment.

Acknowledgments

. This research was supported in part by the Vanderbilt Institute for Integrative Biosystems Research and Education (VIIBRE), the Air Force Office of Sponsored Research (AFOSR) grants FA95500410364 and FA95500510349 as well as NIH grant U01A1061223.

Bibliography

[1] J. M. Ramsey, "The burgeoning power of the shrinking laboratory," *Nature Biotechnology*, vol. 17, no. 11, pp. 1061-1062, 1999.

[2] C. K. Fredrickson and Z. H. Fan, "Macro-to-micro interfaces for microfluidic devices," *Lab on A Chip*, vol. 4, no. 6, pp. 526-533, 2004.

[3] E. Young, *The Penguin Dictionary of Electronics* 2006.

[4] N. H. Bings, C. Wang, C. D. Skinner, C. L. Colyer, P. Thibault, and D. J. Harrison, "Microfluidic devises connected to fused-silica capillaries with minimal dead volume," *Analytical Chemistry*, vol. 71, no. 15, pp. 3292-3296, 1999.

[5] H. Chen, D. Acharya, A. Gajraj, and J. C. Meiners, "Robust interconnects and packaging for microfluidic elastomeric chips," *Analytical Chemistry*, vol. 75, no. 19, pp. 5287-5291, 2003.

[6] Z. H. Fan and D. J. Harrison, "Micromachining of Capillary Electrophoresis Injectors and Separators on Glass Chips and Evaluation of Flow at Capillary Intersections," *Analytical Chemistry*, vol. 66, no. 1, pp. 177-184, 1994.

[7] C. Gonzalez, S. D. Collins, and R. L. Smith, "Fluidic interconnects for modular assembly of chemical microsystems," *Sensors and Actuators B-Chemical*, vol. 49, no. 1-2, pp. 40-45, 1998.

[8] B. L. Gray, D. Jaeggi, N. J. Mourlas, B. P. van Drieenhuizen, K. R. Williams, N. I. Maluf, and G. T. A. Kovacs, "Novel interconnection technologies for integrated microfluidic systems," *Sensors and Actuators A-Physical*, vol. 77, no. 1, pp. 57-65, 1999.

[9] B. L. Gray, S. D. Collins, and R. L. Smith, "Interlocking mechanical and fluidic interconnections for microfluidic circuit boards," *Sensors and Actuators A-Physical*, vol. 112, no. 1, pp. 18-24, 2004.

[10] K. H. Han and A. B. Frazier, "Reliability aspects of packaging and integration technology for microfluidic systems," *Ieee Transactions on Device and Materials Reliability*, vol. 5, no. 3, pp. 452-457, 2005.

[11] J. Liu, C. Hansen, and S. R. Quake, "Solving the "world-to-chip" interface problem with a microfluidic matrix," *Analytical Chemistry*, vol. 75, no. 18, pp. 4718-4723, 2003.

[12] K. W. Oh, C. S. Park, K. Namkoong, J. Kim, K. S. Ock, S. Kim, Y. A. Kim, Y. K. Cho, and C. Ko, "World-to-chip microfluidic interface with built-in valves for multichamber chip-based PCR assays," *Lab on A Chip*, vol. 5, no. 8, pp. 845-850, 2005.

[13] A. V. Pattekar and M. V. Kothare, "Novel microfluidic interconnectors for high temperature and pressure applications," *Journal of Micromechanics and Microengineering*, vol. 13, no. 2, pp. 337-345, 2003.

[14] A. Puntambekar and C. H. Ahn, "Self-aligning microfluidic interconnects for glass- and plastic-based microfluidic systems," *Journal of Micromechanics and Microengineering*, vol. 12, no. 1, pp. 35-40, 2002.

[15] Z. Yang and R. Maeda, "A world-to-chip socket for microfluidic prototype development," *Electrophoresis*, vol. 23, no. 20, pp. 3474-3478, 2002.

[16] R. Freshney, *Culture of Animal Cells: A Manual of Basic Technique, 4th Edition* Wiley-Liss, 2000.

[17] D. Unutmaz, V. N. KewalRamani, S. Marmon, and D. R. Littman, "Cytokine signals are sufficient for HIV-1 infection of resting human T lymphocytes," *Journal of Experimental Medicine*, vol. 189, no. 11, pp. 1735-1746, 1999.

CHAPTER III

MICROFLUIDIC PLATFORM FOR REAL-TIME SIGNALING ANALYSIS OF MULTIPLE SINGLE T CELLS IN PARALLEL

Abstract

T cells are a vital component of the adaptive immune response in humans. Understanding the signaling events that determine reaction versus anergy in these cells is critical in developing successful methods of diagnosis, treatment, and prevention of disease. Studying single cell dynamics over time reveals rare events that might be averaged out in bulk experiments, but these less common events are undoubtedly important for an integrated understanding of a cellular response to its microenvironment The nanophysiometer is a self-contained unit fabricated of optically transparent, bio-inert PDMS on glass and designed to maintain non-adherent cells in a microfluidic environment. In this report we validate the microfluidic nanophysiometer as a platform to facilitate the study and manipulation of multiple single T cells in parallel. As T cells are injected into the cell culture media perfusing the nanophysiometer, they are passively trapped in one of 550 18 μm$\times$18μm$\times$10μm PDMS, bucket-like structures as they pass through the cell trap region. Cell viability analysis revealed that at flow rates of 100 nl/min, more than 70% of CD4+ T cells, held in place using only hydrodynamic forces, remained viable following 24 hours in the nanophysiometer. We then demonstrate the ability to activate T cells within the nanophysimeter using chemical, antibody, and cellular forms of sitmulation. Cytosolic calcium transients were recorded for each form of stimulation. Statistical analysis of T cells from a single stimulation experiment reveal the power of this platform to distinguish different calcium response patterns, an ability that might be utilized to characterize T cell signaling states in a given population.

Introduction

T cells play a central role in cellular mediated adaptive immune responses as they are highly involved in recognizing and responding to foreign/dangerous antigens. Hence, deciphering the signaling pathways governing T cells in activity is of utmost importance understanding the adaptive immune response as a whole. While the intracellular signaling pathways the govern T cell response are some of the most intensely studied, the intricacies of many signaling mechanisms remain unclear. Conventional cell culture methodologies involve analyzing bulk responses from million of T cells which may average out key, rare signaling events important in the progression of a successful immune response[1]. Fluorescence activated cell sorting (FACs) yields single cell data, but cannot provide information on the temporal cellular signaling dynamics[2]. In order to reliably monitor single T cells over time in cell culture dishes, antibodies or other adhesive proteins are required to tether the cells to the surface. This, of course, result in the initiation of unwanted intracellular signaling cascades that alter the signaling state of the cells. Thus, there is a need for a new type of experimental methodology that facilitates the analysis time-resolved signaling dynamics in individual T cells.

The utilization of microfluidic devices for cellular applications has exploded over the past 10 years with the promise of lower production and reagent cost, tighter control of experimental paramenters, and quicker reaction times along with reduced diffusion times compared to traditional cell culture techniques[1;3;4]. The latter point opens the possibility of interrogating cellular activities that occur in time scales to quick to observe with conventional techniques[5]. Flexible and relatively easy fabrication allows incorporation of more complicated microfluidic designs including valves, pumps, and switches which enhance the manipulative ability of the cellular micro-environment[6-8]. Furthermore, culturing cells in a constant flow-thru environment is arguably more physiologically relevant than maintaining cells in a relatively large, stagnant pool of media as done in conventional cell culture.

The ability to maintain mammalian cells for extended periods of time has been demonstrated in adherent cell lines[9-11]. Cells readily adhere to the glass surface (sometimes functionalized to promote adhesion) and are able to be studied individually or en mass. When working with suspension cells, however, the same adhesion problem that plagues traditional cell culture methods is true for microfluidics as well; methods to adhere cells to a surface (antibodies or adhesion proteins) will induce undesired intracellular signaling pathways that alter the state of the cell.

One solution to this problem is to use suction to hold a cell in a “trap”, which has been demonstrated to be very effective with cardiac myocytes[12-14]. However, T cells, one of the main focuses of this research, are extremely small compared to cardiac myocytes with diameters of naïve T cells ranging between 5-7 μm. The diameter of the suction channels would ideally be much smaller than the diameter of the cell, but this aspect ratio is nearing the resolution limit for out current fabrication facilities. Furthermore, T cells are highly deformable and sensitive to pressure. Suction easily lyses these cells and those that remain intact are destined for apoptosis. Thus, for analysis of T cells, it is essential to have a passive trapping process.

A truly passive trapping mechanism was developed by Wheeler et al[15]. A clever device design incorporating on-chip valves allowed high precision control of fluid flow such that individual T cells could be directed into a bucket-shaped chamber. Once trapped, the intricate hydrodynamic controls allowed the cell to be directly addressable by dyes, stimulants, or lysing agents. However, the design was arranged such that only a single cell was trapped and interrogated during a single experiment. This is highly inefficient for collecting information concerning a population of T cells. To maximize the quantity and quality of data extracted from a given experiment, it is desirable to have many (hundreds to thousands) individually trapped

and fluidically addressable T cells within a single microfluidic platform. To our knowledge, such a platform for analysis of T cells does not yet exist.

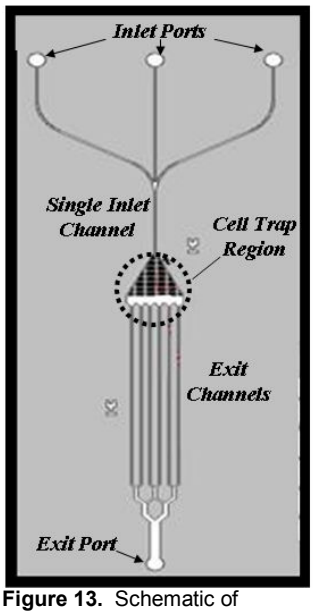

Figure 13. Schematic of microfluidic nanophysiometer. The device is constructed of PDMS and plasma-bonded to a glass coverslip

. As such, we herein report the development and validation of a novel microfluidic platform, the multi-trap nanophysiometer, which addresses these needs. We demonstrate the ability to utilize this platform passively capture primary CD4+ T cells (TCs) using only hydrodynamic forces as well as maintain the cells within the microfluidic the device for more than 24 hours. Furthermore, we show that in this microfluidic environment we are able to stimulate calcium signaling in TCs using chemical, antibody, and cellular methods. Data collection and analysis can be completely automated to sort the resulting calcium traces. The multi-trap nanophysiometer enables the analysis and classification of individual cells based on their dynamic, phenotypic response to stimuli, and requires the use of tiny sample volume, such as might be obtained by a finger stick blood sample, and thus must be considered as a complementary technology to flow cytometry.

A schematic of the microfluidic multi-trap nanophysiometer is shown in **Figure 1**. This platform is a self-contained unit fabricated of optically transparent, bio-inert PDMS on glass and designed to maintain non-adherent cells in a microfluidic environment. Cells are introduced into one of the inlet ports using computer-controlled micro-syringe pumps[16]. As cells flow through the trap region, cells are passively trapped in one of 440 18 $\mu m \times 18\ \mu m \times 10\ \mu m$ PDMS, bucket-like structures (see **Figure 2** for close-up view of cell traps). Fluid flow rate is optimized such that cells remain in traps and receive necessary nutrients while shear stress and waste accumulation are minimized. This provides a method of quickly sequestering cells into individually addressable compartments without using any type of adhesive agents, such as the

normally used cell surface antibodies, poly-l-lysine, or fibronectin, which can themselves induce unwanted intracellular signaling cascades. Furthermore, only relatively small quantities of cells (aliquots as small as 1000 cells), media (~100s of microliters for long-term experiments), and other reagents are required to obtain data on hundreds of single cells in parallel, resulting in decreased labor and material costs. The small size of the device decreases the time required to scan the entire cell trap region during automated, high-magnification microscopy.

Materials & Methods

Experimental Setup

All experiments were performed using an Axiovert 200 microscope (Carl Zeiss), which was equipped to facilitate long-term maintenance of cells during experiments, as shown in **Figure 2**. A plexiglass incubator enclosed the microscope such that the temperature was consistently maintained at 37^{o}C. The multitrap nanophysiometer chip was enclosed within a petri dish (Fisher Scientific, Hampton NH) with holes machined in the bottom to allow microscope viewing, as well as slots in the top for polyethyletylketone (PEEK) tubing passage. In addition, a port was drilled in the side of the dish to allow tubing connected to a gas supply such that a constant flow of 5% CO_2 and 95% air was delivered to the petri dish.

To minimize evaporation, 3 to 4 layers of filter paper (Whatman, Florham Park NJ) saturated with distilled H_20 surrounded the device inside the petri dish. The motorized microscope stage, image acquisition, focus, and filter settings were controlled using Metamorph software (Molecular Devices, Downington PA). Syringe pump flow rates were also under computer control, utilizing software developed by VIIBRE researchers. Images were obtained with the electrically cooled CoolSNAP HQ CCD camera (Photometrics, Tucson AZ).

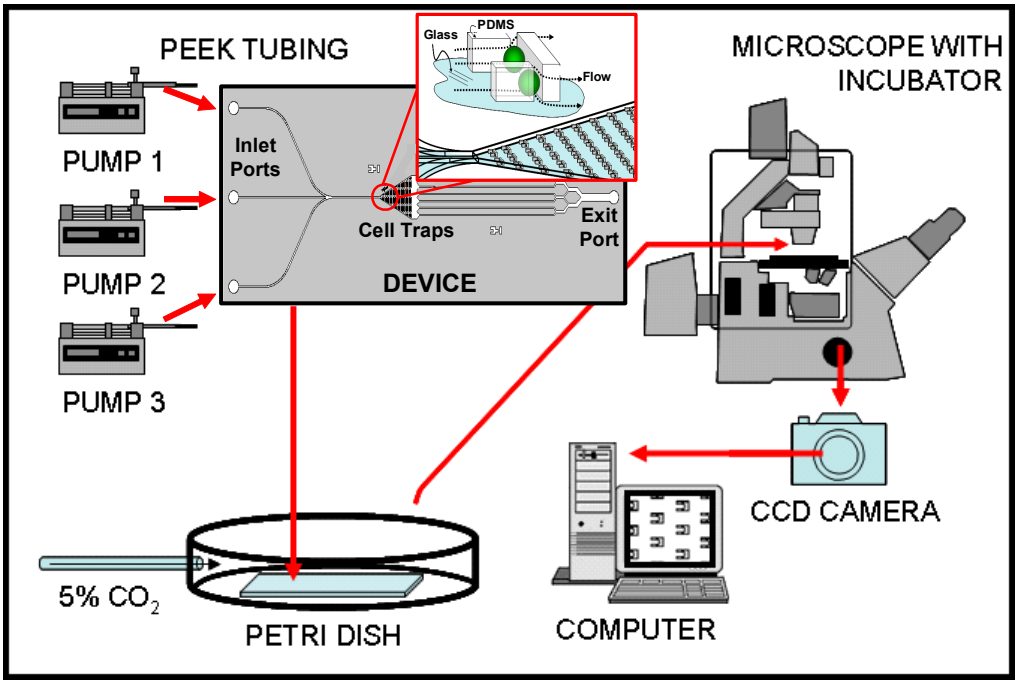

Figure 14. Schematic illustrating the standard experimental setup for the multi-trap nanophysiometer.

Cell Culture

Primary human CD4+ T cells and dendritic cells (derived from human monocytes) were generously provided by the lab of Derya Unutmaz following isolation and purification from human blood donors [17]. Primary CD4+ T cells were thawed from liquid nitrogen aliquots (5×10^5 cells/vial) 24 hours prior to use and cultured using sterile technique in RPMI 1640 cell culture media (ATCC, Manassas VA) supplemented with 10% fetal bovine serum (ATCC, Manassas VA) and 10μg/ml Ciprofloxacin (Mediatech, Herndon VA). Dendritic cells were derived by incubating primary human CD14+ monocytes with 20 ng/ml IL-4 and 100 ng/ml GM-CSF for 4-6 days [17;18]. Mature dendritic cells were generated following 24-hour incubation with 10 ng/ml LPS [17;18]. All cells were incubated in a sterile environment maintained at 37°C, complete with 5% CO_2 and 95% humidity.

Microfluidic Cell Loading

Cell loading followed methods developed by our lab and described in greater detail in a previous publication [16]. Cells were centrifuged to a pellet at 5000 rpm for 1 minute in a 1.5 ml eppendorf tube (Fisher Scientific, Hampton NH) which were then mounted on a glass slide with cellophane tape for microscope viewing. Once the pellet was located using the microscope, 50 μm I.D. PEEK tubing (Upchurch, Oak Harbor WA), connected to 50 μl gas-tight syringe mounted on a computer-controlled syringe pump (Harvard Apparatus, Holliston MA), was guided to the cell pellet. Cells were then aspirated directly into the PEEK tubing using the syringe pump set to withdraw fluid at a flow-rate of 0.5 μl/min.

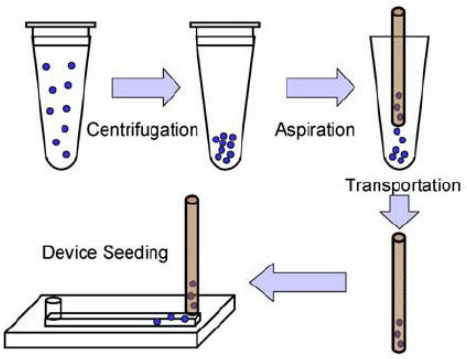

Figure 15. Macro cell culture to micro cell culture in microfluidic devices. Use of ultra small bore tubing to aspirate controllable volumes of high cell-density and seed into device.

The tubing was then inserted to a loading channel of a device pre-cleared with sterile media. This cell loading procedure is illustrated in **Figure 3**. Once all inputs were connected to the device, the pump controlling the cell channel was set to a forward flow rate of 100 nl/min for passive loading of cells into the traps as they traverse the device. Unless otherwise noted, the media used to perfuse the device and the cells contained within consisted of RPMI 1640 supplemented with 10% FBS and 10 μg/ml ciprofloxacin.

Cell Viability Assay

Approximately 5×10^4 primary human CD4+ T cells were loaded with a cytosolic calcium indicator dye by incubating the cells in a solution of 5 μM rhod-2 AM (Invitrogen, Carlsbad CA) for 30 minutes at 37°C. Cells were then loaded into the microfluidic device as described previously. The perfusing media was supplemented with 1.8 mM $CaCl_2$ (Sigma, St. Louis MO) to mimic normal *in vivo* calcium levels [19]. A second syringe was prepared containing normal cell culture media supplemented with 1 nM Yopro-1 viability indicator (Invitrogen, Carlsbad CA). Using Metamorph software, the microscope was programmed to obtain DIC (bright field), FITC (Yopro-1), and TRITC (rhod-2) images for 5 fields of view spanning the cell trap region every 30 minutes for 24 hours. Pump control software generated by VIIBRE researchers was implemented to switch from the perfusing media to media containing Yopro-1 every 2 hours for 5 minutes. Unless otherwise noted, the flow rate was maintained at 100 nl/min.

Cytosolic Calcium Assay

Release of intracellular calcium stores, an early signaling event in T cell activation, was induced chemically, with antibody-coated beads, or by co-incubation with antigen-presenting cells. In all cases, naïve primary CD4+ T cells were first loaded with rhod-2 calcium indicator by incubation in a 5 μM solution for 30 minutes at 37°C. Cells were then loaded into a microfluidic

device (pre-cleared with media to remove air bubbles) and perfused with normal culture media supplemented with 1.8 mM $CaCl_2$. Using Metamorph software, the microsope was programmed to obtain baseline bright field (DIC or phase-contrast) and TRITC (rhod-2 fluorescence) images for 4 to 5 fields of view (FOV) spanning the entire cell trap region of the microfluidic device every 30 seconds.

Chemical Stimulation. A solution consisting of plain culture media supplemented with 1.8 mM $CaCl_2$, 20 ng/ml IL-2, and 8 μM ionomycin, a known calcium ionophore [20], was introduced into an adjacent entrance port. Calcium release from the T cell endoplasmic reticulum was stimulated chemically upon switching perfusate flow completely to the media containing ionomycin.

Bead Stimulation. Protein A coated microspheres (Bangs Laboratories, Fishers IN) were conjugated to anti-CD3 and anti-CD28 antibodies (R & D Systems, Minneapolis MN). Antibody-conjugated beads were loaded in the same manner as cells (aspiration from a centrifuged pellet) and introduced into the device directly following cell trapping. Image acquisition was begun upon bead introduction and continued for the duration of the experiments as described above.

APC Stimulation. Lipopolysaccharide (LPS), a protein found in the membrane of gram-negative bacteria, was used to promote maturation of primary human dendritic cells (DCs) obtained from the Unutmaz lab. Prior to loading, the DCs were made immunogenic by incubation with 5 μg/ml staphylococcal enterotoxin B (SEB), a superantigen that binds to the outer portion of the major histocomplatibility complex (MHC) yielding immunogenic DCs, for thirty minutes at 37°C. DCs were then rinsed with fresh media to remove all unbound SEB. The resuspended cells were then centrifuged to a pellet for cell loading as described above. TCs were trapped first, and then DCs were introduced to the devices. Image acquisition began upon introduction of DCs.

Image Storage and Analysis

Due to the large quantity of potential information that can be extracted from a single experiment when monitoring hundreds of cells with a variety of fluorescent markers over an extended period of time, it was both desirable and necessary to develop an automated analysis program. Metamorph was used to collect images and store them in a stacked format to the hard drive. Analysis of image data was done primarily using Wright Cell Imaging Facility ImageJ bundle and Microsoft Excel along with custom written macros. First, phase contrast and fluorescence images obtained at a single time point are aligned and re-indexed using a modified routine written by Phillippe Thevanez. This algorithm calculates the X and Y translation of each phase contrast (bright field) image relative to a reference image of the same series and saved the data to a file. The resulting translations were applied to the phase contrast and fluorescent images together to ensure proper alignment between each image at a given time point was maintained. The particle analyzer routines embedded with the WCIF ImageJ bundle were used to find the positions of cells in the resulting images, and the mean gray values at these positions were recorded to file.

Microsoft Excel macros were used to segment the data files into trap regions based on the XY positions recorded by the ImageJ particle analyzer. A typical field of view contains up to 85 traps and each trap contains a number of cells to be determined. Segmentation into trap regions requires input regarding the total offset of the image since all the microfluidic traps are spaced very precisely. Segmentation of individual trap zones into individual cells is more complex. Briefly, the first slice which occurred that contained the maximum number (N_{max}) of putative cells for the time series was selected as a cardinal slice. The positions of each of the cells were stored in a 2 x N_{max} array. Every time point is then sequentially compared to the cardinal time point, and the XY positions of the cardinal time point are updated and replaced by the XY positions of each time point weighted by observation. In this way, if a cell is repeatedly

found near one particular position (even if it is not found in the cardinal slice) it is weighted heavily as a probable cell position in the final analysis. Similarly, if a spurious cell or debris is located at a single time point it is weighted less heavily and is less likely to appear in the final analysis. Fluorescence intensities of cells found using this algorithm were automatically plotted out in Excel for further analysis.

Cluster Analysis of Calcium Data

The extracted tracings were automatically sorted or clustered into groups by their responses to a given stimulus. Cluster analysis, or unsupervised learning, is a set of statistical methods used to identify meaningful or informative subgroups within a dataset. For this study, we used hierarchical clustering to identify scales of similarity between T-cells and groups of T-cells. A distance metric must be specified to measure the pair-wise similarity between T-cells. Each cell's time-series is treated as a vector in a multi-dimensional space, and for this study we used the Pearson correlation metric, which is well-suited for measuring differences in shape between two curves.

The clustering algorithm works by creating a pair-wise distance matrix between all cells and creating a cluster by merging the pair of cells with the smallest separating distance. A new distance matrix then is created with the unclustered cells and the merged cells, and the process is repeated. The location of the merged cluster can be defined in different ways, among them: single linkage, complete linkage, and average linkage (the average of the cell vectors). We use complete linkage, though all methods give similar clusters.

Results & Discussion

Device Characterization

Before utilizing the microfluidic device for cellular assays, we evaluated the characteristic flow profiles within the device and the device's cell trapping ability. To visualize the perfusion dynamics within the nanophysiometer, alternating aliquots of fluoroscein and water were passed through the device at various flow rates. Results of this experiment are shown in **Figure 4**. **Figure 4A** illustrates the flow profile of a bolus of fluoroscein through the cell trap region of the nanophysiometer at 50, 100, and 250 nl/min (a, b, and c, respectively). The entire trap region is accessed by the dye within 45 seconds of starting the syringe pumps. **Figure 4B** quantitatively describes the fluorescent images by showing the fluorescence intensity versus time for fixed points in the front, middle, and back of the trap region (P1, P2, and P3, respectively). Finally, **Figure 4C** shows a series of images obtained of a single cell trap during the cell loading process. In this trap, six cells were captured within one minute of cell introduction. With our current cell loading techniques and tight flow control, the trapping efficiency (# traps containing cells/ # traps) of these microfluidic devices approaches 100% in each experiment. Because so few cells are used to load the devices (as little as 1000 cells), this platform offers a unique and highly economic option for studying rare or costly cell types.

The triangular shape of the cell trap region was designed such that the behaviors of cells not exposed to cell secretions (cells trapped nearest the inlet) can be compared to those trapped nearest the exit, which are exposed to all the secretions of cells trapped upstream. This difference in local environment can be a very useful tool in studying intercellular signaling events which are extremely important to immune cell signaling. T cells are known to employ both autocrine and paracrine signaling, such as in IL2 production, in the earliest stages of activation [21-23]. Furthermore, Th1/Th2 differentiation is highly dependant on the cytokine and chemokine gradients existing in the local surroundings[24-28]. These are only two of many examples in which intercellular signals are important in development of immune response. Both the shape and the small volume (~ 25 nl) of the device allows these signals to be studied in real-time and without fear of dilution. In fact, cells downstream may suffer from accumulation of signaling agents as well as waste products. This too is important information with regards to understanding immune cell function as the mechanisms that govern T cell anergy and apoptosis are of great interest to the medical community [29-32]. In a single experiment it is possible to obtain information on cells exposed to an entire spectrum of cellular products concentrations.

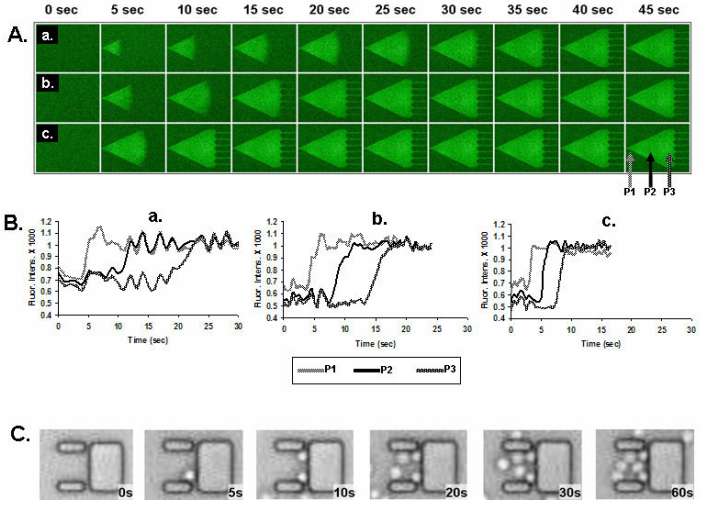

Figure 16. Perfusion dynamics and cell loading characteristics of the microfluidic nanophysiometer. (A)Time response and perfusion dynamics of the nanophysiometer at (a) 50 nl/min, (b) 100 nl/min, and (c) 250 nl/min. (B) Graphs illustrate the fluorescence versus time at points P1, P2 and P3 (shown in the lower right hand corner of A). All traps are accessible via flow switching with similar time-responses at flow rates above 50 nl/min. (C) A single representative cell trap within the nanophysiometer during cell loading. Trapping efficiency (# of traps containing cells/# of traps) approaches 100% within minutes of introducing cells.

Cell Environment and Viability

In order to reliably utilize the nanophysiometer for cellular assays it is important to first validate that T cells are stably

maintained within the microfluidic device over time as they are in traditional cell culture

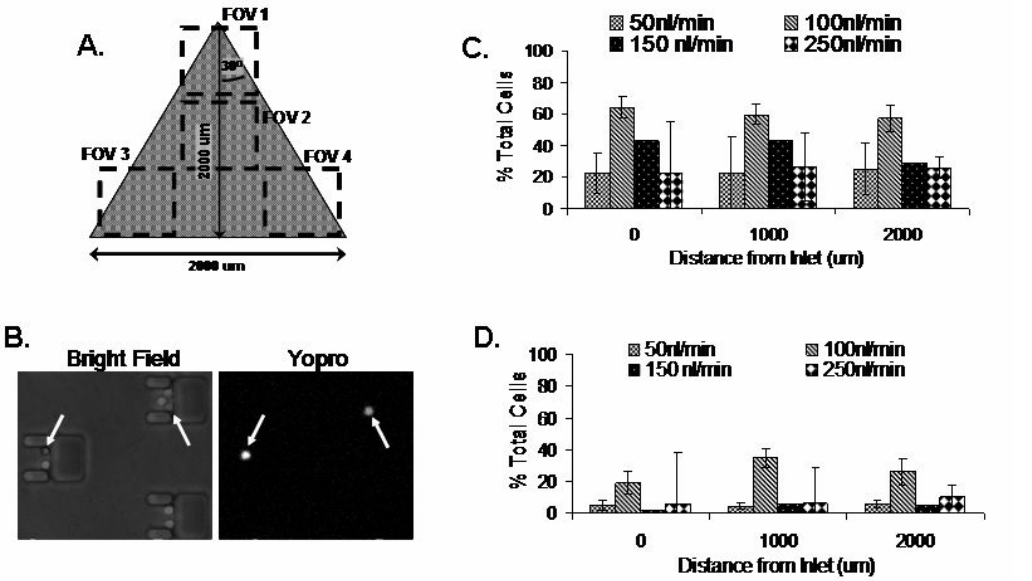

Figure 17. Cell viability analysis within the microfluidic nanophysiometer. (A) Schematic illustrating the four fields of view that were imaged every 20 minutes. (B) An example of images obtained during the viability experiments. Cells exhibiting fluorescence due to yopro-1 staining are dead. (C) Viability as measured by percentage of cells alive after 24 hours with respect to both flow rate and position within the device. (D) Cellular activity as measured as percentage of cells that respond to ionomycin exposure with a measurable cytosolic calcium transient following 24 hours within the device. Results are shown with respect to both flow rate and position within the device.

environments. The rates of perfusion, consumption of nutrients, and production of waste products all affect the viability of cells within the device as well as their ability to respond to stimuli. The following experiments investigate cellular viability and ability to react to ionomycin stimulation with respect to perfusion flow rate.

Since secretion of IL2 and expression of IL2Rα require up to 24 hours following T cell activation, both viability and activity (the ability to elicit a measurable calcium transient in response to ionomycin exposure) measurements were analyzed following 24 hours of incubation within the nanophysiometer. . Cell viability was assessed using Yopro-1, a dye that fluoresces upon interaction with nucleic acids, which was transiently exposed to the cells every two hours. Cell activity, the ability of the T cells to respond to ionomycin stimulation with a measurable cytosolic calcium transient, was tested at the conclusion of the 24 hour experiment by perifusing the device with media containing ionomycin.

Results from the viability experiments are shown in **Figure 5**. Four pump flow rates were evaluated and it was determined that 100 nl/min is optimal for promoting long-term cell viability with nearly 70% of cells alive after 24 hours. This flow rate was also best in terms of cellular activity measurements, with approximately 40% of cells exhibiting a measurable calcium response upon exposure to ionomycin after 24 hours. It is unknown whether this indicates that the inactive cell population (cells not responding to ionomycin) that were counted as viable (i.e. not stained with yopro-1) were in fact in a quiescent state or perhaps the early stages of apoptosis. We are currently developing mathematical models describing fluid dynamics within the device as well as cellular metabolism to aid in predicting cell viability and activity such that we may optimize nutrients, flow rate, temperature, etc. in order to increase the activity of cells during long term maintenance within the microfluidic device. This will be of great importance for long-term activation studies monitoring late indicators of activation such as IL-2 secretion or IL2Rα expression. Activation studies focusing on calcium response, however, involve relatively short duration experiments as calcium release from intracellular stores typically occurs within seconds of proper stimulation. Short duration experiments are extremely well tolerated by cells with greater than 90% remaining viable for up to 12 hours with pump flow rates set to 100 nl/min.

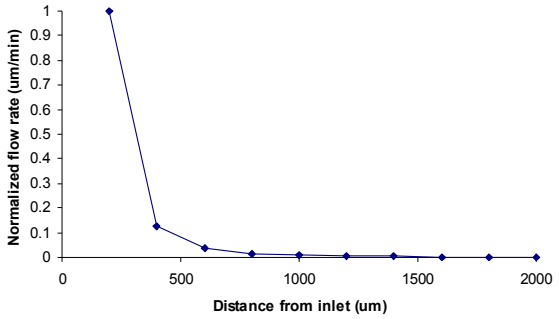

Figure 18. Graph of the predicted decrease in flow rate from inlet to exit of the nanophysiometer cell trap region. Note that cells in the back of the device experience flow rates an order of magnitude less than those close to the inlet.

The triangular shape of the nanophysiometer results in a decrease in linear flow velocity as the media traverses the cell trap region. **Figure 6** shows the predicted decrease in flow velocity with respect to distance from the cell trap region inlet. At low flow rates, cells nearest the inlet survived better than those farthest from inlet. We hypothesize that this was due to the fact, compared to cells near the exit, that the cells in the front of the device had access to

adequate nutrients from the media along with a quicker fluid volume turnover rate which facilitated the removal of waste products. Accordingly, the cells in the back of the device were exposed to media not only depleted of nutrients, but also carrying a larger concentration of cellular wastes. The accumulation of cellular waste increases the acidity of the media, which is known to cause T cells to become inactive and/or enter apoptosis[33;34]. Cells in general fared less well at lower flow rates due the depletion of nutrients by the cells near the inlet, compounded by the exposure to cellular waste. Increasing the media flow rate to 100 nl/min increased cell survival by more than three times that found at 50 nl/min (Figure 4C). At this flow rate, the cells throughout the device are exposed to a nutrient/waste concentration ratio that is more compatible for long-term survival. Interestingly, increasing the flow rate to 150 nl/min and 250 nl/min caused a decrease in cell viability. In addition to taking care to optimize the waste/nutrient ratio cells are exposed to, there is also a factor of shear force impinged on the cells by the fluid flow that can also effect viability. We hypothesize that at the higher flow rates, cell death was associated with too high a shear force, resulting in either cell lysis or apoptosis. This is supported by the observation that the cells exposed to these flow rates died very quickly (within the first few hours, data not shown) of the experiments and the cells near the inlet of the device died more quickly than those in the back of the cell trap region.

While 100 nl/min was still the optimal flow rate for cell activity, the percentage of cells responding to the ionomycin challenge approached only 40% (**Figure 5D**).

Cytosolic Calcium Assay

Once we demonstrated that the primary CD4+ T cells could be trapped and maintained within the nanophysiometer, we then proceeded to demonstrate that we could activate the primary T cells within the device. We employed three methods of activation: chemical stimulation with ionomycin, antibody stimulation with anti-CD3- and anti-CD28-coated microspheres, and cellular stimulation using SEB-pulsed, LPS matured, primary human

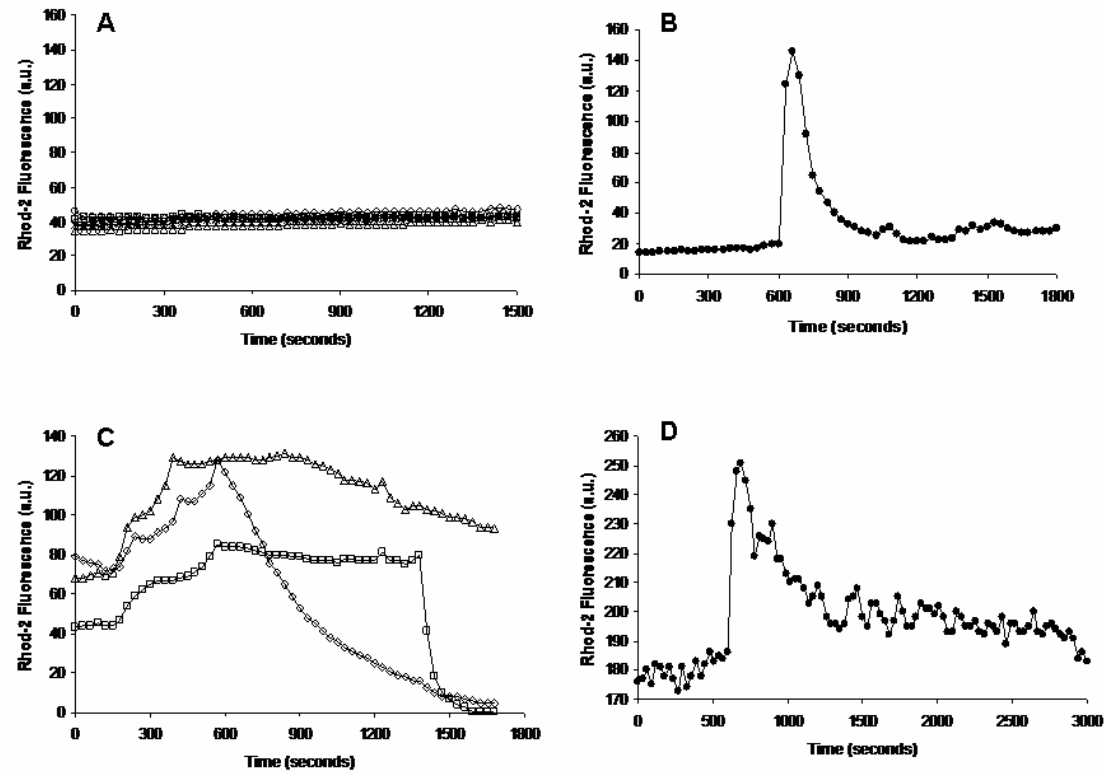

Figure 19. Examples of cyctosolic calcium transients, as indicated via rhod-2 calcium dye, in single primary T cells exposed to (A) plain media, (B) antibody-coated microspheres, (C) ionomycin, and (D) mature, stimulated dendritic cells. Each trace represents a single cell. Three traces are shown in (C) to illustrate the three typical calcium transient patterns observed when stimulating T cells with ionomycin.

dendritic cells. Quantitative results of these experiments are shown in **Figure 7**. In each case we were successful in activating the primary CD4+ T cells as illustrated by the cytosolic calcium transients observed using rhod-2 AM Ester calcium indicator.

The results of the control experiment shown in **Figure 7A** clearly show that rhod-2 loaded cells did not exhibit any cyctosolic calcium increases when exposed to plain media. Introduction of antibody-coated beads (**Figure 7B**), ionomycin (**Figure 7C**), and mature dendritic cells (**Figure 7D**) all resulted in strong calcium responses. The cyctosolic calcium transients induced by antibody-coated beads and dendritic cells are consistent with traces found in literature [35;36].

Ionomycin stimulation of T cells resulted in calcium transients whose shape and duration differed from more physiologic forms of stimulation. This illustrates a key strength of the nanophysiometer platform in that we were able to observe the individual cell responses to

the ionomycin from nearly 800 cells and clearly identify three distinct populations of responses in a single experiment (as shown in representative curves in **Figure 7C**). Automated ImageJ and Excel routines were used to analyze fluorescence images of T cells challenged with ionomycin. The analysis found 809 raw fluorescence traces which included 69 duplicates, 195 truncated curves with insufficient data and 88 flat-lines or unresponsive traces found by calculation of the data trend. There were 457 unique traces for use with automated clustering analysis, the results of which are illustrated in **Figure 8**. A dendrogram plot (**Figure 8**, left) illustrates the distinct clusters of T cells comprising the range of calcium responses to ionomycin as determined by the clustering algorithm. The horizontal axis measures the dissimilarity between cells and clusters of cells. The vertical lines in the diagram tell you the distance between the clusters connected by the tree's horizontal lines. By inspection of the dendrogram in **Figure 8** one can see that there are three major subgroups of cellular calcium responses to ionomycin. In cluster profiles graphic (**Figure 8**, right), we plot the individual time-series profiles for each of the 457 T cell responses with respect to the group with which they are clustered. The distinguishing feature of these subgroups is the fall-time, or time it takes the intensity to return to baseline following the initial intensity rise following exposure to ionomycin, Cluster A is comprised of T cells exhibiting a marked increase in fluorescence upon ionomycin exposure followed by a sharp drop in fluorescence that falls to below initial baseline fluorescence levels, often within a single data point (30 seconds). Cells within cluster B respond to ionomycin with a similar increase in fluorescence intensity, but both the time spent at peak fluorescence intensity ans the time required to return to baseline intensity levels are extended. Finally, cells in cluster C exhibit an increase in fluorescence intensity, but remain at the peak intensity for the duration of the experiment. We theorize that the cells in cluster A are undergoing non-apoptotic cell death because of the dramatic and often complete loss of fluorescence signal. This is perhaps in response to the environmental stress, ionomycin exposure, or combination thereof. Based upon more physiologic types of stimulation, we expect that the initial increase in fluorescence

induced by ionomycin to be transient in nature with intensities returning to baseline levels as in cluster B. It is possible that the fall time of the fluorescent signal in cluster C is longer than the

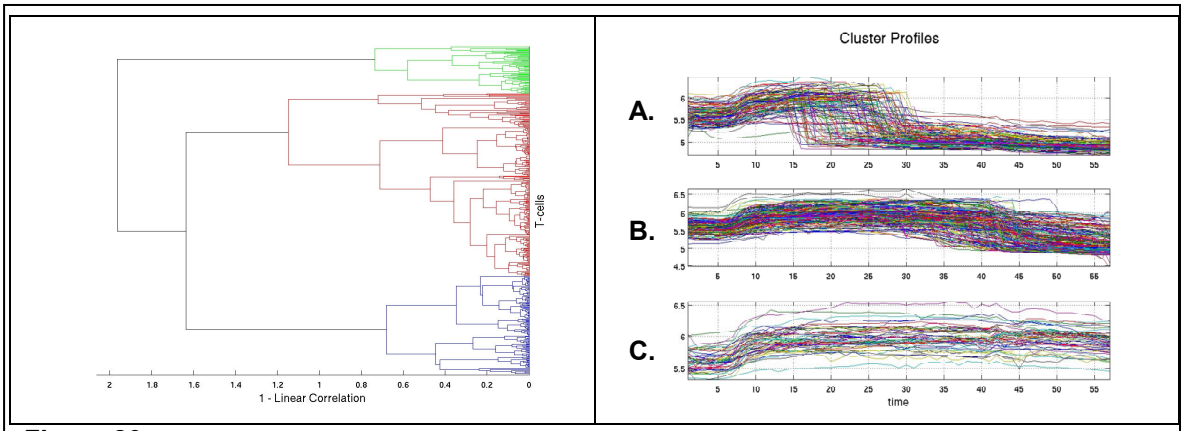

Figure 20. Clustering analysis results of calcium response from ionomysin stimulated T cells within the nanophysiometer. Left: Dendrogram representing the distance in N-dimensional space between green, red and blue type curves, where N is the number of time points. Right: Profiles of the green, red and blue subgroups top, middle and bottom, respectively.

duration of the experiment and that intensity levels would eventually return to baseline. While the exact biological mechanisms resulting in these distinct clusters of response are presently unknown, the ability to tease out such information within a single experiment is a major testament to the usefulness of this platform for the application to cellular signaling analysis. Cell to cell variations, even in specific subsets such as theses CD4+ T cells, can have a large impact upon their response to a given stimuli. This data both illustrates the value and importance of single cell data in combination with bulk analysis as well as highlights the utility of the multi-trap nanophysiometer as it yields valuable statistical information in a minimal amount of time from hundreds of single cells in parallel, including their temporal activation dynamics.

In addition to single cell analysis, another key strength of this platform is the ability to study cell-cell interaction as well. As shown in **Figure 7D** dendritic cell stimulation resulted in measurable pulsing of calcium transients within the T cell as the two cells interacted within the device.

An example of dendritic cell/ T cell interaction is shown in **Figure 9**. Current immunological methods for studying the immune synapse consist of large media:cell volume ratios. One must simply wait for 2 cells to diffuse through the media and find each other in order to extract information about the interaction. Other methods include adhering cells in place using antibody- or fibronectin-covered dishes. This not only reduces time to contact for two cells, but also triggers internal signaling cascades caused by the antibody/fibronectin binding, making the interpretation of data more difficult. The multi-trap nanophysiometer easily traps multiple types of cells passively, quickly, and much more predictably than current methods. This ability alone has the potential for a significant impact on the approach of many immunological studies, since a complete immune response depends heavily on cell-cell interactions.

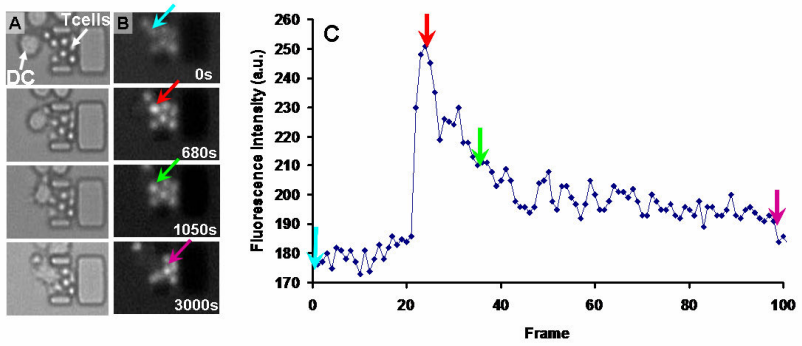

Figure 21. Primary human dendritic cells (DCs), preactivated with LPS and SEB, were trapped with naïve primary human CD4+ T cells preloaded with rhod-2 calcium indicator in the nanophysiometer. Bright field (A) and rhod-2 fluorescence (B) images were obtained every 30 seconds. As shown in graph (C), cytosolic calcium transients were observed in T cells that were in direct contact with DCs, consistent with the early stages of T cell activation and the initiation of the immune synapse.

Conclusions

The nanophysiometer is a unique and powerful microfluidic platform for the study of signaling dynamics in hundreds-to-thousands of single cells in parallel from very small samples. In this respect it is considered complimentary to flow cytometry since the dynamic responses of individual cells to stimuli can be recorded and used to discover phenotypic subtypes. In this report, we demonstrated its ability to passively trap non-adherent, primary CD4+ T cells, taken from samples consisting of less than 50,000 cells, and maintain them such that nearly 70%

remained viable after 24 hours. Furthermore, we successfully induced cytosolic calcium transients in trapped T cells using chemical, antibody, and cellular stimuli.

Acknowledgements

The authors wish to thank Derya Unutmaz and Michelle Tseng for providing the primary cells as well as their invaluable assistance and advice on cell culture. In addition, we would like to thank Walter Georgescu for the use of the pump controller program written by him. Thanks to E. Duco Jansen for the use of cell culture facilities and to Allison Price for her generous help with this manuscript. This research was supported in part by the Vanderbilt Institute for Integrative Biosystems Research and Education (VIIBRE), the Air Force Office of Sponsored Research (AFOSR) grants FA95500410364 and FA95500510349 as well as NIH grant U01A1061223.

Bibliography

[1] J. P. Wikswo, A. Prokop, F. Baudenbacher, D. Cliffel, B. Csukas, and M. Velkovsky, "Engineering challenges of BioNEMS: the integration of microfluidics, micro- and nanodevices, models and external control for systems biology," *IEE. Proc. Nanobiotechnol.*, vol. 153, no. 4, pp. 81-101, Aug.2006.

[2] K. Sachs, O. Perez, D. Pe'er, D. A. Lauffenburger, and G. P. Nolan, "Causal protein-signaling networks derived from multiparameter single-cell data," *Science*, vol. 308, no. 5721, pp. 523-529, Apr.2005.

[3] P. Mitchell, "Microfluidics--downsizing large-scale biology," *Nat Biotechnol.*, vol. 19, no. 8, pp. 717-721, Aug.2001.

[4] S. K. Sia and G. M. Whitesides, "Microfluidic devices fabricated in poly(dimethylsiloxane) for biological studies," *Electrophoresis*, vol. 24, no. 21, pp. 3563-3576, Nov.2003.

[5] J. Voldman, "Engineered systems for the physical manipulation of single cells," *Curr. Opin. Biotechnol.*, vol. 17, no. 5, pp. 532-537, Oct.2006.

[6] M. A. Unger, H. P. Chou, T. Thorsen, A. Scherer, and S. R. Quake, "Monolithic microfabricated valves and pumps by multilayer soft lithography," *Science*, vol. 288, no. 5463, pp. 113-116, Apr.2000.

[7] G. M. Whitesides, E. Ostuni, S. Takayama, X. Jiang, and D. E. Ingber, "Soft lithography in biology and biochemistry," *Annu. Rev. Biomed. Eng*, vol. 3, pp. 335-373, 2001.

[8] G. M. Whitesides, "The origins and the future of microfluidics," *Nature*, vol. 442, no. 7101, pp. 368-373, July2006.

[9] C. D. Di, L. Y. Wu, and L. P. Lee, "Dynamic single cell culture array," *Lab Chip.*, vol. 6, no. 11, pp. 1445-1449, Nov.2006.

[10] L. Kim, Y. C. Toh, J. Voldman, and H. Yu, "A practical guide to microfluidic perfusion culture of adherent mammalian cells," *Lab Chip.*, vol. 7, no. 6, pp. 681-694, June2007.

[11] A. Prokop, Z. Prokop, D. Schaffer, E. Kozlov, J. Wikswo, D. Cliffel, and F. Baudenbacher, "NanoLiterBioReactor: long-term mammalian cell culture at nanofabricated scale," *Biomed. Microdevices.*, vol. 6, no. 4, pp. 325-339, Dec.2004.

[12] N. Klauke, G. Smith, and J. M. Cooper, "Microfluidic systems to examine intercellular coupling of pairs of cardiac myocytes," *Lab Chip.*, vol. 7, no. 6, pp. 731-739, June2007.

[13] N. Klauke, G. L. Smith, and J. M. Cooper, "Microfluidic partitioning of the extracellular space around single cardiac myocytes," *Anal. Chem.*, vol. 79, no. 3, pp. 1205-1212, Feb.2007.

[14] A. A. Werdich, E. A. Lima, B. Ivanov, I. Ges, M. E. Anderson, J. P. Wikswo, and F. J. Baudenbacher, "A microfluidic device to confine a single cardiac myocyte in a sub-nanoliter volume on planar microelectrodes for extracellular potential recordings," *Lab Chip.*, vol. 4, no. 4, pp. 357-362, Aug.2004.

[15] A. R. Wheeler, W. R. Throndset, R. J. Whelan, A. M. Leach, R. N. Zare, Y. H. Liao, K. Farrell, I. D. Manger, and A. Daridon, "Microfluidic device for single-cell analysis," *Anal. Chem.*, vol. 75, no. 14, pp. 3581-3586, July2003.

[16] K. T. Seale, S. L. Faley, and J. P. Wikswo, "Macro to nano: A Simple Method for Transporting Cultured Cells from Milliliter Scale to Nanoliter Scale *(in revision)*," *Lab Chip.*, 2007.

[17] K. Oswald-Richter, V. J. Torres, M. S. Sundrud, S. E. VanCompernolle, T. L. Cover, and D. Unutmaz, "Helicobacter pylori VacA Toxin Inhibits Human Immunodeficiency Virus Infection of Primary Human T Cells," *J. Virol.*, vol. 80, no. 23, pp. 11767-11775, Dec.2006.

[18] K. A. Eger, M. S. Sundrud, A. A. Motsinger, M. Tseng, L. V. Kaer, and D. Unutmaz, "Human natural killer T cells are heterogeneous in their capacity to reprogram their effector functions," *PLoS. ONE.*, vol. 1, p. e50, 2006.

[19] C. Navarrete, R. Sancho, F. J. Caballero, F. Pollastro, B. L. Fiebich, O. Sterner, G. Appendino, and E. Munoz, "Basiliolides, a class of tetracyclic C19 dilactones from Thapsia garganica, release Ca(2+) from the endoplasmic reticulum and regulate the activity of the transcription factors nuclear factor of activated T cells, nuclear factor-kappaB, and activator protein 1 in T lymphocytes," *J Pharmacol. Exp. Ther.*, vol. 319, no. 1, pp. 422-430, Oct.2006.

[20] C. Liu and T. E. Hermann, "Characterization of ionomycin as a calcium ionophore," *J Biol Chem.*, vol. 253, no. 17, pp. 5892-5894, Sept.1978.

[21] J. Rachmilewitz and A. Lanzavecchia, "A temporal and spatial summation model for T-cell activation: signal integration and antigen decoding," *Trends in Immunology*, vol. 23, no. 12, pp. 592-595, Dec.2002.

[22] M. C. Rodriguez-Galan, J. H. Bream, A. Farr, and H. A. Young, "Synergistic effect of IL-2, IL-12, and IL-18 on thymocyte apoptosis and Th1/Th2 cytokine expression," *J Immunol*, vol. 174, no. 5, pp. 2796-2804, Mar.2005.

[23] M. R. Warnement, S. L. Faley, J. P. Wikswo, and S. J. Rosenthal, "Quantum dot probes for monitoring dynamic cellular response: reporters of T cell activation," *IEEE Trans. Nanobioscience.*, vol. 5, no. 4, pp. 268-272, Dec.2006.

[24] N. Bertho, H. Adamski, L. Toujas, M. Debove, J. Davoust, and V. Quillien, "Efficient migration of dendritic cells toward lymph node chemokines and induction of TH1 responses require maturation stimulus and apoptotic cell interaction," *Blood*, vol. 106, no. 5, pp. 1734-1741, Sept.2005.

[25] L. Amati, M. Pepe, M. E. Passeri, M. L. Mastronardi, E. Jirillo, and V. Covelli, "Toll-like receptor signaling mechanisms involved in dendritic cell activation: potential therapeutic control of T cell polarization," *Curr. Pharm. Des*, vol. 12, no. 32, pp. 4247-4254, 2006.

[26] M. Feili-Hariri, D. H. Falkner, and P. A. Morel, "Polarization of naive T cells into Th1 or Th2 by distinct cytokine-driven murine dendritic cell populations: implications for immunotherapy," *J Leukoc Biol*, vol. 78, no. 3, pp. 656-664, Sept.2005.

[27] S. Iwamoto, M. Ishida, K. Takahashi, K. Takeda, and A. Miyazaki, "Lipopolysaccharide stimulation converts vigorously washed dendritic cells (DCs) to nonexhausted DCs expressing CD70 and evoking long-lasting type 1 T cell responses," *J Leukoc Biol*, vol. 78, no. 2, pp. 383-392, Aug.2005.

[28] S. A. Luther and J. G. Cyster, "Chemokines as regulators of T cell differentiation," *Nat Immunol*, vol. 2, no. 2, pp. 102-107, Feb.2001.

[29] L. Chiodetti, S. Choi, D. L. Barber, and R. H. Schwartz, "Adaptive Tolerance and Clonal Anergy Are Distinct Biochemical States," *J Immunol*, vol. 176, no. 4, pp. 2279-2291, Feb.2006.

[30] S. Dillon, S. Agrawal, K. Banerjee, J. Letterio, T. L. Denning, K. Oswald-Richter, D. J. Kasprowicz, K. Kellar, J. Pare, T. van Dyke, S. Ziegler, D. Unutmaz, and B. Pulendran, "Yeast zymosan, a stimulus for TLR2 and dectin-1, induces regulatory antigen-presenting cells and immunological tolerance," *J. Clin. Invest.*, vol. 116, no. 4, pp. 916-928, Apr.2006.

[31] M. B. Lutz and G. Schuler, "Immature, semi-mature and fully mature dendritic cells: which signals induce tolerance or immunity?," *Trends in Immunology*, vol. 23, no. 9, pp. 445-449, Sept.2002.

[32] J. K. H. Tan and H. C. O'Neill, "Maturation requirements for dendritic cells in T cell stimulation leading to tolerance versus immunity," *J Leukoc Biol*, vol. 78, no. 2, pp. 319-324, Aug.2005.

[33] C. G. Sagerstrom, E. M. Kerr, J. P. Allison, and M. M. Davis, "Activation and differentiation requirements of primary T cells in vitro," *Proc Natl Acad Sci U S A*, vol. 90, no. 19, pp. 8987-91, 1993.

[34] M. A. Santana and Y. Rosenstein, "What it takes to become an effector T cell: the process, the cells involved, and the mechanisms," *J Cell Physiol*, vol. 195, no. 3, pp. 392-401, 2003.

[35] E. Donnadieu, G. Bismuth, and A. Trautmann, "Calcium fluxes in T lymphocytes," *J. Biol. Chem.*, vol. 267, no. 36, pp. 25864-25872, Dec.1992.

[36] E. Donnadieu, D. Cefai, Y. P. Tan, G. Paresys, G. Bismuth, and A. Trautmann, "Imaging early steps of human T cell activation by antigen-presenting cells," *J Immunol*, vol. 148, no. 9, pp. 2643-2653, May1992.

CHAPTER V

REAL-TIME MONITORING OF INTERCELLULAR SIGNALING BETWEEN HUMAN DENDRITIC CELL AND CD4+ T CELLS USING THE MICROFLUIDIC NANOPHYSIOMETER

Abstract

It has long been known that stimulation of naïve T cells (TCs) by mature dendritic cells (DCs) occurs through both contact and non-contact-based interactions, although much attention is paid to the immune synapse. However, studying the signaling events surrounding the immune synapse or intercellular signaling between DCs and TCs can be quite difficult using current cell culture methods, especially when one is interested in capturing the earliest signaling events. In this report, we demonstrate a novel microfluidic platform, the nanophysiometer, which overcomes many limitations of current methods to allow easy, real-time data collection in both cell-cell interaction experiments and intercellular signaling studies in non-adherent cell lines. Using the nanophysiometer in both stand-alone and daisy-chain configurations, we were able to observe calcium transients in TCs in response to contact as well as non-contact based interactions with DCs. Further investigation into then non-contact based stimulation, we found that LPS matured DCs, in the absence of antigen, secrete chemical signals that cause strong calcium transients in naïve CD4+ TCs. This signal was not measurable in un-concentrated cell culture supernatants indicating that the signaling agent is produced in small quantities, but was easily detected within the nanphysiometer due to its inherent low cell to media volume ratio. The characteristics of this signaling factor, which remains to be identified, are similar to those reported in the literature for DCs lipid hydrolysis products, prostaglandins, secreted exosomes, or prepackaged chemokine CCL19. Future studies will focus on identifying this signaling factor as well as investigating other intercellular signaling events between DCs and TCs during immune response.

Introduction

It has long been known that stimulation of naïve T cells (TCs) by mature dendritic cells (DCs) occurs through both contact and non-contact-based interactions, although much attention is paid to the immune synapse. In the body, both DCs and TCs rely on a complex and highly specific array of chemokine, cytokine, and other signaling agents to navigate and home to lymph nodes or infection sites, as well as to differentiate into the proper functional cell phenotype for efficient immune response against a particular antigen[2]. However, studying the signaling events surrounding the immune synapse or intercellular signaling between DCs and TCs can be quite difficult using current cell culture methods, especially when one is interested in capturing the earliest signaling events. In this report, we demonstrate a novel microfluidic platform, the nanophysiometer, which overcomes many limitations of current methods to allow easy and fast data collection on both cell-cell interaction experiments and intercellular signaling studies in non-adherent cell lines. We have used this platform to discover and investigate an early intercellular signaling event occurring between DCs and TCs.

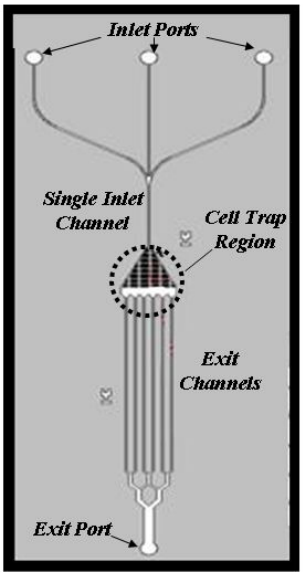

Figure 22. Schematic of microfluidic nanophysiometer. The device is constructed of PDMS and plasma-bonded to a glass coverslip

A schematic of the microfluidic nanophysiometer is shown in **Figure 1**. This platform is a self contained unit fabricated of optically transparent, bio-inert PDMS on glass and designed to maintain non-adherent cells in a microfluidic environment [3]. Cells are injected into one of the inlet ports using computer-controlled micro-syringe pumps. As cells flow through the trap region, cells are passively trapped in one of 550 18 $\mu m \times 18\mu m \times 10\mu m$ PDMS, bucket-like structures (see **Figure 2** for close-up view of cell traps). Media flow rate is optimized such that cells remain in traps and receive necessary nutrients while minimizing shear stress and waste accumulation. The nanophysiometer provides a

method of quickly sequestering cells into individually addressable compartments without using any type of adhering agents, such as cell surface antibodies, poly-l-lysine, or fibronectin, which can themselves induce unwanted intracellular signaling cascades. Furthermore, only relatively small quantities of cells (aliquots as small as 1000 cells), media (~100s of microliters for long-term experiments), and other reagents are required to obtain data on hundreds of single cells in parallel, resulting in decreased labor and material costs.

A major strength of this platform is the ability to easily study cell-cell interaction between two or more cell types. In cell culture, there normally exists a relatively large media volume:cell ratio, resulting in a significant time delay before any cell interaction occurs, as the cells passively diffuse throughout the large media volume and find partners by chance. Two cell types are easily co-cultured in the nanophysiometer, however, by simply flowing both cell types across the trap region. There exists almost no delay time in bringing the two cells together in close contact and since the traps themselves are fixed in place, it is easy to program the computer-controlled stage and camera system to capture images of earliest responses in cell-cell interactions. In addition, the low ceiling of the device (10μm) ensures that cells remain in a single layer within the trap region so that all physical interactions are in the optical plane of the microscope, another feature that is virtually uncontrollable in suspension cell culture.

In addition to easily studying cell-cell interactions, the nanophysiometer has many characteristics that make it a powerful tool for analyzing non-contact-based intercellular signaling events. The fact that the cell trap region of the nanophysiometer has a volume of less than ,20 nL. more than half of which is occupied by traps and cells, means that signaling agents secreted by cells are not diluted by the external media, and remain at biologically realistic concentrations. This allows the observation of autocrine and paracrine signaling in real-time that might otherwise squelched by the preponderance of culture media. The triangular shape of the cell trap region was designed such that the behaviors of cells not exposed to cell secretions (cells trapped in the top of the device) can be compared to those cells trapped in the back of the

device (which are exposed to all the secretions of cells trapped upstream). In this paper, we report the observation of naïve T cell stimulation in T cells trapped downstream of mDC/TC pairs within a single device. This finding led to a group of experiments investigating the early intercellular signals between physically separated DCs and TCs using multiple microfluidic devices in series.

Experimental Setup

All experiments were performed using an Axiovert 200 microscope (Carl Zeiss, Germany). The microscope environment was modified to facilitate long-term maintenance of cells during experiments, as shown in **Figure 2**. A plexiglass incubator enclosed the microscope such that the temperature was maintained at 37°C. The nanophysiometer was enclosed within a modified petri dish (Fisher Scientific, Hampton NH) with holes machined in the bottom to allow microscope viewing, as well as slots in the top for PEEK tubing passage. In addition, a port was drilled in the side of the dish to allow tubing connected to a gas supply such that a constant flow of 5% CO_2 in 95% air was pumped into the petri dish. To minimize evaporation, 3 to 4 layers of filter paper (Whatman, Florham Park NJ) saturated with dH_20 were used to surround the device inside the petri dish. The entire device was rigidly affixed to the mechanized microscope stage. The stage, image acquisition, focus, and filter settings were

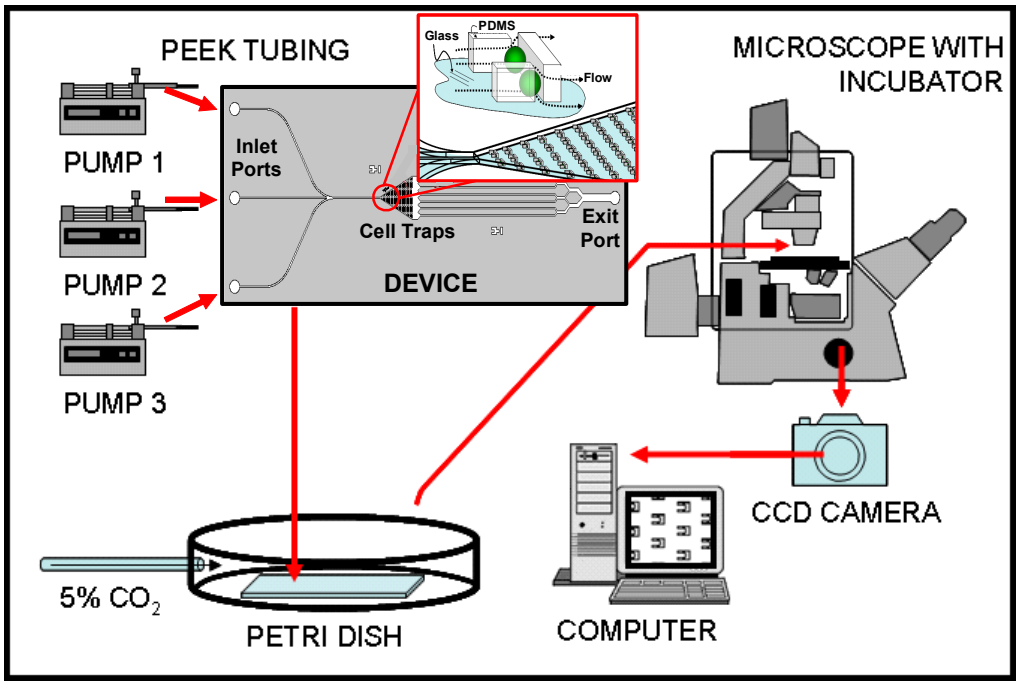

Figure 23. Schematic illustrating the standard experimental setup.

controlled using Metamorph software (Molecular Devices, Downington PA). Syringe pump flow rates were also ,controlled utilizing custom software developed by VIIBRE researchers. Images were obtained with the electrically cooled CoolSNAP HQ CCD camera (Photometrics, Tucson AZ).

Cell Culture

Primary human CD4+ T cells and dendritic cells (derived from human monocytes) were generously provided by the lab of Derya Unutmaz (New York University School of Medicine, New York, NY) following isolation and purification from human blood donors [1]. Primary CD4+ T cells were thawed from liquid nitrogen aliquots ($5*10^5$ cells/vial) 24 hours prior to use and cultured using sterile technique in RPMI 1640 (ATCC, Manassas VA) supplemented with 10% FBS (ATCC, Manassas VA) and 10μg/ml Ciprofloxacin (Mediatech, Herndon VA). Dendritic cells were derived by incubating primary human CD14+ monocytes with 20 ng/ml IL-4 and 100ng/ml GM-CSF for 4-6 days [4]. Mature dendritic cells were generated following 24-hour incubation with 10 ng/ml LPS [4]. All cells were incubated in a sterile environment maintained at 37^{o}C, complete with 5% CO_2 and 95% humidity.

Microfluidic Cell Loading

Cell loading followed methods developed by our lab and described in greater detail in previous publication [5]. Cells were centrifuged to a pellet at 5000 rpm for 1 minute in 1.5 ml eppendorf tubes (Fisher Scientific, Hampton NH) which were then mounted on a glass slide for viewing the pellet with the microscope. Once the pellet was located using the microscope, 50 μm I.D. PEEK tubing (Upchurch, Oak Harbor WA), connected to 50 μl gas-tight syringe mounted on a computer controlled syringe pump (Harvard Apparatus, Holliston MA), was guided to the cell pellet. Cells were then aspirated directly into the PEEK tubing using the

syringe pump set to reverse at a flow-rate of 0.5 μl/min. The tubing was then inserted to a loading channel of a device pre-cleared with sterile media. This cell loading procedure required approximately 10 minutes and is illustrated in **Figure 3**. Once all inputs were connected to the device, the pump controlling the cell channel was set to a forward flow rate of 100 nl/min for passive loading of cells into the traps as they traverse the device. Unless otherwise noted, the media used to perfuse the device and the cells contained within consisted of RPMI 1640 supplemented with 10% FBS and 10μg/ml ciprofloxacin.

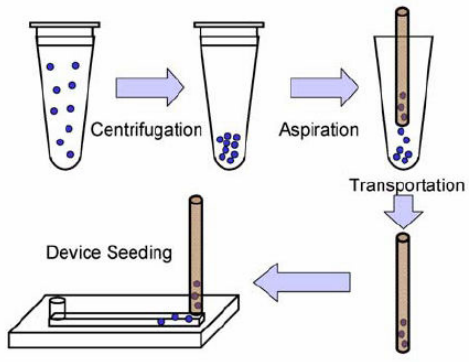

Figure 24 Macro cell culture to micro cell culture in microfluidic devices. Use of ultra small bore tubing to aspirate controllable volumes of high cell-density and seed into device.

Cytosolic Calcium Assay

Release of intracellular calcium stores and subsequent calcium flux, an early signaling event in T cell activation, was induced chemically, with antibody-coated beads, or by co-incubation with antigen-presenting cells. In all cases, naïve primary CD4+ T cells were first loaded with rhod-2 calcium indicator by incubation in a 5μM solution for 30 minutes at 37°C. Cells were then loaded into the nanophysiometer (pre-cleared with media to remove air bubbles) and perfused with normal culture media supplemented with $CaCl_2$ to a final concentration of 1.8 mM[6]. Using Metamorph software, the microsope was programmed to obtain baseline bright field (DIC or phase-contrast) and TRITC (rhod-2 fluorescence) images for 4 to 5 FOVs spanning the entire cell trap region of the microfluidic device every 30 seconds. The images were numbered sequentially and saved automatically to disk.

APC Stimulation. LPS stimulated, primary human dendritic cells (DCs) were obtained from the Unutmaz lab on the day of experiment. Prior to loading, the DCs were incubated with 20 ng/ml of SEB for thirty minutes at 37°C [4]. DCs were then rinsed with fresh media to remove all unbound SEB. The resuspended cells were then centrifuged to a pellet for cell loading as described above. TCs were trapped first, and then DCs introduced to the devices. Image acquisition began upon introduction of DCs.

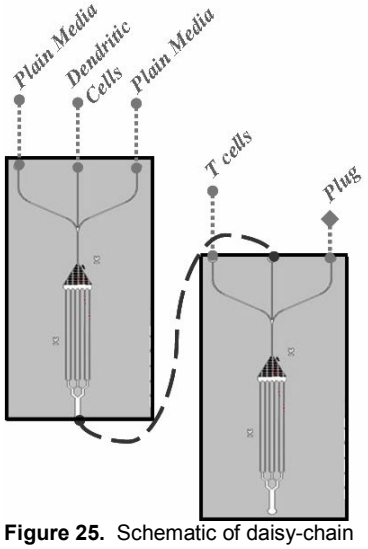

Figure 25. Schematic of daisy-chain device conformation. Prior to daisy-chain connection, the PEEK tubing connecting the two devices is initially connected to a syringe pump pushing plain media through the second (downstream) device. During connection, this line is cut and the cut end is inserted into the exit port of the first device.

Daisy-chain Configuration. Two separate devices were prepared just as described above, except that instead of inserting the devices into a specially cut petri dish, the polystyrene chambers from a single chambered converglass (Nunc, Fisher Scientifc, Hampton, NH) was detached from its original coverslip and adhered to the glass coverslip bonded to the microfluidic device, in order to create a small area to control CO_2 and humidity levels. Both devices were secured to a custom machined stage insert that is capable of accommodating and imaging up to six devices in the same experiment. Filter paper saturated with water and CO_2 were added as before. One device was loaded with naïve CD4+ T cells only. The other device was loaded with the TC stimulus of interest (e.g., mature dendritic cells). Background data was collected every 30 seconds on both devices running on completely separate pump systems. To connect the two devices, one of the inlets on the TC device pushing plain media was cut and the cut end inserted into the exit port of the other device, such that the downstream TCs were exposed to the effluent of the cells in the first device. **Figure 4** illustrates the daisy-chain setup for studying intercellular signaling. Image acquisition was restarted immediately following reconnection and continued for at least one hour.

Results

As shown in **Figure 5**, naïve T cells elicit cytosolic calcium burst when in direct contact with a mature dendritic cell while trapped within the microfluidic nanophysiometer. This is a well-known signaling cascade initiated by the interaction between the MHC (in this case, aided by the super-antigen, SEB) and the T cell receptor which results in calcium release from the sarcoplasmic reticulum. The calcium responses derived from these contact-based interactions are consistent with the literature and were entirely expected. Interestingly, however, during the course of experiments it was noted that some CD4+ T cells that were in no detectable physical contact with dendritic cells also elicited a calcium response. This observation led to a series of experiments investigating the nature of intercellular signaling occurring between dendritic cells and T cells.

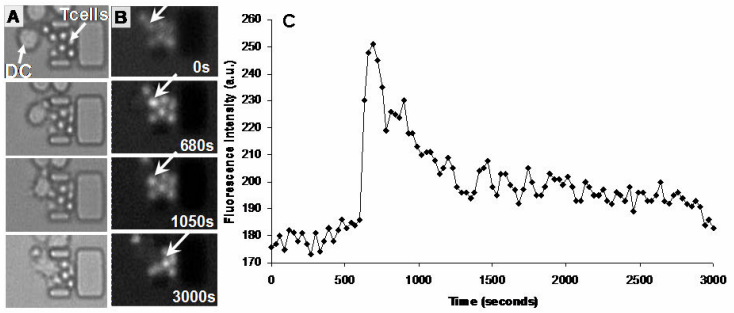

Figure 26. Calcium transient observed in a naïve CD4+ T cell stimulated by interaction with a mature DC. T cells were incubated with 5 μM rhod-2 AM ester prior to experiment[1]. Bright field snapshots of the cells are shown in **(A)** and the corresponding fluorescence images are shown in **(B)**. Graph **(C)** shows the fluctuation in fluorescence over time, indicating a clear cytosolic calcium increase in the TC following contact with the DC.

In order to ensure that what triggered a calcium transient in the naïve CD4+ cells was indeed a factor present in the perifusate, rather than being the result of long, barely visible extensions of the dendritic cells, a new setup was devised to physically separate the two cell populations. Two identical microfluidic devices were utilized to house one cell population each, in a configuration shown in **Figure 4**. After collecting baseline data, the two devices were connected in a daisy-chain fashion, such that the exit port of the first device (containing the stimulus, i.e., dendritic cells) was connected to an inlet port of the second device (containing naïve CD4+ T cells). This arrangement results in the cells in the second device being exposed

to the all the signaling factors secreted into the perifusate by the cells trapped in the upstream device.

The first experiment utilizing the daisy-chain device configuration involved mature dendritic cells and naïve T cells trapped together in the first (upstream) device. The second device contained only naïve T cells. Just as observed in the single trap experiment, calcium transients were observed in both the T cells in contact with the dendritic cells (upstream device) as well as those in the T cells trapped in the downstream device. **Figure 6** illustrates the non-contact-dependent calcium transients induced in the T cells trapped in the second device. Interestingly, the calcium transients were induced very quickly – within minutes of connecting the daisy-chain.

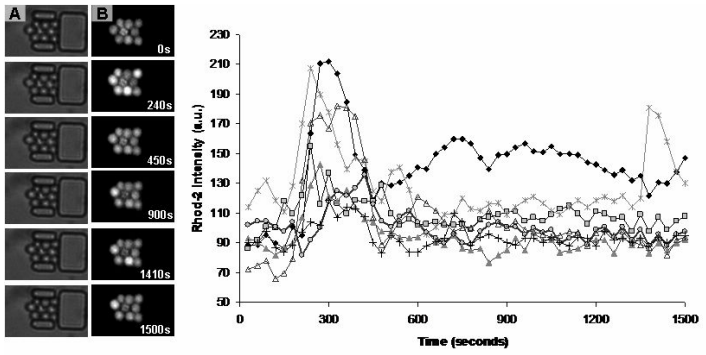

Figure 27. Non-contact based stimulation of cytosolic calcium flux in naïve CD4+ TCs trapped in nanophysiometer daisy-chained downstream of a device containing mature DCs and TC together. Image acquisition began upon daisy-chain connection. Bright field images of the cells are shown in **(A)** with the corresponding fluorescence images shown in **(B)**. TCs were incubated with 5 μM rhod-2 prior to experiment. Graph **(C)** indicates the fluctuation in fluorescence intensities of the cells. Each line represents a single cell. Cytosolic calcium transients are clearly seen in TC within minutes of daisy-chain connection.

Once it was verified that there was indeed a stimulatory factor transmitted in a non-contact-dependent manner, we sought to identify its source. This involved evaluating both different upstream cellular populations as well as chemicals such as SEB and LPS that were undoubtedly being transferred in the media. A comparison of control to experimental data is shown in **Figure 7**. Graphs A – C clearly demonstrate that calcium transients are not induced from plain media, SEB, or LPS. The stimulatory signal is cell-based. In addition, note that a sharp jump in rhod-2 fluorescence is observed in the naïve T-cell population in the downstream device and occurs within seconds to minutes of the daisy-chain being connected. The stimulus in this case was mature dendritic cells pre-pulsed with SEB. The ensuing stimulation of calcium release in the downstream cell revealed that the DCs were in fact the source of the stimulating factor.

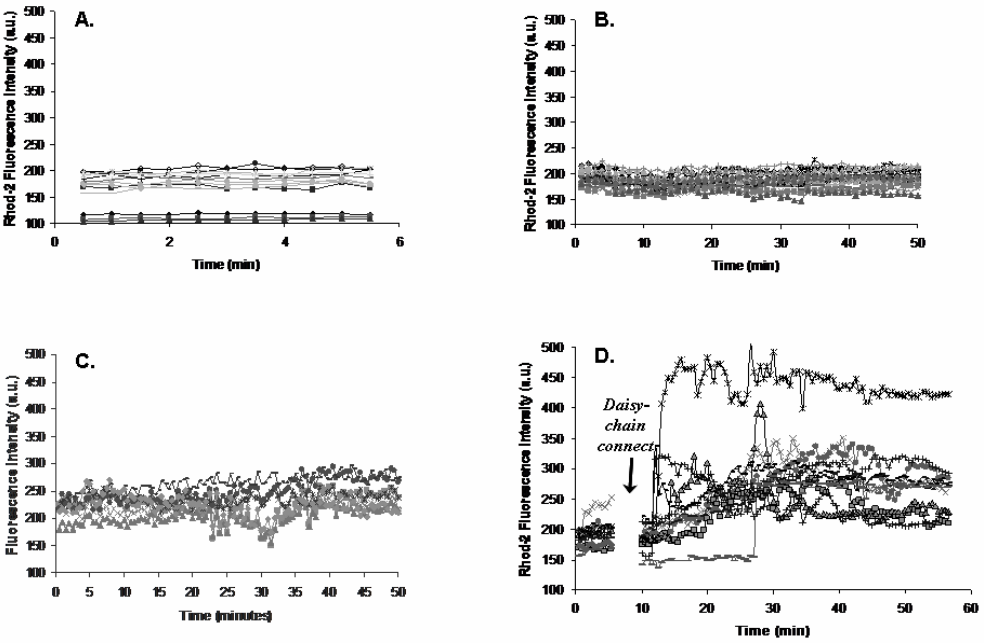

Figure 28. Monitoring cytosolic calcium levels in naïve T cells exposed to **(A)** plain media (RPMI 1640+ 10% FBS+10 μg/ml Cipro+20 ng/ml IL2), **(B)** plain media supplemented with 5 μg/ml LPS, **(C)** plain media supplemented with 5 nM SEB, and **(D)** Daisy-chained to a device upstream which contained mature DCs only. Each line represents a single cell analyzed over the entirety of the experiment. T cells were incubated with 5 μM rhod-2 AM-ester prior to the experiments. No calcium activity is observed in response to plain media or LPS. Some calcium activity is observed with the addition of SEB, as expected, but the relative intensity of this response is quite small compared to that shown in graph D. Within seconds to minutes, T cells respond with distinct cytosolic calcium transient to the effluent from mature DCs. It is clear that the DCs are secreting a signaling factor that stimulates this calcium release in T cells.

Table 1 summarizes the experiments conducted to further characterize the source of the stimulatory factor. We evaluated the stimulation ability of mature DCs pulsed with SEB and paired with naïve T cells, mature DCs pulsed with SEB, mature DCs (no SEB), naïve DCs, naïve TCs, SEB alone, LPS alone, and finally, the supernatant taken from mature DCs (no SEB) incubated in a cell culture dish for 24 hours at a concentration of $5*10^5$ and $5*10^6$ DCs per milliter of media (LPS concentration held constant). The analysis revealed that mature DCs secrete the stimulating factor and that neither pulsing with SEB nor incubation with naïve T cells was necessary for production. In addition, the fact that the supernatant from cultured mature DCs was unable to elicit a calcium response suggests that the stimulatory factor exists in very small concentrations. This hypothesis was supported by the fact that concentrating DCs tenfold

(essentially reducing the media volume:cell ratio) resulted in supernatant that did induce calcium transient in naïve T cells.

While the factor secreted by mature DCs stimulated calcium transients in the naïve T cells, we wanted to determine if it was truly a pro-stimulatory factor, or one that perhaps might have an overall inhibitory effect towards complete T cell activation. To examine this question, mature DCs were daisy-chained upstream of naïve TCs as in previous experiments. After allowing the TCs in the second device to be exposed to the effluent from the first device containing DC, the daisy-chain was disconnected and a bolus of mature, SEB pulsed DCs were injected into the second device. We then compared the calcium response of cells exposed to the secreted factor followed by direct DC contact to those stimulated by DC contact alone. The results are shown in **Figure 8.** We found that cells initially exposed to the stimulatory factor ("factor x" in the graph) were subsequently able to be stimulated by DC contact. This suggests that the factor secreted by DCs does not have an inhibitory effect on TC activation, at least in terms of initiating calcium release from intracellular stores. Whether or not this signaling molecule functions to enhance TC activation, however, still remains to be determined.

Device 1: T Cell Stimulus	Device 2: Ca^{2+} Signal in T Cells?
LPS Matured DCs + SEB + T cells	Yes
LPS Matured DCs + SEB	Yes
LPS Matured DCs	Yes
Immature DCs	No
T cells Only	No
SEB Only	No
LPS Only	No
Supernatant from LPS Matured (24 hrs) DCs in culture ($5*10^5$ cells/ml)	No
Supernatant from LPS Matured (24 hrs) DCs in culture ($5*10^6$ cells/ml)	Yes

Table 1. The left column describes the agent used to stimulate naïve CD4+ TCs within the nanophysiometer. The right hand column indicates whether or not a measurable cytosolic calcium transient was observed in the TCs Each stimulus was exposed to the TCs for at least an hour. Cell-based stimuli were daisy-chained upstream to the naïve TCs while fluid based stimuli (LPS, SEB, cell culture supernatants) were simply introduced in an alternate port of the device containing the TCs..

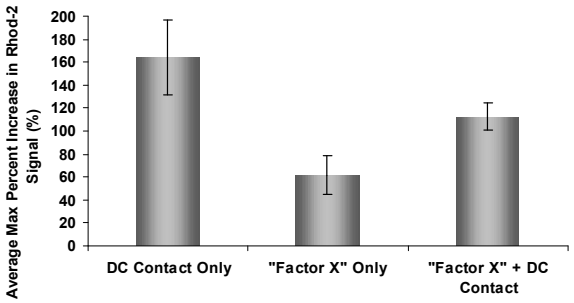

Figure 29. Comparison of rhod-2 signal strength in naïve CD4+TCs exposed to DC contact only, "factor x" only and "factor x" followed by DC contact. While neither "factor x" nor "factor x + DC contact" resulted in the same magnitude of response seen in cells only exposed to DCs, the overall calcium signal did increase once the cell exposed to "factor x" were in contact with DCs. This suggests that "factor x" is at least not inhibitory to TC activation, and is likely a pro-stimulatory agent.

Discussion

In this report we have demonstrated a novel microfluidic platform for studying both cell-cell interactions and intercellular signaling events of non-adherent cells. The nanophysiometer employs hydrodynamic forces to passively trap and retain suspension cells in static, individually addressable, PDMS buckets, thereby bypassing the need for specialized cell isolation or adherence techniques. Previous studies characterizing cell viability within the microfluidic nanophysiometer revealed that the primary TCs remained both viable and active for 24 hours [3]. Results of our cell-cell interaction experiments involving mDCs and naïve TCs revealed cytosolic calcium transients in TCs with clear oscillations, a characteristic calcium burst pattern first reported by Donnadieu et al. [7]. This lends support to our assertion that trapped cells are at least as functional as those utilized in standard cell culture experiments. Compared to standard cell culture techniques, the nanohpysiometer facilitiates the capture of hundreds of these DC-TC interactions in a single experiment, rather than a few chance encounters. Furthermore, the physical interaction between TCs and DCs within the nanophysiometer is quite similar to that observed *in vivo* [8], with rings of nTCs circling individual mDCs (data not shown).

Utilizing the nanophyisiometer in a daisy-chain configuration allowed us to confirm that in the absence of antigen, mDCs release soluble signaling agent(s) that induce cytosolic calcium transient in naïve CD4+ TCs. For the ease of communication, we have termed the TC stimulus "factor x," with the knowledge that the mDCs may be releasing more than one signaling factor that causes the subsequent calcium release. While the existence of intercellular signaling between DCs and TCs is anything but new, these results lend further support to the utility of applying the nanophysiometer to immunological study, especially when analyzing cellular products that may occur in small quantities. Furthermore, these results raise interesting questions into the nature of these early, pre-synaptic communications between DCs and TCs. One could clearly envision "factor x" having chemotactic properties, as mDCs ready for antigen presentation would like to traffic and/or stimulate TCs trafficking to lymph nodes. Increased TC

motility and sampling of nearby mDCs would also be desirable in the early stages of immune response. The concentration of "factor x" is relatively small, suggesting that either it is meant to act locally, as in supporting synapse formation, or the signal is generated in sufficient concentrations *in vivo* to propagate the signal. Another possibility is that mDCs continually produce small amounts of "factor x," thereby causing an accumulation of the signaling agent over time.

Due to the rapid transmission of the stimulatory signal from DCs to TCs upon daisy-chain connection, it is possible that rather than a chemokine/cytokines signal, "factor x" could be a signaling molecule, such as a lipid hydrolysis product[9;10] or prostaglandin, which does not require de novo synthesis, and all of which are known to induce calcium transients in TCs. It is clear that if "factor x" is a cytokine/chemokine, it is one whose production is stimulated by maturation of the DC in the presence of LPS and prepackaged for release. This raises the questions of whether maturation by other agents might effect the expression of "factor x" and at what point during maturation its secretion begins, two areas currently under investigation in our lab.

Because the experiments presented here stop short of identifying "factor x," we can only speculate on its identity and function. However, several reports in the literature provide a few potential candidates. Segura et al. report that both immature and mature DCs secret exosomes that are capable of interacting with nTCs and inducing calcium release [11]. In the absence of antigen, DCs matured using LPS were found to produce exosomes with increased levels of DC86, ICAM-1, and MHC II compared to exosomes produced by immature DCs, all of which can induce calcium transients in naïve CD4+ TCs. Exosomes have even been shown to transfer MHC peptide complexes to nTCs [12]. Furthermore, they found a very similar activation trend, as shown in **Figure 8**. Exosomes secreted by mDCs induced calcium transients in TCs that were weaker than when TCs were stimulated by mDCs (still in the absence of antigen). When stimulated by mDCs following exposure to exosomes, the intensity of the calcium signal

rose, but not to the level of mDC alone[11]. In terms of the identity of "factor x," secreted exosomes are quite feasible given the timescale in which the signal is observed and the similar pattern of calcium transients observed.

Another interesting report by Kaiser et al. asserts that even in the absence of antigen, mDCs secrete chemokine CCL19, which stimulates nTCs via the cell surface receptor, CCR7, resulting in cytosolic calcium transients [13]. Similar to our findings, supernatant taken from LPS matured DCs failed to result in nTC stimulation, although the authors note that presence of supernatant enhanced calcium response in TCs interacting with mDCs. Since CCL19 is not an adhesion protein, it is hypothesized that mDCs release the chemokine to act locally on nearby TCs to enhance synapse formation. Others report that CCL19 is secreted by mDCs *in vivo* as a potent attractor of nTCs [14].

Current experiments in our lab focus on identifying "factor x," including investigating the possibilities of exosomes or CCL19 being the culprit, as well as proteomic analysis of mDC supernatant to yield other possible signaling molecules. In addition, we plan to utilize the nanophysiometer to study in greater depth the events leading up to and surrounding the initiation of secretion of stimulatory signals from DCs, as well as their long-term effects on TC activation. It will be of great interest to learn if these pre-synaptic signals can influence Th1/Th2 orientation since DC chemokine and cytokine secretions are known to have a great impact on this transition [15-19]. As mentioned earlier, we are interested in looking into differences in maturation agents upon the release of chemical signals by mDCs. Because the nanophysiometer allows data collection on hundreds of cells in parallel in any given experiment, we can begin to run statistical analysis on the calcium response patterns, and perhaps even determine whether different DC maturation agents result in characteristic calcium response patterns[2;15-17;20-27].

Conclusions

In this report we demonstrate a unique and powerful microfluidic platform for studying both cell-cell interaction and intercellular signaling events in non-adherent immune cells. The novelty of this platform lies in the ability to passively trap and maintain hundreds of non-adherent cells in parallel, easily and quickly dictate the physical location of cells, obtain temporal data on any given cells, function in low cell:volume environment such that cellular secretions are not diluted and effects are monitored in real-time, and, because of the small dimension, require very few cells and reagents to obtain large amounts of data. We have successfully utilized this platform to show that DCs matured with LPS, but in the absence of antigen, release low concentrations of a chemical signal that stimulates cytosolic calcium release in nTCs. Future experiments will continue to investigate both intercellular and intracellular signaling events surrounding the immune synapse.

Acknowledgements

The authors wish to thank the Unutmaz lab, especially Mindy Leelawong and Michelle Tseng for providing the primary cells as well as their invaluable assistance and advice in cell culture. In addition, we would like to thank Walter Georgescu for the use of the pump controller program written by him. Also, thanks to E. Duco Jansen for the use of cell culture facilities and to Allison Price for her generous help witht his manuscript. . This research was supported in part by the Vanderbilt Institute for Integrative Biosystems Research and Education (VIIBRE), the Air Force Office of Sponsored Research (AFOSR) grants FA95500410364 and FA95500510349 as well as NIH grant U01A1061223.

Bibliography

[1] K. Oswald-Richter, V. J. Torres, M. S. Sundrud, S. E. VanCompernolle, T. L. Cover, and D. Unutmaz, "Helicobacter pylori VacA Toxin Inhibits Human Immunodeficiency Virus Infection of Primary Human T Cells," *J. Virol.*, vol. 80, no. 23, pp. 11767-11775, Dec.2006.

[2] J. Banchereau, F. Briere, C. Caux, J. Davoust, S. Lebecque, Y. J. Liu, B. Pulendran, and K. Palucka, "Immunobiology of Dendritic Cells," *Annual Review of Immunology*, vol. 18, no. 1, pp. 767-811, 2000.

[3] S. L. Faley, K. T. Seale, J. Hughey, J. P. Wikswo, and F. J. Baudenbacher, "Microfluidic platform for real-time signaling analysis of multiple single T cells in parallel (in preparation)," *Lab Chip.*, 2007.

[4] K. A. Eger, M. S. Sundrud, A. A. Motsinger, M. Tseng, L. V. Kaer, and D. Unutmaz, "Human natural killer T cells are heterogeneous in their capacity to reprogram their effector functions," *PLoS. ONE.*, vol. 1, p. e50, 2006.

[5] K. T. Seale, S. L. Faley, and J. P. Wikswo, "Macro to nano: A Simple Method for Transporting Cultured Cells from Milliliter Scale to Nanoliter Scale *(in revision)*," *Lab Chip.*, 2007.

[6] S. Kunerth, G. W. Mayr, F. Koch-Nolte, and A. H. Guse, "Analysis of subcellular calcium signals in T-lymphocytes," *Cell Signal.*, vol. 15, no. 8, pp. 783-792, Aug.2003.

[7] E. Donnadieu, D. Cefai, Y. P. Tan, G. Paresys, G. Bismuth, and A. Trautmann, "Imaging early steps of human T cell activation by antigen-presenting cells," *J Immunol*, vol. 148, no. 9, pp. 2643-2653, May1992.

[8] M. J. Miller, O. Safrina, I. Parker, and M. D. Cahalan, "Imaging the single cell dynamics of CD4+ T cell activation by dendritic cells in lymph nodes," *J Exp. Med.*, vol. 200, no. 7, pp. 847-856, Oct.2004.

[9] A. Legradi, V. Chitu, V. Szukacsov, R. Fajka-Boja, S. K. Szekely, and E. Monostori, "Lysophosphatidylcholine is a regulator of tyrosine kinase activity and intracellular Ca(2+) level in Jurkat T cell line," *Immunol Lett.*, vol. 91, no. 1, pp. 17-21, Jan.2004.

[10] C. G. Radu, L. V. Yang, M. Riedinger, M. Au, and O. N. Witte, "T cell chemotaxis to lysophosphatidylcholine through the G2A receptor," *Proc. Natl. Acad. Sci. U. S. A*, vol. 101, no. 1, pp. 245-250, Jan.2004.

[11] E. Segura, S. Amigorena, and C. Thery, "Mature dendritic cells secrete exosomes with strong ability to induce antigen-specific effector immune responses," *Blood Cells, Molecules, and Diseases*, vol. 35, no. 2, pp. 89-93, 2005.

[12] C. Thery, L. Duban, E. Segura, P. Veron, O. Lantz, and S. Amigorena, "Indirect activation of naive CD4+ T cells by dendritic cell-derived exosomes," *Nat Immunol*, vol. 3, no. 12, pp. 1156-1162, Dec.2002.

[13] A. Kaiser, E. Donnadieu, J. P. Abastado, A. Trautmann, and A. Nardin, "CC Chemokine Ligand 19 Secreted by Mature Dendritic Cells Increases Naive T Cell Scanning Behavior and Their Response to Rare Cognate Antigen," *J Immunol*, vol. 175, no. 4, pp. 2349-2356, Aug.2005.

[14] V. N. Ngo, H. Lucy Tang, and J. G. Cyster, "Epstein-Barr Virus-induced Molecule 1áLigand Chemokine Is Expressed by Dendritic Cells in Lymphoid Tissues and Strongly Attracts Naive T Cells and Activated B Cells," *J. Exp. Med.*, vol. 188, no. 1, pp. 181-191, July1998.

[15] N. Bertho, H. Adamski, L. Toujas, M. Debove, J. Davoust, and V. Quillien, "Efficient migration of dendritic cells toward lymph node chemokines and induction of TH1 responses require maturation stimulus and apoptotic cell interaction," *Blood*, vol. 106, no. 5, pp. 1734-1741, Sept.2005.

[16] M. Feili-Hariri, D. H. Falkner, and P. A. Morel, "Polarization of naive T cells into Th1 or Th2 by distinct cytokine-driven murine dendritic cell populations: implications for immunotherapy," *J Leukoc Biol*, vol. 78, no. 3, pp. 656-664, Sept.2005.

[17] S. Iwamoto, M. Ishida, K. Takahashi, K. Takeda, and A. Miyazaki, "Lipopolysaccharide stimulation converts vigorously washed dendritic cells (DCs) to nonexhausted DCs expressing CD70 and evoking long-lasting type 1 T cell responses," *J Leukoc Biol*, vol. 78, no. 2, pp. 383-392, Aug.2005.

[18] M. Mandron, M. F. Aries, R. D. Brehm, H. S. Tranter, K. R. Acharya, M. Charveron, and C. Davrinche, "Human dendritic cells conditioned with Staphylococcus aureus enterotoxin B promote TH2 cell polarization," *J Allergy Clin. Immunol*, vol. 117, no. 5, pp. 1141-1147, May2006.

[19] M. C. Rodriguez-Galan, J. H. Bream, A. Farr, and H. A. Young, "Synergistic effect of IL-2, IL-12, and IL-18 on thymocyte apoptosis and Th1/Th2 cytokine expression," *J Immunol*, vol. 174, no. 5, pp. 2796-2804, Mar.2005.

[20] M. L. Albert, M. Jegathesan, and R. B. Darnell, "Dendritic cell maturation is required for the cross-tolerization of CD8+ T cells," *Nat Immunol*, vol. 2, no. 11, pp. 1010-1017, Nov.2001.

[21] P. Berthe, J. L. Cousin, and J. P. Breittmayer, "Intracellular Ca2+ regulation in CD3 stimulated Jurkat T cells involves H+ fluxes," *Cell Signal.*, vol. 3, no. 5, pp. 453-459, 1991.

[22] J. Delon, N. Bercovici, G. Raposo, R. Liblau, and A. Trautmann, "Antigen-dependent and -independent Ca2+ Responses Triggered in T Cells by Dendritic Cells Compared with B Cells," *J. Exp. Med.*, vol. 188, no. 8, pp. 1473-1484, Oct.1998.

[23] M. Kelleher and P. C. L. Beverley, "Lipopolysaccharide Modulation of Dendritic Cells Is Insufficient to Mature Dendritic Cells to Generate CTLs from Naive Polyclonal CD8+ T

Cells In Vitro, Whereas CD40 Ligation Is Essential," *J Immunol*, vol. 167, no. 11, pp. 6247-6255, Dec.2001.

[24] M. B. Lutz and G. Schuler, "Immature, semi-mature and fully mature dendritic cells: which signals induce tolerance or immunity?," *Trends in Immunology*, vol. 23, no. 9, pp. 445-449, Sept.2002.

[25] E. Real, A. Kaiser, G. Raposo, A. Amara, A. Nardin, A. Trautmann, and E. Donnadieu, "Immature Dendritic Cells (DCs) Use Chemokines and Intercellular Adhesion Molecule (ICAM)-1, But Not DC-Specific ICAM-3-Grabbing Nonintegrin, to Stimulate CD4+ T Cells in the Absence of Exogenous Antigen," *J Immunol*, vol. 173, no. 1, pp. 50-60, July2004.

[26] J. K. H. Tan and H. C. O'Neill, "Maturation requirements for dendritic cells in T cell stimulation leading to tolerance versus immunity," *J Leukoc Biol*, vol. 78, no. 2, pp. 319-324, Aug.2005.

[27] Y. Valdez, W. Mah, M. M. Winslow, L. Xu, P. Ling, and S. E. Townsend, "Major Histocompatibility Complex Class II Presentation of Cell-associated Antigen Is Mediated by CD8{alpha}+ Dendritic Cells In Vivo," *J. Exp. Med.*, vol. 195, no. 6, pp. 683-694, Mar.2002.

CHAPTER VI

A REPORT OF DYE TRANSFER BETWEEN DENDRITIC CELLS AND CD4+ T CELLS DURING SYNAPSE FORMATION

Abstract

A concert of intricate exchanges between immune cells lies at the core of adaptive immune response, whereby critical antigenic information is communicated and the general environmental survey performed by antigen presenting cells is transformed into a highly specific cell-mediated attack against the infecting agent. While it is clear that some information is passed by way of cell surface ligand/receptor binding events during the immunological synapse between dendritic cells and T cells, there are also paracrine intercellular signaling events that impact the development of immune response. Understanding how immune cells communicate with one another is key to fully deciphering the signals leading to immune response, tolerance, and anergy. We have developed a microfluidic platform, termed the nanophysiometer, to study non-adherent immune cell interactions and signaling pathways. Utilizing the nanophysiometer to investigate calcium signaling in T cells during the immunological synapse, dye transfer between T cells and dendritic cells was observed. Further analysis revealed that bi-directional dye transfer occurs during the immunological synapse. This suggests that the communication between T cells and dendritic cells during the immune synapse involves cytosolic transfer.

Introduction

A concert of intricate exchanges between immune cells lies at the core of adaptive immune response, whereby critical antigenic information is communicated and the general environmental survey performed by antigen presenting cells is transformed into a highly specific cell-mediated attack against the infecting agent [1]. The immunological synapse, perhaps the

most well known of these intercellular exchanges, is widely accepted as the physical medium by which dendritic cells (DCs) transmit antigen information to naïve T cells (TCs), resulting in TC activation [2-4]. While it is clear that some information is passed by way of cell surface ligand/receptor binding events which trigger intracellular signaling cascades, a complete understanding of what information and the method by which it is translated remains under investigation [5-9]. Understanding how immune cells communicate with one another is key to fully deciphering the signals leading to immune response, tolerance, and anergy.

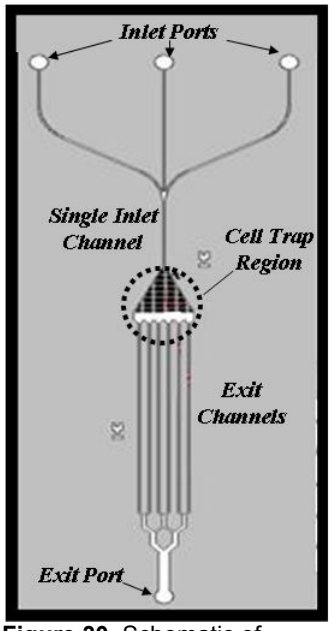

Figure 30. Schematic of microfluidic nanophysiometer. The device is constructed of PDMS and plasma-bonded to a glass coverslip.

We have developed a microfluidic platform, termed the nanophysiometer, to study non-adherent immune cell interactions and signaling pathways. A schematic of the microfluidic nanophysiometer is shown in **Figure 1**. This platform is a self-contained unit fabricated of optically transparent, bio-inert PDMS on glass and designed to maintain non-adherent cells in a microfluidic environment [10]. Cells are injected into one of the inlet ports using computer-controlled micro-syringe pumps. As cells flow through the trap region, they are passively trapped in one of 550 18 $\mu m \times 18 \mu m \times 10 \mu m$ PDMS, bucket-like structures. Media flow rate is optimized such that cells remain in traps and receive necessary nutrients while minimizing shear stress and waste accumulation. The nanophysiometer provides a method of quickly sequestering cells into individually addressable compartments without using any adhering agents, such as cell surface antibodies, poly-l-lysine, or fibronectin, which can themselves induce unwanted intracellular signaling cascades. Furthermore, only relatively small quantities of cells (aliquots as small as 1000 cells), media (less than 1 ml is required for long-term experiments), and other reagents are required to obtain data on hundreds of single cells in parallel, resulting in decreased labor and material costs compared with bulk cell culture techniques.

We utilized the nanophysiometer to investigate interactions between mDCs and TCs. In this paper, we report the observation of bi-directional dye transfer between DCs and TCs at various stages of immune synapse formation. We hypothesize that this reveals a very important communication method employed by both cell types during the development of effective immune response.

Materials & Methods

A description of the experimental setup, nanophysiometer preparation, and cell loading can be found in [11]. Primary human CD4+ T cells and dendritic cells (derived from human monocytes) were generously provided by the lab of Derya Unutmaz (New York University School of Medicine, New York, NY) following isolation and purification from human blood donors [12]. Primary CD4+ T cells were thawed from liquid nitrogen aliquots ($5*10^5$ cells/vial) 24 hours prior to use and cultured using sterile technique in RPMI 1640 (ATCC, Manassas VA) supplemented with 10% FBS (ATCC, Manassas VA) and 10μg/ml Ciprofloxacin (Mediatech, Herndon VA). Dendritic cells were derived by incubating primary human CD14+ monocytes with 20 ng/ml IL-4 and 100ng/ml GM-CSF for 4-6 days [13]. Mature dendritic cells were generated following 24-hour incubation with 10 ng/ml LPS [13]. All cells were incubated in a sterile environment maintained at 37°C, complete with 5% CO_2 and 95% humidity.

Naïve primary CD4+ T cells were first loaded with rhod-2 calcium indicator by incubation in a 5μM solution for 30 minutes at 37°C. The same protocol was utilized to load mDCs with CellTracker Green (Molecular Probes), except the media contained a 1mM concentration of the dye. Cells were then loaded into the nanophysiometer (pre-cleared with media to remove air bubbles) and perfused with normal culture media supplemented with $CaCl_2$ to a final concentration of 1.8 mM [14]. Using Metamorph software, the microscope was programmed to obtain baseline bright field (DIC or phase-contrast) and TRITC (rhod-2 fluorescence) images for

4 to 5 FOVs spanning the entire cell trap region of the microfluidic device at precise time intervals.

Results

The first observation of dye transfer occurred during an experiment investigating long-term calcium signaling in primary, naïve CD4+ TCs during immune synapse interaction with mature, SEB pulsed DCs. Only the TCs were loaded with rhod-2 calcium indicator dye prior to the experiment. Unexpectedly, we found that roughly 10% of the DCs interacting with TCs exhibited a measurable fluorescent signal for short periods of time. An example is shown in **Figure 2**. Because the only known source of rhod-2 calcium dye was that free in the cytosol of the TCs, it is hypothesized that the fluorescent signal seen in the DCs is a result of cytosolic transfer from the TC to the DC during their interactions. To test if the observed transfer was due to the dye associating with the TC membrane, the experiment was repeated using CellTracker Green with the same results (data not shown).

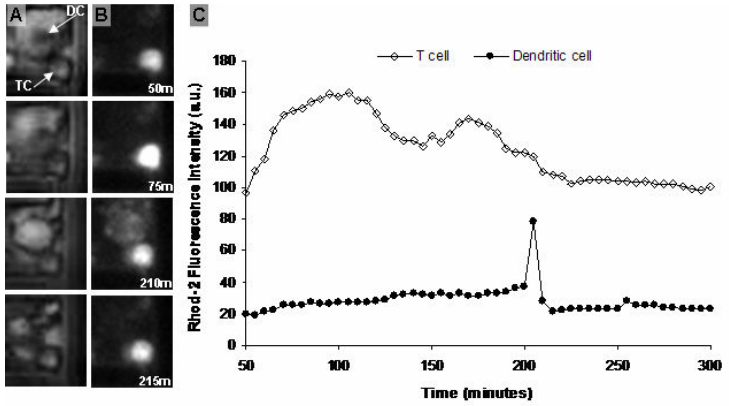

Figure 31. Dye transfer from rhod-2 loaded, naïve primary CD4+ TC trapped alongside a mature, SEB pulse DC. Bright field images are shown in (A) and the corresponding fluorescence images in (B). A graphical representation of the fluorescence intensity of the two cells over time is shown in (C).

Following the observation of the TC to DC dye transfer, we asked whether such a transfer could occur in the opposite direction, from DCs to TCs. For this experiment, only the DCs were loaded with CellTracker Green prior to the experiment. Although the DC to TC dye transfer was a rarer occurrence, we were able to capture several events, one of which is shown in **Figure 3**. In this series of images, a DC uses its cellular extensions to capture a TC as it

passes. One striking difference observed in the DC to TC dye transfer events is the time scale on which it occurs. The DC to TC transfers occur very quickly after physical contact, while TC to DC transfer occurs only after the two cells have maintained physical contact for an extended periods of time.

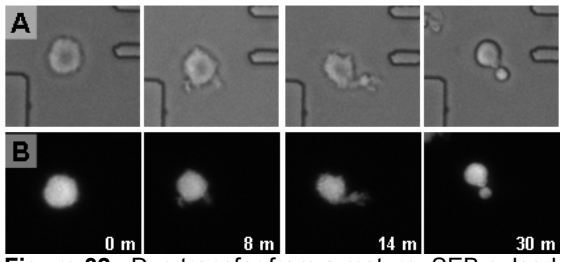

Figure 32. Dye transfer from a mature, SEB pulsed DC loaded with CellTracker Green to a naïve CD4+ T cell. The bright field images are shown in (A) and the corresponding fluorescence images in (B).

Discussion

In this brief report we present evidence for a new type of interaction occurring between mDCs and TCs during the immune synapse which includes the exchange of cytosolic material, as shown through dye transfer observations. It is our hypothesis that the immunological synapse , in addition to facilitating the interaction of cell surface proteins for the exchange of information, may also include a conduit for the direct exchange of mass. What molecular species may be transferred this way remains to be identified. There are reports of cell membrane proteins, such as MHC II, being transferred from DCs to TCs[15;16]. If these proteins are transferred in patches of cell membrane in a process known as trogocytosis that occurs in DCs and TCs [17-19], it is feasible to think that perhaps bits of cytosol are transferred as well.

Another possibility is that there are channels or junctions formed during the immunological synapse. Gap junctions have been demonstrated as a method of peptide transfer between two cells [20] and have selective permeabilities [21]. There are reports of DCs forming gap junctions with neighboring DCs as well as other cell types, such as B cells and other endothelial cells [22-24]. In fact, it is thought that intercellular communication between DCs in the lymph nodes is essential to effective DC maturation [22]. Gap junctions are formed

by organization of connexin proteins within the cell membrane. DCs are known to express connexin 40 and 43 [25;26]. While direct evidence of gap junction formation during the immune synapse has yet to be proven, it is known that TCs also express connexin 43 and thus have the potential to form gap junctions with other cells [27].

Another interesting observation in these dye transfer experiments is the time scale on which the transfer took place. It appears as though DC to TC dye transfer occurs very quickly following physical contact of the two cells while TC to DC transfer takes place several hours into their interaction. Currently this is simply an observation, as not enough events have been documented to yield statistical significance in any case. We can speculate, however, that it is not improbable for DCs to be eager to quickly transmit antigenic information to nTCs when seeking to stimulate an immune response. It is important for DCs to find a TC that responds to the captured antigen as quickly as possible, often briefly interacting with hundreds to thousands of TCs in the process. The TC to DC transfer may only occur after the immunological synapse is fully organized. In any case, this presents a very interesting area for further investigation into the interaction between DCs and TCs. Perhaps it can yield greater insight into the methods utilized by these cells to decide between immune response or suppression.

Conclusions

Because immune cells are non-adherent, traditional cell culture methods are ill-equipped to study cell-cell interactions and must utilize additional adhesion methods to secure cells to a known physical place. These adhesion techniques often obscure normal cell morphology and induce intracellular signaling pathways that may interfere with data analysis. Using a novel microfluidic platform, we examined the interactions between mDCs and naïve CD4+ TCs during the immunological synapse. We observed bi-directional dye transfer between mDCs and TCs that suggest cytosolic exhange occurs during their interactions. The direction of dye transfer was dependent upon the duration of interaction with DC to TC transfer very quickly following

physical contact, while TC to DC transfer occurred several hours into synapse formation. This may hold many clues as to how and when information is communicated between DCs and TCs during the immunological synapse.

Bibliography

[1] J. Banchereau, F. Briere, C. Caux, J. Davoust, S. Lebecque, Y. J. Liu, B. Pulendran, and K. Palucka, "Immunobiology of Dendritic Cells," *Annual Review of Immunology*, vol. 18, no. 1, pp. 767-811, 2000.

[2] M. L. Dustin, S. Y. Tseng, R. Varma, and G. Campi, "T cell-dendritic cell immunological synapses," *Current Opinion in Immunology*, vol. 18, no. 4, pp. 512-516, Aug.2006.

[3] J. C. Stinchcombe, G. Bossi, S. Booth, and G. M. Griffiths, "The immunological synapse of CTL contains a secretory domain and membrane bridges," *Immunity*, vol. 15, no. 5, pp. 751-761, Nov.2001.

[4] J. K. H. Tan and H. C. O'Neill, "Maturation requirements for dendritic cells in T cell stimulation leading to tolerance versus immunity," *J Leukoc Biol*, vol. 78, no. 2, pp. 319-324, Aug.2005.

[5] M. B. Lutz and G. Schuler, "Immature, semi-mature and fully mature dendritic cells: which signals induce tolerance or immunity?," *Trends in Immunology*, vol. 23, no. 9, pp. 445-449, Sept.2002.

[6] J. Rachmilewitz and A. Lanzavecchia, "A temporal and spatial summation model for T-cell activation: signal integration and antigen decoding," *Trends in Immunology*, vol. 23, no. 12, pp. 592-595, Dec.2002.

[7] E. Segura, S. Amigorena, and C. Thery, "Mature dendritic cells secrete exosomes with strong ability to induce antigen-specific effector immune responses," *Blood Cells, Molecules, and Diseases*, vol. 35, no. 2, pp. 89-93, 2005.

[8] C. Thery, L. Duban, E. Segura, P. Veron, O. Lantz, and S. Amigorena, "Indirect activation of naive CD4+ T cells by dendritic cell-derived exosomes," *Nat Immunol*, vol. 3, no. 12, pp. 1156-1162, Dec.2002.

[9] J. Delon, "The immunological synapse," *Curr. Biol*, vol. 10, no. 6, p. R214, Mar.2000.

[10] S. L. Faley, K. T. Seale, J. Hughey, J. P. Wikswo, and F. J. Baudenbacher, "Microfluidic platform for real-time signaling analysis of multiple single T cells in parallel (in preparation)," *Lab Chip.*, 2007.

[11] S. L. Faley, K. T. Seale, S. E. VanCompernolle, D. Unutmaz, and J. P. Wikswo, "Real-time monitoring of intercellular signaling between human dendritic cell and cd4+ t cells using the microfluidic nanophysiometer *(in preparation)*," *Undecided*, 2007.

[12] K. Oswald-Richter, V. J. Torres, M. S. Sundrud, S. E. VanCompernolle, T. L. Cover, and D. Unutmaz, "Helicobacter pylori VacA Toxin Inhibits Human Immunodeficiency Virus Infection of Primary Human T Cells," *J. Virol.*, vol. 80, no. 23, pp. 11767-11775, Dec.2006.

[13] K. A. Eger, M. S. Sundrud, A. A. Motsinger, M. Tseng, L. V. Kaer, and D. Unutmaz, "Human natural killer T cells are heterogeneous in their capacity to reprogram their effector functions," *PLoS. ONE.*, vol. 1, p. e50, 2006.

[14] S. Kunerth, G. W. Mayr, F. Koch-Nolte, and A. H. Guse, "Analysis of subcellular calcium signals in T-lymphocytes," *Cell Signal.*, vol. 15, no. 8, pp. 783-792, Aug.2003.

[15] S. A. Wetzel and D. C. Parker, "MHC transfer from APC to T cells following antigen recognition," *Crit Rev. Immunol*, vol. 26, no. 1, pp. 1-21, 2006.

[16] S. A. Wetzel, T. W. McKeithan, and D. C. Parker, "Peptide-Specific Intercellular Transfer of MHC Class II to CD4+ T Cells Directly from the Immunological Synapse upon Cellular Dissociation," *J Immunol*, vol. 174, no. 1, pp. 80-89, Jan.2005.

[17] E. Joly and D. Hudrisier, "What is trogocytosis and what is its purpose?," *Nat Immunol*, vol. 4, no. 9, p. 815, Sept.2003.

[18] S. Bourbie-Vaudaine, N. Blanchard, C. Hivroz, and P. H. Romeo, "Dendritic Cells Can Turn CD4+ T Lymphocytes into Vascular Endothelial Growth Factor-Carrying Cells by Intercellular Neuropilin-1 Transfer," *J Immunol*, vol. 177, no. 3, pp. 1460-1469, Aug.2006.

[19] J. Caumartin, J. Lemaoult, and E. D. Carosella, "Intercellular exchanges of membrane patches (trogocytosis) highlight the next level of immune plasticity," *Transpl. Immunol*, vol. 17, no. 1, pp. 20-22, Dec.2006.

[20] J. Neijssen, C. Herberts, J. W. Drijfhout, E. Reits, L. Janssen, and J. Neefjes, "Cross-presentation by intercellular peptide transfer through gap junctions," *Nature*, vol. 434, no. 7029, pp. 83-88, Mar.2005.

[21] G. S. Goldberg, V. Valiunas, and P. R. Brink, "Selective permeability of gap junction channels," *Biochimica et Biophysica Acta (BBA) - Biomembranes*, vol. 1662, no. 1-2, pp. 96-101, Mar.2004.

[22] H. Matsue, J. Yao, K. Matsue, A. Nagasaka, H. Sugiyama, R. Aoki, M. Kitamura, and S. Shimada, "Gap junction-mediated intercellular communication between dendritic cells (DCs) is required for effective activation of DCs," *J Immunol*, vol. 176, no. 1, pp. 181-190, Jan.2006.

[23] C. W. Wong, T. Christen, and B. R. Kwak, "Connexins in leukocytes: shuttling messages?," *Cardiovascular Research*, vol. 62, no. 2, pp. 357-367, May2004.

[24] T. Krenacs and M. Rosendaal, "Immunohistological detection of gap junctions in human lymphoid tissue: connexin43 in follicular dendritic and lymphoendothelial cells," *J. Histochem. Cytochem.*, vol. 43, no. 11, pp. 1125-1137, Nov.1995.

[25] P. I. Jara, M. P. Boric, and J. C. Saez, "Leukocytes Express Connexin 43 After Activation with Lipopolysaccharide and Appear to Form Gap Junctions with Endothelial Cells After Ischemia-Reperfusion," *PNAS*, vol. 92, no. 15, pp. 7011-7015, July1995.

[26] E. Oviedo-Orta and W. H. Evans, "Gap junctions and connexins: potential contributors to the immunological synapse," *J Leukoc Biol*, vol. 72, no. 4, pp. 636-642, Oct.2002.

[27] E. Oviedo-Orta and W. Howard Evans, "Gap junctions and connexin-mediated communication in the immune system," *Biochimica et Biophysica Acta (BBA) - Biomembranes*, vol. 1662, no. 1-2, pp. 102-112, Mar.2004.

CHAPTER VII

CONCLUSIONS & FUTURE DIRECTIONS

This body of work describes the major accomplishments attained towards the development, validation, and application of a novel microfluidic platform designed to study T cell signaling. Platform compatible, antibody-conjugated QDs were shown to be accurate indicators of IL2Rα cell surface expression in T cells during activation. These will be useful for future long-term activation studies within the nanophysiometer as IL2Rα expression peaks 24 hours following T cell activation. In terms of the platform itself, the results presented here validate the nanophysiometer as a powerful, cell-based instrument to study multiple single cells in parallel. Not only was it demonstrated that primary T cells can be passively contained within the cell trap region using only hydrodynamic forces, but also that cells can be maintained under continuous flow conditions for 24 hours with viability approaching 70%. Furthermore, we successfully activated T cells within the nanophysiometer using chemical, antibody, and cellular based stimulation methods.

Following this validation, we then employed the nanophysiometer to study signaling events associated with the early stages of T cell activation. By utilizing the nanophysiometer in a daisy-chain configuration, we were able to confirm that DCs matured with LPS, but in the absence of antigen, release small quantities of a chemical signal that induces cytosolic calcium transients in naïve T cells without any physical interaction. This intercellular signaling phenomenon was not apparent in a standard cell culture environment due to the large volume of media diluting the signal, highlighting another attribute of the nanophysiometer as the 20 nanoliter volume of the cell trap region greatly decreases the cell to media volume ratio and allows the effects of low concentration chemical signals to be observed. Because autocrine and

paracrine signaling is highly influential during immunological synapse formation and the progression of immune response, the nanophysiometer has the potential to have a significant impact upon immunological research as there exist very few tools to study large quantities of individual suspension cells over time while maintaining a low cell to media volume ratio. Furthermore, the ability to either study cell-cell interaction or to physically separate the cells offers a useful flexibility to the platform for modeling various biologically relevant situations, such as the signaling events between DCs and TCs during the immunological synapse compared to DC cells in the lymph node with TCs in the periphery.

Finally, we report evidence of dye transfer between mature DCs and naïve TC during early interactions leading to the immunological synapse. The relative number of cell pairs that showed signs of dye transfer was only 10%, but observation was made possible by monitoring hundreds of cell-cell interactions over time within the nanophysiometer. Dye transfer was observed from TCs to DCs and vice versa, although on different time scales suggesting some specificity in information communicated between the cells. DC to TC dye transfer occurred very quickly after making superficial contact while TC to DC transfers occurred following hours of interaction. These results suggest that communication between DCs and TCs during the immunological synapse is not limited to cell surface ligand-receptor pairs initiating intracellular signaling cascades. Understanding the biology behind the observed dye transfer events will undoubtedly reveal important information concerning the role of the immunological synapse in effective immune response.

Future directions for the further development of the nanophysiometer include modeling the fluid dynamics as well as incorporating additional technologies to probe cellular signaling states. Currently, sensors to monitor cellular metabolism as well as technology to detect cellular secretions, such as cytokines or chemokines, are under development and planned to be incorporated into the nanophysiometer platform, thus expanding our detection capabilities. The applications of the nanophysiometer to study immune biology are practically endless. We plan

to continue studying the interactions between DCs and TCs during the immunological synapse in the immediate future. Experiments include narrowing down the possible identity of “factor x” from the list of potential culprits. It will also be interesting to examine whether various maturing agents affect the chemical signals secreted by DCs. Furthermore, to study how the chemical signals impact T cell activities in the presence or absence of DC contact. Of course, the dye transfer experiments are still in the very early phases and warrant further investigation into the nature of the channel/junction that facilitates cytosolic exchange.

A secondary impetus for this work is derived from dire need for reliable chemical and biological warfare (CBW) detection system. Recent world events have resulted in heightened concern over the threat of chemical & biological warfare (CBW) agents and renewed interest in elucidating mechanisms of detection, prevention, treatment, and containment of large scale disease epidemics. While detection systems and treatment protocols against naturally occurring diseases such as small pox and anthrax are already being implemented, these efforts do not address the more concerning issue of maliciously engineered biological agents. This yields the question: how do you construct a detection system with the ability to sense novel pathogens with completely unknown pathogenesis? We believe that the adaptive immune response is an ideal model for such a system as this is exactly what the immune system is designed to accomplish within the body. Since T cells are posses’ inherent discriminatory ability along with responsive intracellular signaling pathways, we believe that they are excellent candidates for utilization as biosensors. The same microfluidic platform designed to study the signaling pathways of T cells has the potential to be a useful tool in the field or field laboratory due to is small size, ease and low cost of production, as well as the ability to be integrated with multiple detection modalities. Thus, the development of this microfluidic platform can not only impact the necessary basic biological research of T cell signaling pathways during the course of an immune response, but may also potentially be utilized as a tool for detecting unknown CBW toxins in the field.

There is much more detail to the activation of T cells than is discussed within this dissertation, much if which is still under investigation. The choice between T cell activation versus anergy is a function of TCR affinity for MHC + pathogenic peptide [1] , presence of co-factors and adhesion proteins[2;3], cytoskeletal rearrangements [4], inflammatory cytokines[5], the activation of any cytosolic inhibitory proteins [6], as well as signals yet to be identified. Furthermore, activated CD4+ cell then differentiate into either TH1 or TH2 effector cells depending upon the interactions occurring during the immune synapse which determined whether there will be a humoral or cell based T cell response[7]. There are situations such as pregnancy and tumorigenesis that, according to the traditional model of adaptive immune

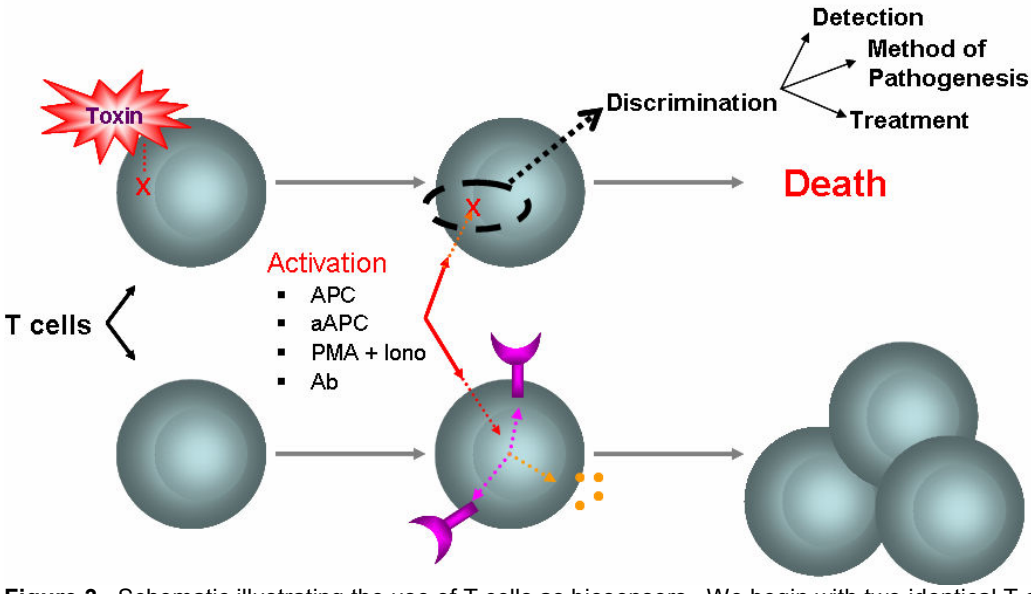

Figure 3. Schematic illustrating the use of T cells as biosensors. We begin with two identical T cells, one of which is exposed to an unknown toxin. The two cells are then exposed to activating factors which may consist of antigen presenting cells (APCs), artificial antigen presenting cells (aAPCs), chemicals such as PMA and ionomycin, or antibodies. The normal T cell will go on to upregulate IL2R and IL2, as well as other known processes associated with T cell activation. The cell exposed to toxin, however, will have an altered activation process. This may take the form of anergy, or upregulation of atypical proteins for activation. In the end, the normal cell that is completely activated will begin to divide whereas the toxin exposed cell might die or become anergic. We plan to go back and determine what signaling pathways the toxin effects within the T cell. By doing so, we hypothesize that the manner in which the toxin effects the cell can be used to discriminate between toxins. In addition, because we are dealing with cells of the immune system, understanding what pathways have been disturbed will aid in understanding a toxin's method of pathogenesis and provide valuable insights into treatment.

response, should lead to acute inflammatory reaction and rejection, but, for reasons not entirely clear, result in immune tolerance. Conversely, a completely MHC matched donated organ

suffers from acute and chronic immune rejection despite the use of immune suppressive medications. Matzinger proposed the concept that T cells are capable of not just discriminating between self and non-self, but actually goes a step further and differentiates between dangerous versus non-dangerous signals[8;9]. Clearly, there exists a high level of complexity and discriminatory ability within the signaling pathways of T cells. These characteristics not only allow these cells to be highly effective for mediating immune response against novel pathogens, but also to be utilized as biosensors to gain insight into methods of detection, prevention, and treatment for biological warfare agents (see Figure . The premise being that T cells exposed directly (not via APCs) to a particular toxin will subsequently yield unique signatures in the form of promotion or inhibition of particular signaling events or molecules. After toxin exposure, T cells that are subsequently activated using chemicals or artificial APCs will exhibit changes in the known signaling cascades that can be identified and used for identification and discrimination against other potential CBW agents. Studies concerning anthrax toxin conducted by Paccani et al support the feasibility of this premise as they have shown both the lethal factor (LF) and edema factor (EF) of anthrax toxin suppress T cell activation by inhibiting the MAPK dependant NFAT and AP-1 signaling pathways [10]. This work illustrates an additional benefit of using T cells as biosensors in that the information collected is not only useful for identifying pathogens, but also provides details concerning its impact upon the adaptive immune response. This is highly relevant is developing preventative and therapeutic treatments.

Ultimately, however, the nanophysiometer is intended to be a tool to be utilized to gather important information regarding T cell signaling states. Significant progress towards this goal had been made by validating the nanophysiometer as a platform capable of sustaining primary T cells and demonstrating that valuable information can be extracted. In order to continue to progress it is necessary to develop and incorporate optical probes to study the intracellular signaling pathways as well as the additional detection technologies for monitoring cellular metabolism and secretions. In addition, it is necessary to also works towards identifying the

pathways of importance beyond those already known during T cell activation. The results presented here prove that the current capabilities of this platform are quite powerful and that it should be continued to be developed as both a tool for CBW detection as well as a technology to investigate cellular signaling activities in general.

Bibliography

[1] J. D. Ashwell, "Antigen-driven T cell expansion: affinity rules," *Immunity*, vol. 21, no. 5, pp. 603-4, 2004.

[2] C. A. Janeway, Jr., "The T cell receptor as a multicomponent signalling machine: CD4/CD8 coreceptors and CD45 in T cell activation," *Annu Rev Immunol*, vol. 10, pp. 645-74, 1992.

[3] R. Konig and W. Zhou, "Signal transduction in T helper cells: CD4 coreceptors exert complex regulatory effects on T cell activation and function," *Curr Issues Mol Biol*, vol. 6, no. 1, pp. 1-15, 2004.

[4] D. Sancho, M. Vicente-Manzanares, M. Mittelbrunn, M. C. Montoya, M. Gordon-Alonso, J. M. Serrador, and F. Sanchez-Madrid, "Regulation of microtubule-organizing center orientation and actomyosin cytoskeleton rearrangement during immune interactions," *Immunol Rev*, vol. 189, pp. 84-97, 2002.

[5] J. M. Curtsinger, C. S. Schmidt, A. Mondino, D. C. Lins, R. M. Kedl, M. K. Jenkins, and M. F. Mescher, "Inflammatory cytokines provide a third signal for activation of naive CD4+ and CD8+ T cells," *J Immunol*, vol. 162, no. 6, pp. 3256-62, 1999.

[6] D. Mary, J. F. Peyron, P. Auberger, C. Aussel, and M. Fehlmann, "Modulation of T cell activation by differential regulation of the phosphorylation of two cytosolic proteins. Implication of both Ca2+ and cyclic AMP-dependent protein kinases," *J Biol Chem*, vol. 264, no. 24, pp. 14498-502, 1989.

[7] M. A. Santana and Y. Rosenstein, "What it takes to become an effector T cell: the process, the cells involved, and the mechanisms," *J Cell Physiol*, vol. 195, no. 3, pp. 392-401, 2003.

[8] P. Matzinger, "Introduction to the series. Danger model of immunity," *Scand J Immunol*, vol. 54, no. 1-2, pp. 2-3, 2001.

[9] P. Matzinger, "The danger model: a renewed sense of self," *Science*, vol. 296, no. 5566, pp. 301-5, 2002.

[10] S. R. Paccani, F. Tonello, R. Ghittoni, M. Natale, L. Muraro, M. M. D'Elios, W. J. Tang, C. Montecucco, and C. T. Baldari, "Anthrax toxins suppress T lymphocyte activation by disrupting antigen receptor signaling," *J Exp Med*, vol. 201, no. 3, pp. 325-31, 2005.